IDENTIFICATION OF THE VARIANCE OF THE WAVE EXCITING ROLLING MOMENT USING SHIP'S RANDOM RESPONSE

ZHILIANG XING

Identification of the Variance of the Wave Exciting Rolling Moment Using Ship's Random Response

BY

© Zhiliang Xing

A thesis submitted to the

School of Graduate Studies

in partial fulfilment of the

requirements for the degree of

Master of Engineering

Faculty of Engineering and Applied Science
Memorial University of Newfoundland

May 2003

St. John's Newfoundland Canada

Abstract

In this research, the variance of wave exciting rolling moment has been identified using ship roll response only. The data of ship rolling motion were obtained from ship rolling simulations as well as from ship model tests. The random decrement technique has been used to extract the free roll decay curves from the stationary random response. The roll damping and restoring moments can then be obtained from the extracted free decay curves using a neural network technique. The predicted rolling parameters were then used to calculate the variance of wave exciting rolling moment.

The simulated data are used to demonstrate the validity of the proposed method. The application of the method to the experimental data showed the influence of the wave model frequency, the wave height, and the GM value on the variance of the wave exciting rolling moment in irregular beam waves. This method is only based on the time history of the ship rolling displacement to estimate the variance of wave exciting rolling moment. Moreover, the roll response of a ship can be easily measured using an accelerometer while the ship is at sea. The analysis can be done on line at sea. The estimated variance value will give captains an important parameter for the assessment of ship safety.

Acknowledgements

I would like to take this opportunity to express my sincere appreciation to my supervisor, Dr. M. R. Haddara, for his guidance and support both on the finance and the spirit during my master study at Memorial University of Newfoundland.

Special thanks to Mr. Jim Gosse, the technician at wave tank of MUN, for his technique support in the model experiments.

Table of Contents

Abstract..... i

Acknowledgements..... ii

Table of Contents..... iii

List of Figures..... vi

List of Tables..... viii

1. Introduction..... 1

1.1 Objective..... 1

1.2 Research Outline..... 2

1.3 Organization..... 2

2. Literature Review..... 3

2.1 Ship Rolling Motion in Random waves..... 3

2.2 Random Decrement Technique..... 6

2.3 Neural Network Technique..... 8

2.4 Review Summary..... 9

3. Mathematical Analysis..... 11

3.1 Rolling Equation in Random Waves..... 11

3.2 Fokker-Plank Equation..... 13

3.3 Mean Values Propagation..... 15

3.4 Variance Propagation..... 17

3.5 Damping and Restoring Moment Model..... 20

4. Numerical Simulation Method.....22

4.1 Simulation of the Random Roll Response.....22

4.2 Random Decrement Signature.....26

4.3 Estimation of the Parameters using Neural Networks..... 27

4.4 Comparison of the Regular Responses.....31

4.5 Estimation of the Variance of Wave Exciting Moment.....31

5. Ship Model Experiments.....33

5.1 General Arrangement.....33

5.2 Ship Model Descriptions.....35

5.3 Experimental Set-up.....38

5.4 Roll Tests in Towing Tank.....42

5.4.1 Inclining Tests.....43

5.4.2 Free Roll Tests.....45

5.4.3 Forced Roll Tests in Random Beam Waves.....48

5.5 Experimental Data Analysis Method.....51

6. Results and Discussion.....52

6.1 Simulation Results and Discussion.....52

6.1.1 Validation of Predicted Equivalent Linear Roll Parameters.....52

6.1.2 Validation of the Variance ψ Prediction.....54

6.2 Experiment Results and Discussion.....56

7. Conclusions and Recommendations.....73

7.1 Conclusions.....73

7.2 Recommendations.....75

Reference.....76

Appendix A Comparison of Regular Response Curves.....79

Appendix B Programs.....95

List of Figures

Figure 4.1: Simulated Roll Angle History of Case 511.....23

Figure 4.2: Special 20 Seconds Roll Angle History of Case 511.....23

Figure 4.3: The Random Decrement Curve of Case 511.....27

Figure 4.4: Neural Network.....28

Figure 5.1: Towing Tank Layout.....34

Figure 5.2: Body Plan of "R-class Icebreaker" Ship Model.....35

Figure 5.3: "Series 60" Model Test.....41

Figure 5.4: "R-class Icebreaker" Model Test.....42

Figure 5.5: Incling Result Plot for "R-class".....44

Figure 5.6: Incling Result Plot for "Series 60".....45

Figure 5.7: 10-degree free decay for 'R-class' case 1.....46

Figure 5.8: 10-degree free decay for 'R-class' case 2.....46

Figure 5.9: 10-degree free decay for 'R-class' case 3.....47

Figure 5.10: 10-degree free decay for 'Series 60' case 1.....47

Figure 5.11: 10-degree free decay for 'Series 60' case 2.....47

Figure 5.12: 10-degree free decay for 'Series 60' case 3.....48

Figure 6.1: Compare the regular response of Case 511.....54

Figure 6.2: Variance ψ vs. Fm for "Series 60" GM=1.8cm.....60

Figure 6.3: Variance ψ vs. Fm for "Series 60" GM=1.62cm.....60

Figure 6.4: Variance ψ vs. Fm for "Series 60" GM=1.52cm.....60

Figure 6.5: Variance ψ vs. Fm for "R-class" GM=4.33cm.....61

Figure 6.6: Variance ψ vs. Fm for "R-class" GM=4.9cm.....61

Figure 6.7: Variance ψ vs. Fm for "R-class" GM=5.47cm.....61

Figure 6.8: Variance ψ vs. GM for "Series 60" Hs=7cm.....62

Figure 6.9: Variance ψ vs. GM for "Series 60" Hs=10cm.....62

Figure 6.10: Variance ψ vs. GM for "Series 60" Hs=13cm.....62

Figure 6.11: Variance ψ vs. GM for "R-class" Hs=7cm.....63

Figure 6.12: Variance ψ vs. GM for "R-class" Hs=10cm.....63

Figure 6.13: Variance ψ vs. GM for "R-class" Hs=13cm.....63

Figure 6.14: Variance ψ vs. Hs for "Series 60" fm=0.5Hz.....64

Figure 6.15: Variance ψ vs. Hs for "Series 60" fm=0.6Hz.....64

Figure 6.16: Variance ψ vs. Hs for "Series 60" fm=0.7Hz.....64

Figure 6.17: Variance ψ vs. Hs for "R-class" fm=0.5Hz.....65

Figure 6.18: Variance ψ vs. Hs for "R-class" fm=0.6Hz.....65

Figure 6.19: Variance ψ vs. Hs for "R-class" fm=0.7Hz.....65

Figure 6.20: Residual vs. Case Number Plot.....67

List of Tables

Table 4.1: Parameters Applied in the Simulations.....25

Table 4.2: Calculation for ωe and ζe of Case 511.....30

Table 5.1: Hydrostatic Particulars for "R-class Icebreaker" Model.....36

Table 5.2: Hydrostatic Particulars for "Series 60" Ship Model.....37

Table 5.3: Inclining Test Data of "R-class Icebreaker" Model.....43

Table 5.4: Inclining Test Data of "Series 60" Model.....44

Table 5.5: Natural Frequencies from Free Roll Tests.....46

Table 5.6: "Series 60" Data Files and Experimental Conditions.....49

Table 5.7: "R-class Icebreaker" Data Files and Experimental Conditions....50

Table 6.1: Comparison of the Regular Responses.....53

Table 6.2: Comparison of the estimated ψ and the true ψa 55

Table 6.3: "Series 60" Ship Model Experiment Results.....58

Table 6.4: "R-class" Ship Model Experiment Results 59

Table 6.5: MR including all Interaction Terms.....68

Table 6.6: MR including all Interaction Terms for Two Models.....69

Table 6.7: MR Results for Two Models.....69

Table 6.8: MR excluding GM Term for Two Models.....70

Table 6.9: MR Results including GM^2 and V_H Terms.....70

Table 6.10: R^2 Value for Different Function.....71

Chapter 1

Introduction

1.1 Objective

Wave force is one of the most important factors in determining the stability and safety of a ship at sea. Therefore, it is very helpful to study the characteristics of wave excitation on a ship sailing in a realistic sea. The excitation of waves is a random process, which may be described with the mean value, the variance, the correlation function and the spectral density function. The variance is the most common variable to describe the deviation of a signal away from its mean value. It is also a measure of the energy of the wave. The measured wave excitation data can be used to determine the variance of wave exciting rolling moment to a ship at sea. However, it is generally not possible to obtain time records of the wave excitation to a full-scale ship sailing at sea. However, it is easy to collect the rolling motion data when a ship is sailing in a realistic sea.

The main objective of this thesis is to develop a particular method for identification of the variance of wave exciting rolling moment from the ship rolling time history. Furthermore, the study of two ship model data showed the influence of the wave frequency, the wave height, and the GM value on the variance of the wave exciting rolling moment in irregular beam waves.

1.2 Research outline

Applying the Fokker-Plank equation to the nonlinear ship roll motion in random sea, differential equations that govern the propagation of the expected value and the variance of the nonlinear motion are obtained. For steady state, a formula is derived to identify the variance of wave exciting rolling moment from parameters of nonlinear rolling equation. Neural network technique was used to obtain a nonlinear function, G, from training the random decrement equation, which is calculated from the random roll response. The function, G, can be used to identify the parameters of nonlinear roll motion using regression technique. The identified rolling motion parameters are then used to estimate the variance of wave exciting rolling moment.

The proposed method is applied to experimental data as well as to simulated data. Model tests of "series 60" and "R-class Icebreaker" ship models are carried in the wave tank at MUN. From the simulated data, the validity of the method has been proved. From the experimental data, the effect of the wave frequency, the wave height, and the GM value has been checked using multiple regressions.

1.3 Organization

Chapter 2 presents a review of the literature. In Chapter 3, the theoretical basis of the proposed method is presented. In Chapter 4, the numerical simulation method is introduced step by step. In Chapter 5, the experimental program and the analysis of the experimental data are presented. In Chapter 6, the validity and accuracy of the proposed method are examined using the simulation method; also a discussion of the experimental results is presented. Finally, the conclusions and recommendations are presented in Chapter 7.

Chapter 2

Literature Review

2.1 Ship Rolling Motion in Random Waves

Any particular ship's motion time history can be represented by a combination of the time histories of three translations (surge, sway and heave) and three rotations (roll, pitch and yaw) about a right-handed orthogonal axis system. In these six displacements, rolling motion may be the most severe angular motion, often exceeding the "small angle" range of fifteen degree. By far, it is yet understood least, especially in irregular waves.

The shortcoming of the linear approach was widely recognized but further progress did not occur until St. Denis and Pierson (1953) first introduced the linear-random theory to the naval architecture field for the study of ship motions in irregular waves. The theory for the response of a linear system to random excitation was developed in the field of electromagnetic communications (Rice, 1944). St Denis and Pierson suggested that a ship could be treated as a "black box" filter, which amplified or attenuated different frequency components of the waves to produce ship motions as output. There are two crucial assumptions underlying the theory. First, the short-term ocean waves are stationary, zero-mean, Gaussian random process. Second, ship responses are linear transformations of the

wave elevation or slope. Based on these assumptions the probability structure and the statistical parameters of the wave elevation and the ship response are constant in the short term. In a stationary, zero-mean, Gaussian process, the only necessary statistical parameter to describe the process is its variance. Linear-random theory is intended for predicting the stationary statistics of the ship response. It is assumed that the filter is "linear" in the sense that the output signal amplitude (the ship motion) at any given frequency is linearly proportional to the input signal amplitude (the wave). However, this general rule failed to recognize the rolling motion in random waves because viscous roll damping is a nonlinear function of the roll velocity (Lloyd, 1998).

It is a typical method building a single-degree-of-freedom second-order nonlinear differential equation to simulate the rolling motion of a ship in random waves. The equation includes four parameters: the total moment of inertia, the damping moment, the hydrostatic restoring moment, and the random wave excitation moment. Usually, the equation is normalized with respect to the total moment of inertia. Then, only three quantities are required to be determined. In principle it is possible to deduce all the required parameters in a single degree of freedom ship roll model if a stochastic model of the excitation is assumed (Roberts et al., 1991). For a linear model, it is easy to estimate the linear roll natural frequency by spectral analysis method. And the linear damping coefficient may also be estimated by applying the random decrement method (Vandiver et al., 1982). For large amplitude motion, the estimation of rolling parameters is much more difficult because the effects of nonlinearities are significant.

Since Froude (1955) demonstrated that nonlinearities exist in the damping and the restoring moments, several forms have been presented in the literature to describe the

nonlinear term in the roll damping and restoring moment models. He suggested the linear plus quadratic velocity dependent roll damping moment, which has not been doubted about two decades as a classical form because of general supposition of the viscous damping proportional to the square of the roll velocity. In 1971, Haddara introduced the linear plus cubic velocity dependent roll damping moment to overcome some analytical difficulties arising from applying the quadratic form. Further, Haddara (1984) presented a linear dependence on the product of the roll angle and roll velocity and a quadratic dependence on the angle of roll. It seems that none of these models is obviously better in describing the roll damping as long as the model is used in the range of the experimental data applied to estimate the parameters in the model (Haddara 1984; Mathisen *et al.* 1977). The method of slowly varying parameters and a least squares technique were used to investigate various damping models to find an equation for the rate of decay curve as a function of the damping moment (Haddara 1984). This method was not suitable for large amplitude motion. Robert (1985) used a loss function to derive the parameters of the roll damping moment by means of a least squares method. It is suitable for nonlinear restoring moments, but failed to identify the angle-dependent components of the same order of magnitude as the velocity-dependent component because of using the averaging technique. Mathisen and Price (1984) used a perturbation method to identify the roll damping parameters and approximate the free rolling response of a vessel. It assumes that the nonlinear response is a small perturbation of the linear response that makes the method valid for small nonlinearities only. Haddara (1989) investigated a set of experimental data by the energy method to show the relationship between the damping

moment and rolling angle. The results explained why the linear plus cubic damping model in many cases was more effective than the quadratic model.

Roll damping is derived from four sources: wave making, eddy shedding, skin friction and the appendage forces. The wave making damping arises because the oscillating hull radiate energy in the form of waves that travel away from the ship. Hull forms with relatively sharp corners at the bilges and /or at the keel will shed eddies as ship roll, which absorbs energy. Skin friction forces on the surface of the rolling hull may be significant and appendages will generate drag and/or lift forces that provide contributions to the roll damping. In strip theory, only wave making damping, which is a small fraction of total damping in some cases, is considered. Other three sources are neglected because they result from the influence of viscosity. Wave making roll damping and the damping due to the appendage forces are directly proportional to the roll velocity at high forward speed. Viscous roll damping is nonlinear and is generally proportional to the square of the roll velocity. This is why roll damping is so difficult to be recognized in the numerical calculations and simulations. (Lloyd, 1998)

2.2 Random Decrement Technique

The random decrement technique has been used widely in the analysis of experimental vibration data in the aerospace since Cole (1971) developed it. Through the analysis of a specific case, Vandiver et al. (1982) established the mathematical basis for the random decrement technique for vibration signature analysis. The basic concept of the random decrement curve is based on the fact that a random response of a structure due to a random input is composed of two parts: 1) deterministic part, and 2) random part, which

is assumed to have a zero mean. By averaging enough samples of the same random response, the random part of the response will filter out, leaving the deterministic part of the response (Ibrahim, 1977). An equivalent definition of the random signature can be obtained using the concept of ensemble averages. For a linear, time-invariant system excited by a stationary Gaussian random process, the response will also be a stationary Gaussian random process. The random decrement signature of the system is only the product of the correlation function and the trigger level. Vandiver (1982) indicated that a free decay curve could be obtained using the concept of ensemble average only when the random process is ergodic. Accordingly, averages computed from a single time history are equivalent to averages computed across the ensemble of all potential time histories of the process. It means that the random decrement curve is simply the conditional expected value of the random process. In conditioning the expected value, members of the ensemble are excluded from the computation unless they possess the specified values for the initial conditions. The choice of too low a trigger level would grossly increase the error of the estimate if the noise were present. Vandiver believed that the random decrement signature of the output would exactly represent the transient decay of the system from a trigger level only when the input to the system is white noise. However, a lightly damped single degree of freedom system, excited by a band-limited force often yields results that are to a sufficient degree of accuracy equivalent to the response to white noise.

Haddara and Wu (1993) studied the validity of the random decrement technique for the ship rolling identification, which involved a lightly damped system under the band-limited excitations. The technique was further tested by Haddara *et al.* (1994) using

model experiments and full-scale data. Haddara and Zhang (1994) extended the technique to the case of a narrow band excitation. The general conclusion from these studies indicates that a random decrement curve can be extracted to identify the ship roll parameters. However, Haddara *et al* (1994) found a common problem that the damping moments parameters did not always produce unique values especially when the number of parameters to be identified is large.

2.3 Neural Networks Technique

A new identification technique, which is a combination of the neural networks technique (Haddara, 1995) and the random decrement technique (Haddara, 1992), has been developed to estimate the roll damping parameters from the stationary roll response in random waves (Haddara, 2000). Neural networks technique is inspired by the human brain functions to learn some rules through an off-line or on-line training process. A network consists of several layers of neurons. The input feeds into each of the first layer neurons, the outputs of this layer feed into each of the second layer neurons, and so on (Hush *et al.* 1993). The neural networks technique provides a method to model complex systems without a priori knowledge of the physical mechanisms. In the past decade, neural networks have become a very popular choice as a universal "black box" model for nonlinear systems (Ljung, 1999).

Individual neuron is the basic computing unit in the network structure. Static networks are characterized by the memoryless neuron functions, thus the output is a function only of the current inputs. Dynamic networks, on the other hand, are systems with memory. Their neural functions are typically described by differential equations. In the multiplayer

perception network, which is the most widely used static network till now, individual neurons are arranged in successive layers with the sigmoid nonlinearity as neuron equation. Each layer is fully connected to the adjacent layers and information is passed only forward from the input layer through the hidden layers to the output layer. Linear neurons are commonly used in the output layer to make learning easier. The connecting weights between the layers are the adjustable parameters that fully determine the relationship between the inputs and the outputs. During the supervised learning process, the neural network is presented with a set of input-output points and trained to implement a mapping that matches the sample points as closely as possible. The most popular learning method for multiplayer perception network is the backpropagation algorithm, which uses a gradient technique to find the optimum values for the connecting weights. It is an iterative process of computing the gradient and adjusting the weight values until a minimum error is located or a maximum iteration times is reached. A "black box" model is selected finally through the training process.

In the marine field, Haddara (1995) found an approach combining the neural network technique with the free roll decay curves to identify the ship stability parameters. Further applications are developed by Haddara & Hinchey (1995) to free roll decay curves and Haddara (2000) to the stationary random roll response for identification of the damping parameters. The results showed that the neural network technique is robust and produces unique results for the damping moment.

2.4 Review Summary

An extensive review of the literature indicates that ship roll motion is a complicated phenomenon because the roll damping is difficult to estimate or calculate in irregular

waves. Until now, the method, which combines the neural networks technique and the random decrement technique, is the best choice to estimate the ship roll parameters in random waves. The reason lies in the similarity of the neural networks and ship as a "black box" model of nonlinear system. Another reason is that the method only uses rolling time history and therefore can be applied at sea.

Chapter 3

Mathematical Analysis

This chapter presents the mathematical basis for a new method to estimate the variance of the wave exciting rolling moment per unit virtual mass moment of inertia for a ship in a random sea. Using the Fokker-Plank equation of the nonlinear ship motion in random waves, the differential equations of the mean value and the variance of the motion are derived (Haddara, 1974). For the steady state, a formula is derived to calculate the variance of the wave exciting rolling moment per unit virtual mass moment of inertia of a ship in random waves.

3.1 Rolling Equation in Random Waves

The rolling motion of a ship in random waves is governed, at least approximately, by the following nonlinear, single degree of freedom equation of motion (Roberts, 1982):

$$I\ddot{\phi} + B(\dot{\phi}) + C(\phi) = M(t) \qquad (3.1)$$

where ϕ denotes roll displacement of the ship; I is the total virtual moment of inertia (including added fluid inertia) along a longitudinal axis, passing through the center of gravity of the ship; B is the moment of the damping forces; C is the hydrostatic restoring

moment and M is the wave excitation moment. A dot over the variable ϕ indicates differentiation with respect to time.

A more convenient form of the equation (3.1) is obtained by dividing throughout by I (Haddara, 1992).

$$\ddot{\phi} + N(\dot{\phi}) + D(\phi) = K(t) \qquad (3.2)$$

where $K=M/I$, is the wave exciting moment per unit virtual moment of inertia. $D=C/I$, is the nonlinear restoring moments per unit virtual moment of inertia; $N=B/I$, is the nonlinear damping moments per unit virtual moment of inertia;

The excitation $K(t)$, should be stationary random Gaussian process and satisfies the following equations.

$$\begin{aligned} &< K(t) >= 0 \\ &< K(t_1)K(t_2) >= \psi\delta(t_1 - t_2) \end{aligned} \qquad (3.3)$$

where < > means the ensemble average of the process; δ is the Dirac delta function; ψ is the variance of the wave exciting moment per unit virtual moment of inertia of a ship. Furthermore, the excitation is assumed to be Gaussian. These assumptions, while simplify the analysis greatly, do not limit the applicability of the results obtained. The highly resonant nature of rolling justifies this.

Using the change of variables, $y_1 = \phi$ and $y_2 = \dot{\phi}$, one can rewrite equation (3.2) as:

$$\begin{aligned} \dot{y}_1 &= y_2 \\ \dot{y}_2 &= K(t) - N(y_2) - D(y_1) \end{aligned} \qquad (3.4)$$

The matrix form of the equation (3.4) is

$$\dot{Y} = F(Y, t) + E(t) \qquad (3.5)$$

where

$$Y = \begin{bmatrix} y_1 \\ y_2 \end{bmatrix}, F = \begin{bmatrix} y_2 \\ -N(y_2) - D(y_1) \end{bmatrix}, E = \begin{bmatrix} 0 \\ K(t) \end{bmatrix}$$

3.2 Fokker-Plank Equation

A stochastic process *Y(t)*, is called Markov process if the conditional probability that Y lies in the interval $(y_n, y_n + dy_n)$ at time t_n, given that Y is equal to y_1 at time t_1, y_2 at time $t_2, \ldots,$ and y_{n-1} at time t_{n-1}, depends only the values of Y at time t_{n-1} (Haddara,1974). Thus, for a Markov process, one has

$$P_n(y_1 t_1, y_2 t_2, \ldots, y_{n-1} t_{n-1} | y_n t_n) = P_2(y_{n-1} t_{n-1} | y_n t_n) \qquad (3.6)$$

where $P_2(y_1 t_1 | y_2 t_2) dy_2$ is the probability that Y will lie in the interval $(y_2 + dy_2)$ at time t_2 given that $Y = y_1$ at time t_1. Then the conditional probability density function P_2 describes a Markov process completely.

A Markov process may also be associated with a first-order differential equation of the form of equation (3.5). Then the two-dimensional stochastic process (y_1, y_2) of equation (3.4) is Markov. The process may be described by conditional probability density function $P_2(y_{10} y_{20} | y_1, y_2, t)$ where y_{10} and y_{20} are the initial values of the angle and velocity of rolling motion.

It can be easily shown that the conditional probability density function that describes the Markov process (y_1, y_2) satisfies the following partial differential equation (Caughey, 1963):

$$\frac{\partial P}{\partial t} = -\sum_{i=1}^{2} \frac{\partial}{\partial y_i}(a_i P) + \frac{1}{2}\sum_{i,j=1}^{2} \frac{\partial^2}{\partial y_i \partial y_j}(b_{ij} P) \qquad (3.7)$$

where

$$a_i = \lim_{\Delta t \to 0} \frac{<\Delta y_i>}{\Delta t}, \qquad b_{ij} = \lim_{\Delta t \to 0} \frac{<\Delta y_i \Delta y_j>}{\Delta t}$$

Haddara (1974) evaluated the averages of a and b as following:

$$a_1 = \lim_{\Delta t \to 0} \frac{<\Delta y_1>}{\Delta t} = y_2$$

$$a_2 = \lim_{\Delta t \to 0} \frac{<\Delta y_2>}{\Delta t} = \lim_{\Delta t \to 0} \frac{<-(N+D)\Delta t + \int_t^{t+dt} K(u)du>}{\Delta t} = -<N+D>$$

$$b_{11} = \lim_{\Delta t \to 0} \frac{<\Delta y_1 \Delta y_1>}{\Delta t} = 0$$

$$b_{22} = \lim_{\Delta t \to 0} \frac{<\Delta y_2 \Delta y_2>}{\Delta t} = \lim_{\Delta t \to 0} \frac{<\{-(N+D)\Delta t + \int_t^{t+dt} K(u)du\}^2>}{\Delta t} = Var(K(t)) = \psi$$

$$b_{12} = \lim_{\Delta t \to 0} \frac{<\Delta y_1 \Delta y_2>}{\Delta t} = 0$$

Substituting the above results of a and b into equation (3.7), one can obtain the following partial differential equation:

$$\frac{\partial P}{\partial t} = -\frac{\partial}{\partial y_1}(y_2 P) + \frac{\partial}{\partial y_2}(N + D)P + \frac{\psi}{2}\frac{\partial^2 P}{\partial y_2^2} \qquad (3.8)$$

where the short hand notation P is used to replace $P_2(y_{10} y_{20} | y_1, y_2, t)$. The solution of equation (3.8) subject to the initial condition $P(y_{10} y_{20} | y_1, y_2, t) = \delta(t_1 - t_{10})\delta(t_2 - t_{20})$ as $t \to 0$, yields the conditional probability density function which describes the process (y_1, y_2) completely.

It is difficult to solve equation (3.8) directly except in some special cases. One can convert this equation into a stochastic differential equation.

$$dP(y_{10}, y_{20} | y_1, y_2, t) = P(y_{10}, y_{20} | y_1, y_2, t + dt) - P(y_{10}, y_{20}, t)$$

$$= [-\frac{\partial}{\partial y_1}(y_2 P) + \frac{\partial}{\partial y_2}\{(N + D)P\} + \frac{\psi}{2}\frac{\partial^2 P}{\partial y_2^2}]dt \qquad (3.9)$$

Equation (3.9) can be used to derive the differential equations that govern the propagation of the mean values and variances of y_1 and y_2.

3.3 mean values propagation

Before integrating the equation (3.9), we assume the following boundary conditions:

$$y_1 y_2 P \Big|_{y_1=-\infty}^{y_1=\infty} = (N + D)P \Big|_{y_2=-\infty}^{y_2=\infty} = \frac{\partial P}{\partial y_2}\Big|_{y_2=-\infty}^{y_2=\infty} = 0 \qquad (3.10)$$

$$P \Big|_{y_i=-\infty}^{y_i=\infty} = y_i (N + D) P \Big|_{y_i=-\infty}^{y_i=\infty} = 0 \ , \quad i = 1, 2 \qquad (3.11)$$

Multiplying equation (3.9) by y_1 and integrating the equation with respect to y_1 and y_2 from $-\infty$ to ∞, we have the left hand side of the equation as

$$\int_{-\infty}^{\infty}\int_{-\infty}^{\infty} y_1[P(y_{10}, y_{20}|y_1, y_2, t+dt) - P(y_{10}, y_{20}, t)]dy_1 dy_2$$
$$= \mu_1(t+dt) - \mu_1(t) \tag{3.12}$$

and the right hand side

$$dt\int_{-\infty}^{\infty}\int_{-\infty}^{\infty} y_1[-\frac{\partial}{\partial y_1}(y_2 P) + \frac{\partial}{\partial y_2}(N+D)P + \frac{\psi}{2}\frac{\partial^2 P}{\partial y_2^2}]dy_1 dy_2$$
$$= dt\{\mu_2 - \int_{-\infty}^{\infty}(y_1 y_2 P\Big|_{y_1=-\infty}^{y_1=\infty})dy_2 + \int_{-\infty}^{\infty} y_1[(N+D)P\Big|_{y_2=-\infty}^{y_2=\infty}]dy_1 + \frac{\psi}{2}\int_{-\infty}^{\infty} y_1(\frac{\partial P}{\partial y_2}\Big|_{y_2=-\infty}^{y_2=\infty})dy_1\}$$
$$= dt\mu_2 \tag{3.13}$$

Then equations (3.12) and (3.13) are divided by dt, to obtain

$$\dot{\mu}_1 = \mu_2 \tag{3.14}$$

where μ_1 and μ_2 are the mean values of y_1 and y_2 respectively.

Using same process, we multiply the two sides of equation (3.9) by y_2 and integrate the equation with respect to y_1 and y_2 from $-\infty$ to ∞, to get

$$\int_{-\infty}^{\infty}\int_{-\infty}^{\infty} y_2[P(y_{10}, y_{20}|y_1, y_2, t+dt) - P(y_{10}, y_{20}, t)]dy_1 dy_2$$
$$= \mu_2(t+dt) - \mu_2(t) \tag{3.15}$$

$$dt\int_{-\infty}^{\infty}\int_{-\infty}^{\infty} y_2[-\frac{\partial}{\partial y_1}(y_2 P) + \frac{\partial}{\partial y_2}(N+D)P + \frac{\psi}{2}\frac{\partial^2 P}{\partial y_2^2}]dy_1 dy_2$$
$$= dt\{-\int_{-\infty}^{\infty} y_2(y_2 P\Big|_{y_1=-\infty}^{y_1=\infty})dy_2 + \int_{-\infty}^{\infty} y_2[(N+D)P\Big|_{y_2=-\infty}^{y_2=\infty}]dy_1 - \int\int_{-\infty}^{\infty}(N+D)P dy_1 dy_2$$
$$+\frac{\psi}{2}\int_{-\infty}^{\infty} y_2(\frac{\partial P}{\partial y_2}\Big|_{y_2=-\infty}^{y_2=\infty})dy_1 - \frac{\psi}{2}\int_{-\infty}^{\infty} P\Big|_{y_2=-\infty}^{y_2=\infty} dy_1\}$$
$$= dt < -N - D > \tag{3.16}$$

Then equations (3.15) and (3.16) are divided by dt, to obtain

$$\dot{\mu}_2 = -< N(y_2) + D(y_1) > \tag{3.17}$$

Expanding equation (3.17) in its Taylor series about μ_1 and μ_2, and retaining the first-order terms only, we have

$$\dot{\mu}_2 = -< N(\mu_2) + D(\mu_1) + (y_1 - \mu_1)\frac{\partial}{\partial y_1}(N + D) + (y_2 - \mu_2)\frac{\partial}{\partial y_2}(N + D) >$$

$$= -N(\mu_2) - D(\mu_1) \tag{3.18}$$

Substituting equation (3.14) into equation (3.18), we obtain

$$\ddot{\mu}_1 + N(\dot{\mu}_1) + D(\mu_1) = 0 \tag{3.19}$$

From this equation, we can see that the mean value of the random roll motion satisfies a first order approximation to the differential equation of its free roll motion. Based on this principle, we apply the random decrement technique to the nonlinear roll motion of a ship in irregular waves.

3.4 Variance propagation

Using the same boundary conditions in equation (3.10) and (3.11), we multiply the two sides of equation (3.9) by y_1^2/dt and integrate the equation with respect to y_1 and y_2 from $-\infty$ to ∞. The different result of the integration are given as:

$$\int\int_{-\infty}^{\infty} y_1^2 \frac{\partial P(y_{10}, y_{20} | y_1, y_2, t)}{\partial t} dy_1 dy_2 = \dot{V}_{11} \tag{3.20}$$

$$-\int\int_{-\infty}^{\infty} y_1^2 \frac{\partial}{\partial y_1}(y_2 P)dy_1 dy_2 = -\int_{-\infty}^{\infty} y_1^2 (y_2 P\Big|_{y_1=-\infty}^{y_1=\infty})dy_2 + 2\int\int_{-\infty}^{\infty} y_1 y_2 P dy_1 y_2$$

$$= 2V_{12} \qquad (3.21)$$

$$\int\int_{-\infty}^{\infty} y_1^2 \frac{\partial}{\partial y_2}[(N+D)P]dy_1 dy_2 = \int_{-\infty}^{\infty} y_1^2 [(N+D)P\Big|_{y_2=-\infty}^{y_2=\infty}]dy_1 = 0$$

(3.22)

$$\frac{\psi}{2}\int\int_{-\infty}^{\infty} y_1^2 \frac{\partial^2 P}{\partial y_2^2}dy_1 dy_2 = \frac{\psi}{2}\int_{-\infty}^{\infty} y_1^2 (\frac{\partial P}{\partial y_2}\Big|_{y_2=-\infty}^{y_2=\infty})dy_1 = 0 \qquad (3.23)$$

Then, from equations (3.20) to (3.23), we have

$$\dot{V}_{11} = 2V_{12} \qquad (3.24)$$

Multiplying the two sides of equation (3.9) by y_2^2/dt and integrating the equation with respect to y_1 and y_2 from $-\infty$ to ∞, we have:

$$\int\int_{-\infty}^{\infty} y_2^2 \frac{\partial P(y_{10}, y_{20}|y_1, y_2, t)}{\partial t}dy_1 dy_2 = \dot{V}_{22} \qquad (3.25)$$

$$-\int\int_{-\infty}^{\infty} y_2^2 \frac{\partial}{\partial y_1}(y_2 P)dy_1 dy_2 = -\int_{-\infty}^{\infty} y_2^2 (y_2 P\Big|_{y_1=-\infty}^{y_1=\infty})dy_2 = 0 \qquad (3.26)$$

$$\int\int_{-\infty}^{\infty} y_2^2 \frac{\partial}{\partial y_2}[(N+D)P]dy_1dy_2 = \int_{-\infty}^{\infty} y_2^2(N+D)P\Big|_{y_2=-\infty}^{y_2=\infty} dy_1 - 2\int_{-\infty}^{\infty} y_2(N+D)Pdy_2$$
$$= -2 < y_2(N+D) > \qquad (3.27)$$

$$\frac{\psi}{2}\int\int_{-\infty}^{\infty} y_2^2 \frac{\partial^2 P}{\partial y_2} dy_1 dy_2 = \frac{\psi}{2}[\int_{-\infty}^{\infty} y_2^2(\frac{\partial P}{\partial y}\Big|_{y_2=-\infty}^{y_2=\infty})dy_1 - \int\int_{-\infty}^{\infty} y_2 \frac{\partial P}{\partial y_2} dy_1 dy_2]$$
$$= -\frac{\psi}{2}[\int_{-\infty}^{\infty} y_2 P\Big|_{y_2=-\infty}^{y_2=\infty} dy_1 - 2\int\int_{-\infty}^{\infty} Pdy_1dy_2] \qquad (3.28)$$
$$= \psi$$

Then, from equation (3.25) to (3.28), we have

$$\dot{V}_{22} = -2 < y_2(N+D) > +\psi \qquad (3.29)$$

Multiplying the two sides of equation (3.9) by $y_1 y_2/dt$ and integrating the equation with respect to y_1 and y_2 from $-\infty$ to ∞, we have:

$$\int\int_{-\infty}^{\infty} y_1 y_2 \frac{\partial P(y_{10}, y_{20}|y_1, y_2, t)}{\partial t} dy_1 dy_2 = \dot{V}_{12} \qquad (3.30)$$

$$-\int\int_{-\infty}^{\infty} y_1 y_2 \frac{\partial}{\partial y_1}(y_2 P)dy_1 dy_2 = -\int_{-\infty}^{\infty} y_1 y_2 (y_2 P\Big|_{y_1=-\infty}^{y_1=\infty})dy_2 + \int\int_{-\infty}^{\infty} y_2^2 P dy_1 y_2$$
$$= V_{22} \qquad (3.31)$$

$$\int\int_{-\infty}^{\infty} y_1 y_2 \frac{\partial}{\partial y_2}[(N+D)P]dy_1dy_2 = \int_{-\infty}^{\infty} y_1 y_2[(N+D)P\Big|_{y_2=-\infty}^{y_2=\infty}]dy_1 - \int_{-\infty}^{\infty} y_1(N+D)Pdy_2$$
$$= - < y_1(N+D) > \qquad (3.32)$$

$$\frac{\psi}{2}\int\int_{-\infty}^{\infty} y_1 y_2 \frac{\partial^2 P}{\partial y_2^2} dy_1 dy_2 = \frac{\psi}{2}[\int_{-\infty}^{\infty} y_1 y_2 (\frac{\partial P}{\partial y_2}\Big|_{y_2=-\infty}^{y_2=\infty}) dy_1 - \int\int_{-\infty}^{\infty} y_1 \frac{\partial P}{\partial y_2} dy_1 dy_2]$$

$$= -\frac{\psi}{2}\int_{-\infty}^{\infty} y_1 P\Big|_{y_2=-\infty}^{y_2=\infty} dy_1 = 0 \qquad (3.33)$$

Then, from equation (3.30) to (3.33), we have

$$\dot{V}_{12} = V_{22} - < y_1 (N + D) > \qquad (3.34)$$

where V_{11} , V_{22} , and V_{12} are the variance and covariance of y_1 and y_2 respectively.

3.5 Damping and Restoring Moment Model

A mixed linear-plus-cubic model is used to describe both the damping and the restoring moment. This has been shown to be reasonable both qualitatively and quantitatively (Haddara, 1980). Thus the damping and restoring moments are expressed as

$$\begin{aligned} N(\dot{\phi}) &= 2\zeta\omega_n(\dot{\phi} + \varepsilon_1 \dot{\phi}^3) \\ D(\phi) &= \omega_n^2(\phi + \varepsilon_2 \phi^3) \end{aligned} \qquad (3.35)$$

where ζ and ε_1 are the nondimensional linear and nonlinear damping coefficients respectively. ω_n is the natural frequency. ε_2 is the nondimensional nonlinear restoring moment coefficient.

Substituting equation (3.35) into the ensemble averages on the right hand side of the equation (3.29) and (3.34), we have

$$< y_1(N + D) >= 2\zeta\omega_n < y_1 y_2 + \varepsilon_1 y_1 y_2^3 > + \omega_n^2 < y_1^2 + \varepsilon_2 y_1^4 >$$

$$= 2\zeta\omega_n V_{12}(1 + \varepsilon_1 V_{22}) + \omega_n^2 (V_{11} + 3\varepsilon_2 V_{11}^2) \qquad (3.36)$$

$$< y_2(N + D) >= 2\zeta\omega_n < y_2^2 + \varepsilon_1 y_2^4 > + \omega_n^2 < y_1 y_2 + \varepsilon_2 y_1^3 y_2 >$$

$$= 2\zeta\omega_n(V_{22} + 3\varepsilon_1 V_{22}^2) + \omega_n^2 V_{12}(1 + \varepsilon_2 V_{11}) \qquad (3.37)$$

For steady state, one has

$$\dot{V}_{11} = \dot{V}_{22} = \dot{V}_{12} = 0 \qquad (3.38)$$

From equation (3.24), we obtain

$$V_{12} = 0 \qquad (3.39)$$

Then equation (3.36) change into

$$< y_1(N + D) >= \omega_n^2(V_{11} + 3\varepsilon_2 V_{11}^2) \qquad (3.40)$$

$$< y_2(N + D) >= 2\zeta\omega_n(V_{22} + 3\varepsilon_1 V_{22}^2) \qquad (3.41)$$

Finally, substituting equations (3.38), (3.40) and (3.41) into equations (3.29) and (3.34), we get

$$V_{22} = \omega_n^2(V_{11} + 3\varepsilon_2 V_{11}^2) \qquad (3.42)$$

$$\psi = 4\zeta\omega_n(V_{22} + 3\varepsilon_1 V_{22}^2) \qquad (3.43)$$

The equation (3.43) shows that the variance ψ of the wave excitation would be identified as long as ship roll parameters can be estimated in random waves. In the following research, we will verify this method using ship roll response data obtained from numerical simulation and ship model test in random beam waves.

Chapter 4

Numerical Simulation Method

Numerical simulation with the variable parameters in the mathematical model is a convenient way to test the validity and accuracy of the method proposed in the last chapter to identify the variance of the wave excitation to a ship. In this research, the random decrement and neural network technique is used to identify the ship roll parameters in random waves.

4.1 Simulation of the Random Roll Response

Using the damping and restoring moment model in equation (3.35), the rolling motion of a ship in random beam waves can be simulated using the following second-order nonlinear ordinary stochastic differential equation.

$$\ddot{\phi} + 2\zeta\omega_n[\dot{\phi} + \varepsilon_1 \dot{\phi}^3] + \omega_n^2[\phi + \varepsilon_2\phi^3] = k(t) \qquad (4.1)$$

k(t) is the random wave excitation per unit virtual mass moment of inertia. Based on Borgman (1969), the expression of *k(t)* is written as follows:

$$k(t) = \sum_{k=0}^{n} A_k \sin(\omega_k t + \theta_k) \qquad (4.2)$$

This equation shows that superposing a number of sinusoidal functions with the same amplitude A_k, varying frequencies ω_k and random phase angles θ_k simulates the random wave excitation.

$$\omega_k = \omega_1 + \frac{k}{n}(\omega_2 - \omega_1) \qquad k = 0,1,2,\cdots,n$$

$$\theta_k = 2\pi\gamma \qquad 0 \le \gamma \le 1 \tag{4.3}$$

ω_1 and ω_2 define a band-limited white noise. γ is a uniform random number chosen such that the phase angle θ_k varies between 0 and 2π.

Figure 4.1: Simulated Roll Angle History of case 511

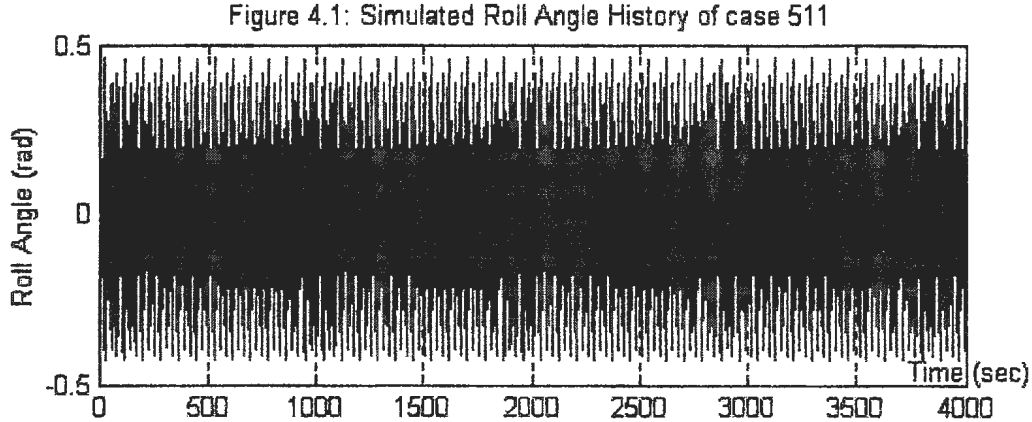

Figure 4.2: Special 20 Seconds Roll Angle History of case 511

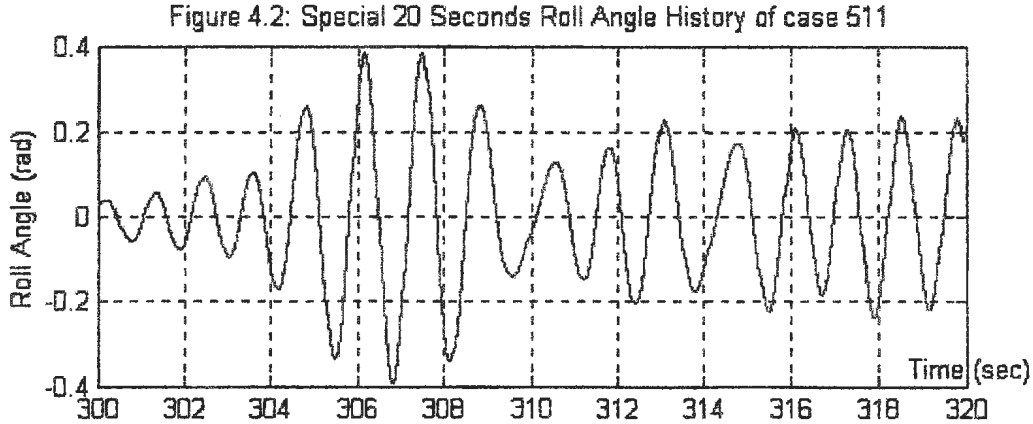

Random rolling records were generated using MATLAB function "ode45"(see Appendix B Simulation Programs). One example of the simulated roll motion records is shown in Figure 4.1; and the selected roll angle curve from 300 second to 320 second has been expanded in Figure 4.2. Total of 31 cases are designed to verify the proposed method. Table 4.1 shows all the parameters used to simulate the rolling motion. Time is the sample record length (4000 seconds) and Δt is the time interval (0.05 second) to be used in the integration.

Table 4.1 Parameters applied in the simulations

Case	ω_n rad/sec	ζ	ε_1	ε_2	ω_1 rad/sec	ω_2 rad/sec	$\Delta\omega$ rad/sec	A_k Meter	Time Second	Δt Second
511	5	0.06	0.01	0.01	3	6	0.075	0.2	4000	0.05
513	5	0.06	0.01	0.03	3	6	0.075	0.2	4000	0.05
515	5	0.06	0.01	0.05	3	6	0.075	0.2	4000	0.05
531	5	0.06	0.03	0.01	3	6	0.075	0.2	4000	0.05
533	5	0.06	0.03	0.03	3	6	0.075	0.2	4000	0.05
535	5	0.06	0.03	0.05	3	6	0.075	0.2	4000	0.05
551	5	0.06	0.05	0.01	3	6	0.075	0.2	4000	0.05
553	5	0.06	0.05	0.03	3	6	0.075	0.2	4000	0.05
555	5	0.06	0.05	0.05	3	6	0.075	0.2	4000	0.05
51010	5	0.06	0.1	0.1	3	6	0.075	0.2	4000	0.05
611	3	0.06	0.01	0.01	1.5	4.5	0.075	0.08	4000	0.05
613	3	0.06	0.01	0.03	1.5	4.5	0.075	0.08	4000	0.05
615	3	0.06	0.01	0.05	1.5	4.5	0.075	0.08	4000	0.05
631	3	0.06	0.03	0.01	1.5	4.5	0.075	0.08	4000	0.05
633	3	0.06	0.03	0.03	1.5	4.5	0.075	0.08	4000	0.05
635	3	0.06	0.03	0..05	1.5	4.5	0.075	0.08	4000	0.05
651	3	0.06	0.05	0.01	1.5	4.5	0.075	0.08	4000	0.05
653	3	0.06	0.05	0.03	1.5	4.5	0.075	0.08	4000	0.05
655	3	0.06	0.05	0.05	1.5	4.5	0.075	0.08	4000	0.05
61010	3	0.06	0.1	0.1	1.5	4.5	0.075	0.08	4000	0.05
61050	3	0.06	0.1	0.5	1.5	4.5	0.075	0.08	4000	0.05
63050	3	0.06	0.3	0.5	1.5	4.5	0.075	0.08	4000	0.05
411	3	0.04	0.1	0.1	1.5	4.5	0.075	0.08	4000	0.05
413	3	0.04	0.1	0.3	1.5	4.5	0.075	0.08	4000	0.05
415	3	0.04	0.1	0.5	1.5	4.5	0.075	0.08	4000	0.05
431	3	0.04	0.3	0.1	1.5	4.5	0.075	0.08	4000	0.05
433	3	0.04	0.3	0.3	1.5	4.5	0.075	0.08	4000	0.05
435	3	0.04	0.3	0.5	1.5	4.5	0.075	0.08	4000	0.05
451	3	0.04	0.5	0.1	1.5	4.5	0.075	0.08	4000	0.05
453	3	0.04	0.5	0.3	1.5	4.5	0.075	0.08	4000	0.05
455	3	0.04	0.5	0.5	1.5	4.5	0.075	0.08	4000	0.05

4. 2 Random Decrement Signature.

A random decrement curve is simply the trace formed by a waveform averaging a number of specially selected segments from an observed time history. Each of the segments shares the common attribute of known initial condition for the angle, but different initial slope (Vandiver et al, 1982). In this research, the rolling motion data from the simulation were processed to obtain the roll random decrement signature. A rolling motion record is divided into N equal length τ segments with same trigger value ϕ_t, and then these segments are ensemble averaged to get the conditional expected value.

$$\mu(\tau) = \frac{1}{N}\sum_{i=1}^{N} \phi_i(t_i + \tau) \qquad (4.4)$$

A MATLAB program was written to obtain the random decrement curves consisted of three steps: 1) interpolating trigger value ϕ_t to find start time t_i of each segment; 2) drawing out each segment from each start time t_i to time length τ; 3) calculating the ensemble average value μ of all segments in a rolling motion record.

In this research, the trigger values were chosen 0.16 or 0.2 radians with the purpose of finding enough large number of segments (at least 100). Time length τ is 4 or 7 seconds. There were 80 or 140 data points in every random decrement signature with the time interval of 0.05 second. One example of the results has been shown in Figure 4.3. μ is the roll angle random decrement curve.

Figure 4.3: The Random Decrement Curve of case 511

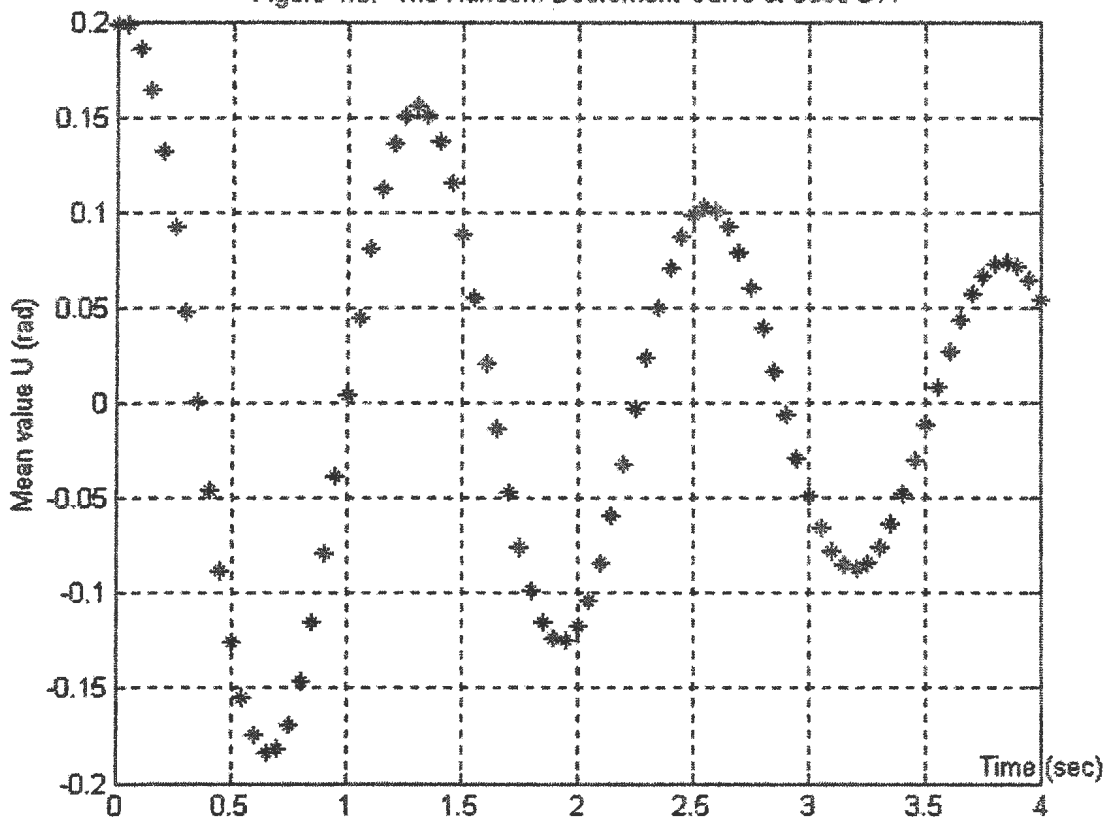

4. 3 Estimation of the Parameters Using Neural Networks.

The Neural Networks technique is inspired by the human brain functions to learn some rules from the training process. In practical, training a neural network is the process of adjusting the values of the weights between input and output data.

Using equations (3.19) and (3.35), it can be shown that the expected value μ of the random roll motion approximately satisfies the following differential equation.

$$\ddot{\mu} + 2\zeta\omega_n[\dot{\mu} + \varepsilon_1 \dot{\mu}^3] + \omega_n^2[\mu + \varepsilon_2\mu^3] = 0 \qquad (4.5)$$

Equation (4.5) is replaced by an equivalent linear equation given by,

$$\ddot{\mu} + 2\zeta_e\omega_e \dot{\mu} + \omega_e^2\mu = 0 \qquad (4.6)$$

where ω_e is the equivalent linear natural frequency, ζ_e is the equivalent linear damping coefficient.

In order to apply the neural networks, we define a new function, G,

$$G(\mu, \dot{\mu}) = (\omega_e^2 - \omega_d^2)\mu + 2\zeta_e \omega_e \dot{\mu} \qquad (4.7)$$

The random decrement equation can be written as follows:

$$\ddot{\mu} + \omega_d^2 \mu + G(\mu, \dot{\mu}) = 0 \qquad (4.8)$$

Then ω_d can be easily obtained from the random decrement curve. The function G was identified using a neural network method shown in Figure 4.4.

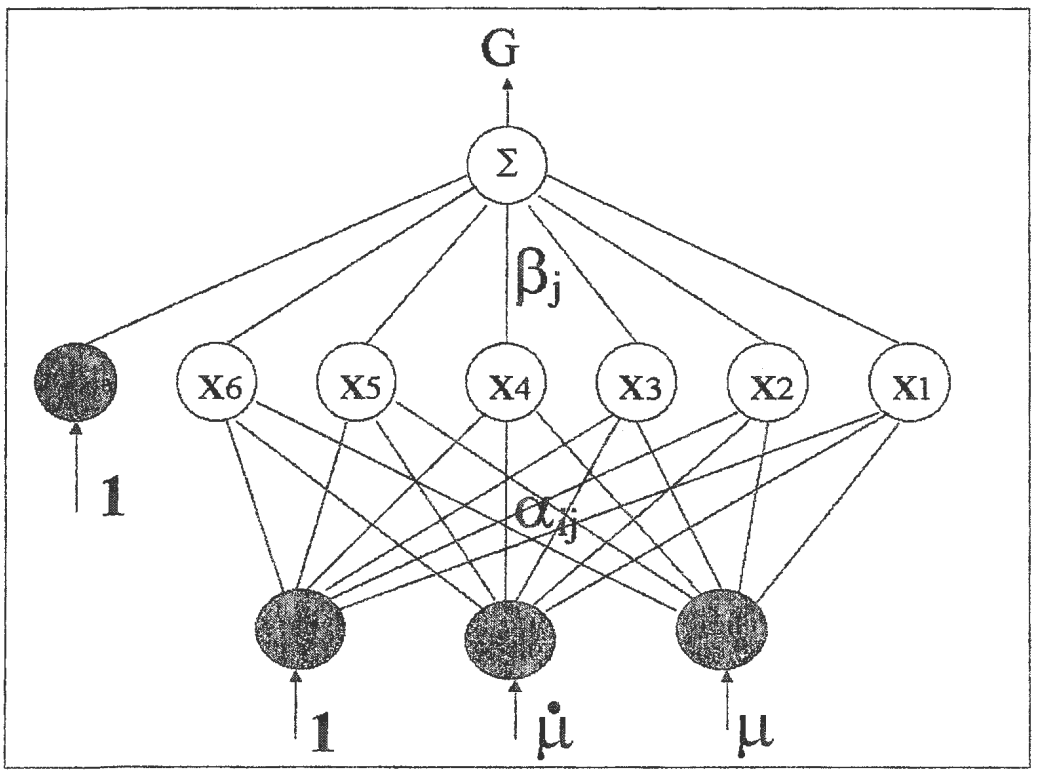

Figure 4.4: Neural Network

The αij and βj are called the synaptic weights. The inputs are a bias, 1, and the mean values of roll angle and roll velocity, which can be obtained from the random decrement curve. G is the output. The relationship between the input vector and hidden layer input is given as:

$$x_j = \alpha_{1j} + \alpha_{2j}\dot{\mu} + \alpha_{3j}\mu \qquad (4.9)$$

The sum x_j is then passed through an activation function $z_j(x_j)$. The hyperbolic tangent function is used for the activation function.

$$Z_j(x_j) = \frac{1 - e^{-x_j}}{1 + e^{-x_j}} \qquad (4.10)$$

The network output is calculated as:

$$G(\mu, \dot{\mu}) = \sum_{j=1}^{n} (\beta_j Z_j) \qquad (4.11)$$

The purpose is to find the value of G, which could be substituted into equation (4.8), and get the equal values for $\dot{\mu}$ and μ as those obtained from the random decrement curve. The process of training the neural network to get G includes three steps. First, a random set of weights was introduced into the neural network to obtain a value of G. Second, using the obtained value for G integrates equation (4.8) is integrated to obtain data for μ. Third, a steepest descent technique is applied to adjust the weights α_{ij} and β_j to minimize the square error between the integrated μ and the measured μ. A Fortran program (see Appendix B) for neural networks was written by Dr. M.R.Haddara (see Haddara 1995) to determine G.

Substituting $\omega_d = \omega_e \sqrt{1-\zeta_e^2}$ into equation (4.7) and letting $h = \omega_e \zeta_e$, one can easily obtain the following equation.

$$\mu h^2 + 2\dot{\mu} h - G = 0 \qquad (4.12)$$

Using the input and output data (μ, $\dot{\mu}$ and G) of the neural network, solving equation (4.12), one can obtain the values for h. Then, the equivalent natural frequency and the equivalent damping coefficient can be identified by the following equations.

$$\omega_e = \sqrt{\omega_d^2 + h^2} \quad , \qquad \zeta_e = h / \omega_e \qquad (4.13)$$

Table 4.2 shows one example of the calculation process for ω_e and ζ_e in Microsoft Excel.

Table 4.2: Calculation for ω_e and ζ_e of case 511

time	μ	dμ	G	h	ω_e	ζ_e	ω_d
0.00	0.1980	0.1180	0.2941	-1.9525			4.8332
0.05	0.1980	-0.1150	0.1808	-0.5374			
0.10	0.1860	-0.3430	0.0607	-0.0865			
0.15	0.1640	-0.5500	-0.0585	0.0536	4.8335	0.0111	
0.20	0.1320	-0.7240	-0.1696	0.1184	4.8347	0.0245	
0.25	0.0924	-0.8550	-0.2656	0.1566	4.8358	0.0324	
0.30	0.0475	-0.9340	-0.3408	0.1833	4.8367	0.0379	
0.35	-0.0001	-0.9570	-0.3911	0.2043	4.8375	0.0422	
0.40	-0.0473	-0.9230	-0.4137	0.2228	4.8384	0.0461	
0.45	-0.0915	-0.8340	-0.4079	0.2414	4.8392	0.0499	
0.50	-0.1300	-0.6940	-0.3746	0.2634	4.8404	0.0544	
0.55	-0.1600	-0.5150	-0.3163	0.2937	4.8421	0.0607	
0.60	-0.1810	-0.3050	-0.2373	0.3522	4.8460	0.0727	
0.65	-0.1900	-0.0800	-0.1427	0.5425	4.8636	0.1116	
0.70	-0.1890	0.1480	-0.0390	1.6882	5.1196	0.3298	
					4.8640	**0.0728**	Average

4.4 Comparison of the Regular Responses

To validate the technique, the predicted equivalent natural frequency ω_e and the equivalent damping coefficient ζ_e in Table 6.1 are substituted into the following equation.

$$\ddot{\phi} + 2\zeta_e \omega_e \dot{\phi} + \omega_e^2 \phi = F_0 \sin \omega t \qquad (4.14)$$

Equation (4.14) is integrated to obtain the value of the roll angle. This angle is compared with roll angle obtained from the integration of the following equation

$$\ddot{\phi} + 2\zeta\omega_n[\dot{\phi} + \varepsilon_1 \dot{\phi}^3] + \omega_n^2[\phi + \varepsilon_2 \phi^3] = F_0 \sin \omega t \qquad (4.15)$$

The values of the parameters in equation (4.15) are the same as those used to obtain the roll motion simulation in irregular waves. The initial conditions and excitations for two equations are same. For all cases, F_0 is taken 12; ω is 7 radians per second; time is 20 seconds and time step is 0.02 second.

4. 5 Estimation of the Variance of the Wave Exciting Moment

For the stationary case, using the linear terms of equations (3.42) and (3.43), the variance, ψ, of the wave exciting rolling moment per unit virtual mass moment of inertia can be predicted from equation (4.16),

$$\psi = 4\zeta_e \omega_e V_{22}, \qquad (4.16)$$

$$V_{22} = \omega_e^2 V_{11} \qquad (4.17)$$

where V_{11} and V_{22} are the variances of the roll angle and roll velocity, respectively. V_{12} is the covariance of roll angle and roll velocity.

The variance of the wave exciting rolling moment can be calculated from equation (4.18),

$$\psi_{\alpha} = \sum_{k=1}^{n} \frac{A_k^2}{2} \qquad (4.18)$$

where A_k is the wave excitation amplitude used in the simulation, which values are shown in Table (4.1). The value of n is 41 for all cases.

Chapter 5

Ship Model Experiments

The validity and accuracy of the method to identify the variance ψ of the wave exciting moment per unit virtual mass moment of inertia using simulated data has been verified in the last chapter. In this chapter we apply the technique to experimental data. Real data reflect the physical response of a system to natural environment whereas simulated data are obtained from an assumed equation. Ship model experiments in a wave tank can simulate to a certain extent the behaviour of real ships at sea, and also allow the method to be tested in a controlled environment. Furthermore, model experiments enable us to assess the variation of the wave excitation for different models under various loading conditions and various wave excitations.

5.1 General Arrangement

The ship model tests were performed in the towing tank of Memorial University of Newfoundland using two ship models. One is a 1:40 'R-class icebreaker' ship model, and the other is a 1:40 series-60 ship model (without appendages). The facility consists of a large wave tank, an instrumented towing carriage, and a fully equipped control room.

The interior dimensions of the tank are 58.27m in length, 4.57m in width, and 3.04m in depth. At one end of the wave tank is the hydraulically operated, piston-type wave generator installed behind the waveboard. The waveboard is fabricated from aluminium with a watertight Teflon seal around its periphery. At the other end of the wave tank is a parabolic beach consisting of an aluminium frame covered by wooden slats. This wave-absorbing beach is intended to reduce the energy contained in the reflected wave, thus maintaining a minimum reflection coefficient. Both regular and irregular waves, in a frequency range between 0.3 and 1.2 Hz, can be generated through the translatory motion of the waveboard driven by a hydraulic actuator. Electronic control for the waveboard is provided from the control room. Computer in the control room generates control signals for irregular wave spectra and the resultant time series are transferred to a microcomputer-controlled digital to analog converter, which allows reproduction of any theoretical spectrum.

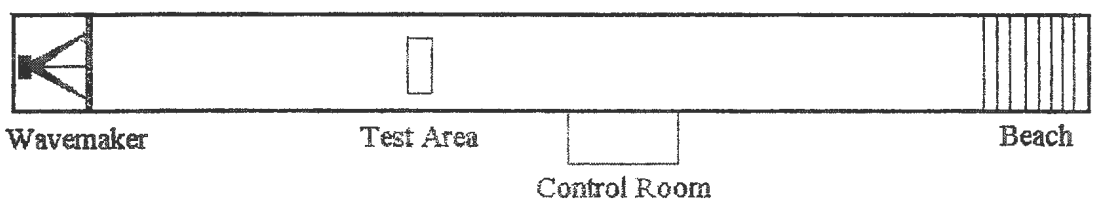

Figure 5.1: Towing Tank Layout

The experiments were conducted at zero forward speed, so the models were positioned across the tank at the test area, whose centre is 20m away from the wavemaker end (see Figure 5.1). The waves generated by the wavemaker at one end of the tank approached the model from its starboard with an encounter angle of 90 degree, namely a beam sea. In

every test run, two parameters were measured and recorded in the form of time history. They are:

- Wave Height (cm)
- Angular roll displacement (degree)

A vertical gyroscope is used to measure the roll response of the ship models. A wave probe is employed to monitor the time history of the wave profile. Data from the vertical gyroscope and wave probe are recorded in analog format on one or more multi-channel instrumentation recorders, and simultaneously digitized with a multi-channel analog to digital converter and a computer, which are installed on the towing carriage. The measurement range of the gyroscope is ±30 degree.

5.2 Ship Models Descriptions

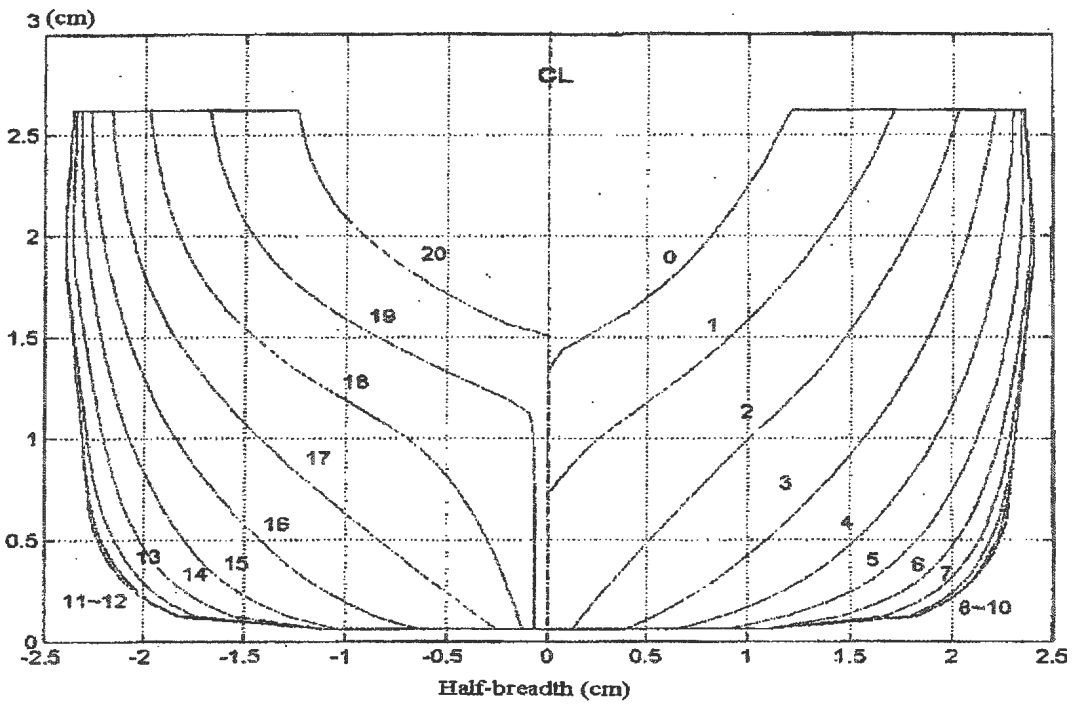

Figure 5.2: Body Plan of "R-class Icebreaker" Ship Model

One of the models used for the tests is a 1:40 scale 'R-class icebreaker'. The hydrostatic particulars of the ship model are presented in Table 5.1, and the body plan is shown in Figure 5.2. The model hull was made of glass reinforced plastic.

Table 5.1: Hydrostatic Particulars for "R-class Icebreaker" Ship Model

Length Between Perpendiculars (LPP)	2.1985 m
Length of Waterline (LWL)	2.3250 m
Waterline Beam at Midships	0.4840 m
Waterline Beam at Maximum Section	0.4845 m
Maximum Waterline Beam	0.4845 m
Draught at Midships	0.1735 m
Draught at Maximum Section	0.1745 m
Draught at Aft Perpendicular	0.1790 m
Draught at Forward Perpendicular	0.1675 m
Equivalent Level Keel Draught	0.1735 m
Maximum Section Forward of Midships	- 0.1850 m
Area of Maximum Section	0.0773 m^2
Center of Buoyancy Forward of Midships (LCB)	- 0.0080 m
Center of Buoyancy above Keel (KB)	0.0970 m
Wetted Surface Area	1.3347 m^2
Volume of Displacement	0.1990 m^3
Center of Floatation Forward of Midships (LCF)	- 0.0175 m
Center of Floatation above Keel	0.1735 m
Area of Waterline Plane	0.8990 m^2
Transverse Metacentric Radius (BM)	0.1220 m
Longitudinal Metacentric Radius (BML)	2.4000 m
Center of Area of Profile Plane Forward of Midships	- 0.0195 m
Center of Area of Profile Plane above Keel	0.0895 m
Area of Profile Plane	0.3580 m

Table 5.2: Hydrostatic Particulars for "Series 60 Block 60" Model

Length Between Perpendiculars (LPP)	3.048 m
Length of Waterline (LWL)	3.092 m
Waterline Beam at Midships	0.4065 m
Waterline Beam at Maximum Section	0.4065 m
Maximum Waterline Beam	0.4065 m
Draught at Midships	0.1625 m
Draught at Maximum Section	0.1625 m
Maximum Draught	0.1625 m
Draught above Datum	0.1625 m
Maximum Section Forward of Midships	0.0380 m
Parallel Middle Body from Forward of Midships	- 0.0380 m
Parallel Middle Body from Aft of Midships	0.0380 m
Area of Midships Section	0.1295 m^2
Area of Maximum Section	0.1295 m^2
Center of Buoyancy Forward of Midships (LCB)	0.0455 m
Center of Aft Body Buoyancy Forward of Midships	- 0.5070 m
Center of fore Body Buoyancy Forward of Midships	0.5420 m
Center of Buoyancy above Keel (KB)	0.0870 m
Wetted Surface Area	1.5924 m
Volume of Displacement	0.1206 m^3
Center of Floatation Forward of Midships (LCF)	0.1155 m
Center of Floatation (aft body) Forward of Midships	- 0.5300 m
Center of Floatation (fore body) Forward of Midships	0.6290 m
Area of Waterline Plane	0.8767 m^2
Transverse Metacentric Radius (BM)	0.07675 m
Longitudinal Metacentric Radius (BML)	3.4050 m
Center of Area of Profile Plane Forward of Midships	- 0.0175 m
Center of Area of Profile Plane above Keel	0.0815 m
Area of Profile Plane	0.4852 m^2

The second model used for the tests is a 1:40 "series-60 Block60" ship model (without appendages). The hydrostatic particulars of the ship model are presented in Table 5.2 *(Note: The information is courtesy of the Institute of Marine Dynamics of the National Research Council of Canada).*

Before the experiments, the models were prepared to meet the requirements specified in the hydrostatic particulars list provided by the Institute for Marine Dynamics, National Research Council of Canada. This work involved ballasting the model until the required waterline is reached and then arranging the weights in the model to adjust the centre of gravity and the radius of gyration. After being ballasted and trimmed in the above way, each model has the proper draft, centre of gravity and roll natural frequency.

In the procedure of adjusting the mass distribution in the model, the centre of gravity and the roll natural frequency need to be checked repeatedly. The roll natural frequency of the model can be determined by conducting a free roll test and recording the time required by the model to perform a specific number of roll cycles. The vertical position of the centre of gravity is usually estimated from an inclining test.

5.3 Experimental Set-up

Two parameters, wave height and roll response, were recorded during model tests. The wave height was measured using a capacitance type wave probe, which was attached to a platform at a fixed location about 1.2m away from the model at the midship section in the direction towards the wavemaker. Two different techniques are usually used for measuring roll motion. One is to use a vertical gyroscope and the other is to use a dynamometer. In the tests, roll angles were measured using the vertical gyroscope located

on the vertical line through the center of gravity of the model. The vertical gyroscope is composed of a linear bearing, a pivot and an angular induction transducer. As shown in Figure 5.3 and Figure 5.4, the models were tethered from its bow and stern by two strings running through a pair of steel plates, which were securely attached and bent so that they hang over the edge of the model. On each steel plate, holes are drilled at a height at the same level as the center of gravity. To prevent the model from drifting down the tank during tests, the cord joining the two tethering points in the bow and stern passes through the center of gravity of the model. Two 2kg weights for "series 60" model and two 5kg weights for "R-class icebreaker" model were fastened at the loose end of each cord, which moves freely up and down in the water to restore the position of the model when displaced. The sway and roll modes are normally coupled but this coupling was found to be weak and negligible. During tests, the models were covered with plastic bags and sealed with duct sealing tape to prevent water spray into the models when the models are in severe waves. Moving a set of weights vertically in the model changed the center of gravity of the model, while keeping the displacement constant. Thus the different GM values were obtained. The signals from the vertical gyroscope and the wave probe were sent through a filter and stored on a microcomputer. The microcomputer was connected to a data acquisition unit: a two-channel digital signal analyzer.

Random wave generation consists of five steps: 1) definition of the target wave spectrum; 2) synthesis of a random target wave train with energy distribution defined by the target spectrum; 3) calculation of the control signal for wave machine; 4) generation and measurement of the waves in the towing tank; 5) spectral analysis of the measured wave train and comparison with the desired target spectrum.

In the simulation, the exciting moment departed from the Gaussian white noise, which was assumed in obtaining the theoretical formulation. Evidence from previous work has shown that the assumption of the white noise spectrum can be relaxed because of the narrow bounded nature of the rolling motion. Haddara *et al.* (1994), however, pointed out that because of the narrow banded nature of rolling motion, the random decrement technique could still be applied in this case. A typical wave in the North Atlantic has been found under the Joint North Sea Wave Project (JONSWAP) from a series of wave measurements at the North Sea. The unidirectional JONSWAP sea-spectrum was used for random rolling experiments. The JONSWAP spectrum, expressed as a function of frequency, is given by

$$S(f) = \frac{A}{f^5}\exp(-B/f^4)\gamma^{\alpha}$$

where

$$A = \frac{5}{16}\frac{H_s^2 f_m^4}{\gamma^{\frac{1}{3}}},$$

$$B = \frac{5}{4} f_m^4,$$

$$\alpha = \exp[-\frac{(f - f_m)^2}{2\sigma^2 f_m^2}]$$

The JONSWAP spectrum depends on four parameters: significant wave height H_s, wave modal frequency f_m, peak enhancement factor γ, and shape parameter σ. The following value proposed by Ewing (1974) were used in the experiments:

$$\gamma = 3.3,$$

$$\sigma = 0.07 \text{ for } f \le f_m,$$

$$\sigma = 0.09 \text{ for } f > f_m \ .$$

Wave modal frequency f_m or wave predominant frequency (PF) is the peak frequency of a wave spectrum. In this research, the values of wave modal frequency f_m are 0.5, 0.6 and 0.7 Hz. The significant wave height H_s is the average of the one-third highest waves, which is defined as $H_s = 4\sqrt{m_0}$ where m_0 is the area under the wave spectrum. In this research, the values of H_s are 7, 10 and 13 cm.

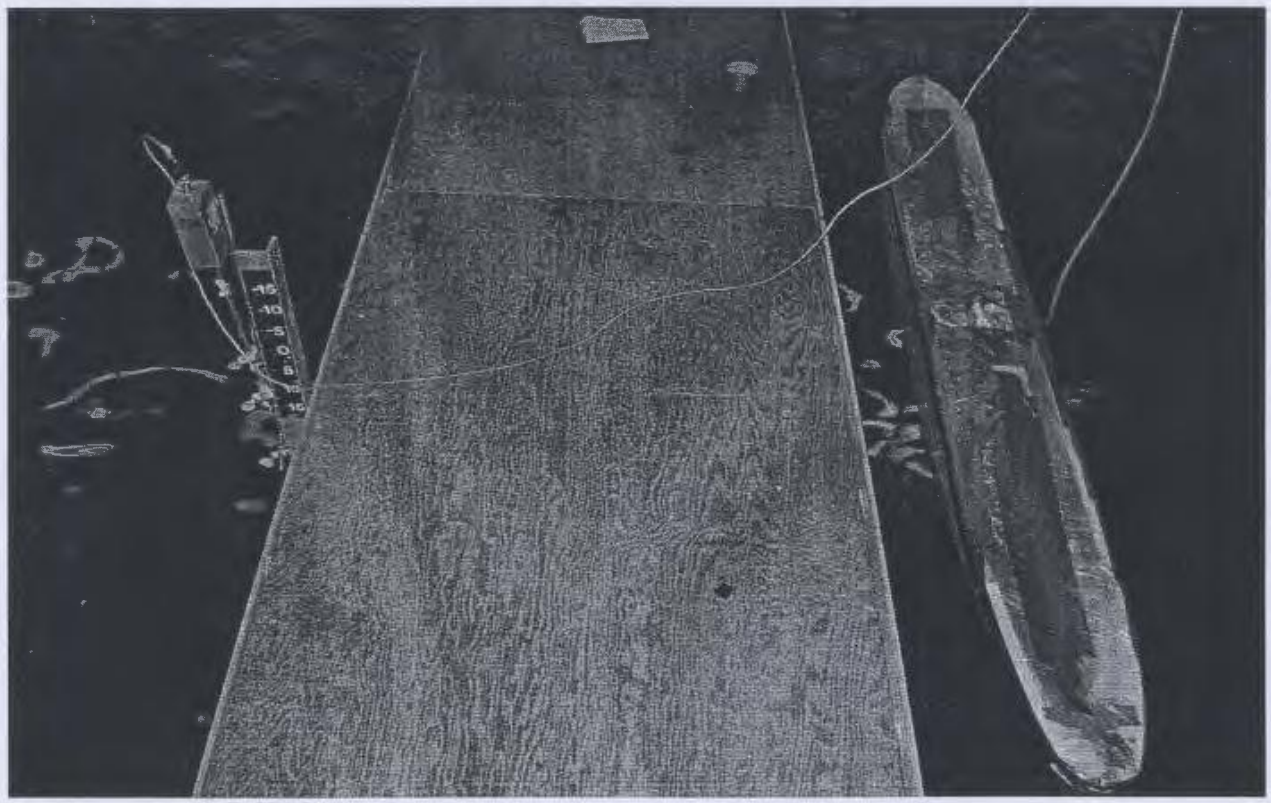

Figure 5.3: "Series 60" Model Test

Figure 5.4: "R-class Icebreaker" Model Test

5.4 Roll Tests in Towing Tank

The vertical gyroscope and the wave probe were calibrated. The rolling tests were performed for each model at a series of GM values, wave modal frequencies and significant wave heights. During the experiments, the mass of each model remained constant but the center of gravity changed vertically to give a series of different GM values. For each model at each GM value, the experiment included three parts: inclining test, free roll tests and roll tests in random beam waves.

5.4.1 Inclining Test

The GM value is a measure of the initial transverse stability of a ship. A low GM value will put the ship in a dangerous situation, even capsizing. The purpose of the inclining test is to check the value of the transverse metacentric height GM for each loading condition. To avoid error from measurements, a weight was moved transversely through five positions on the model and 9 measurements were taken for each case. The 2kg weight was moved on the "R-class Icebreaker" model and the 1.234kg weight for the "Series 60" model. The displacements of "R-class" and "Series 60" models are 128.1kg and 73.61kg, respectively. Table 5.3 and Table 5.4 give the inclining test data for the two models in each case.

Table 5.3: Inclining Test Data of "R-class Icebreaker" Model

	Case 1	Case 2	Case 3
D (cm)	φ (degree)	φ (degree)	φ (degree)
0	0.12	- 0.28	- 0.11
7 s	0.75	0.28	0.59
14 s	1.39	0.86	1.32
7 s	0.76	0.27	0.6
0	0.13	- 0.28	- 0.11
7 p	- 0.51	- 0.87	- 0.85
14 p	- 1.15	- 1.44	- 1.55
7 p	- 0.52	- 0.89	- 0.86
0	0.12	- 0.29	- 0.12
GM	9.79 cm	10.93 cm	8.66 cm
KG	12.11 cm	10.97 cm	13.24 cm

"s": moved weight towards starboard. "p": moved weight towards port.

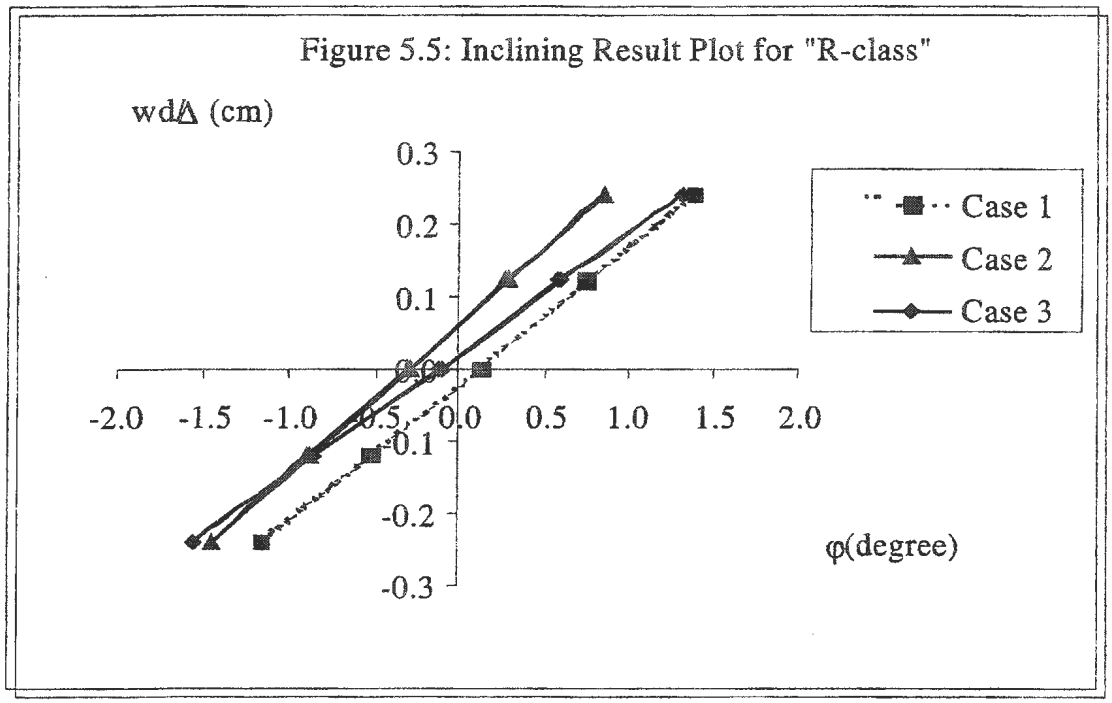

Table 5.4: Inclining Test Data of "Series 60 Block 60" Model

	Case 1	Case 2	Case 3
d (cm)	φ (degree)	φ (degree)	φ (degree)
0	0.02	- 1.52	- 3.7
2 s	0.58	- 0.86	- 3.08
4 s	1.11	- 0.23	- 2.53
2 s	0.61	- 0.87	- 3.13
0	0.07	- 1.44	- 3.71
2 p	- 0.44	- 2.09	- 4.37
4 p	- 1.02	- 2.67	- 4.86
2 p	- 0.47	- 2.04	- 4.36
0	0.06	- 1.5	- 3.73
GM	3.61 cm	3.43 cm	3.23 cm
KG	12.76 cm	12.94cm	13.14 cm

"s": moved weight towards starboard. "p": moved weight towards port.

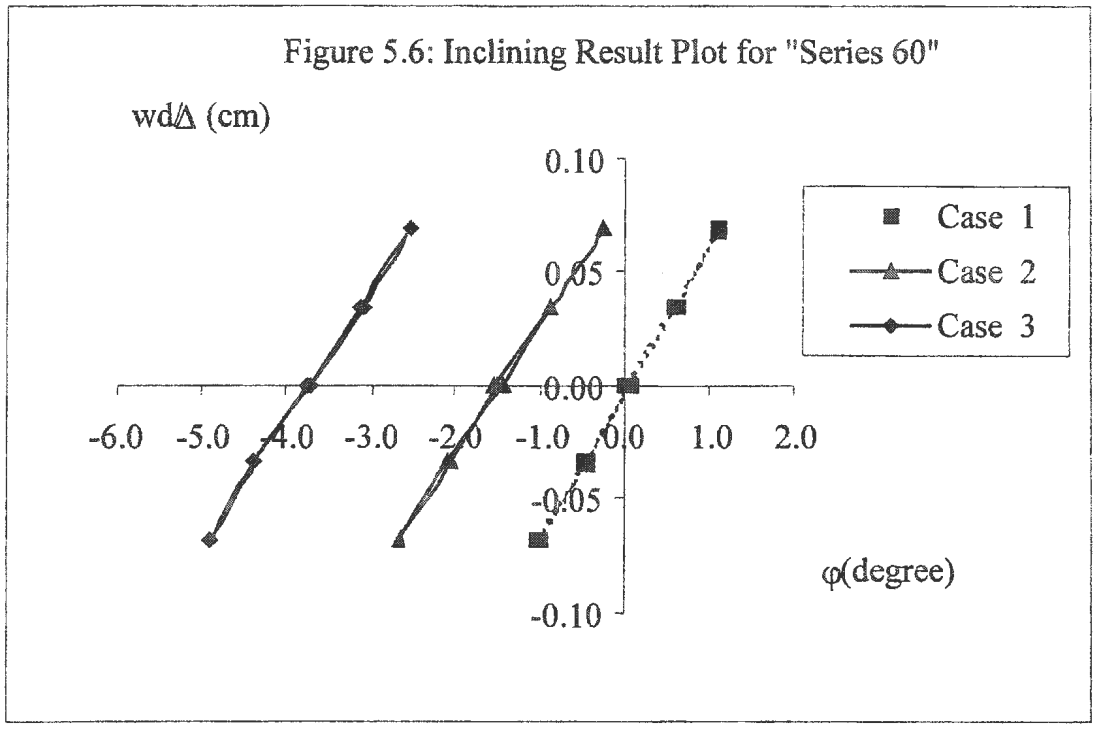

5.4.2 Free Roll Tests

In order to compare the results from the random decrement curves with those from the free roll decay curve, a set of free roll tests was calculated. The model was heeled respectively to port or starboard at 3 different initial angles: 5degree, 10 degree and 15 degrees in calm water and left to roll under its own inertia. Measurements were taken at a rate of 50 points per second and the test duration was 25 seconds. The results of the free decay test for all cases are shown in Figure 5.7 to Figure 5.12. The natural frequencies of the ship response are also determined from the free roll response (see Table 5.5).

Table 5.5: Natural Frequencies from Free Roll Tests

	"R-class"		"Series 60"	
	GM (cm)	Frequency (Hz)	GM (cm)	Frequency (Hz)
Case1	9.79	1.03	3.61	1.24
Case 2	10.93	1.15	3.43	1.22
Case 3	8.66	0.92	3.23	1.17

Figure5.7: 10 degree free decay for 'R-class' case1

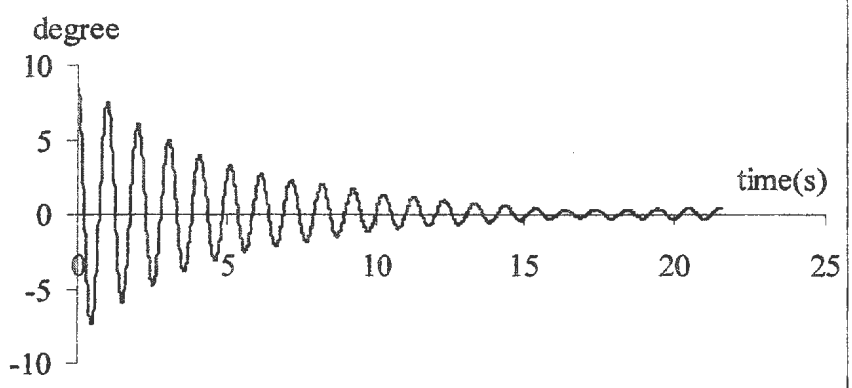

Figure5.8: 10 degree Free decay for 'R-class'case 2

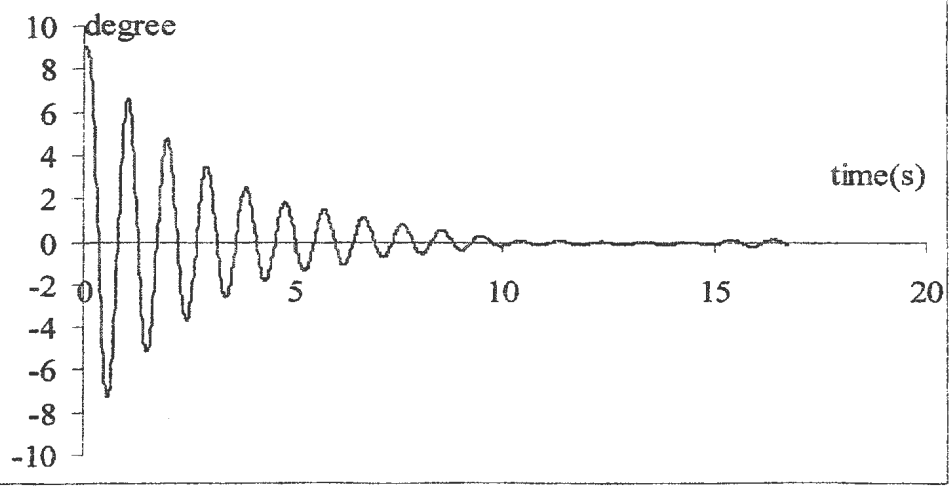

Figure 5.9: 10 degree free decay for 'R-class' case 3

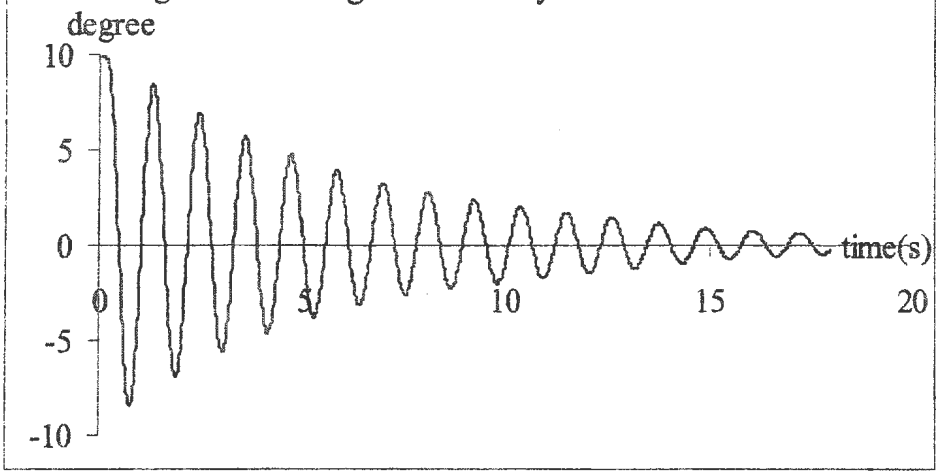

Figure 5.10: 10 degree free decay of "Series 60" case 1

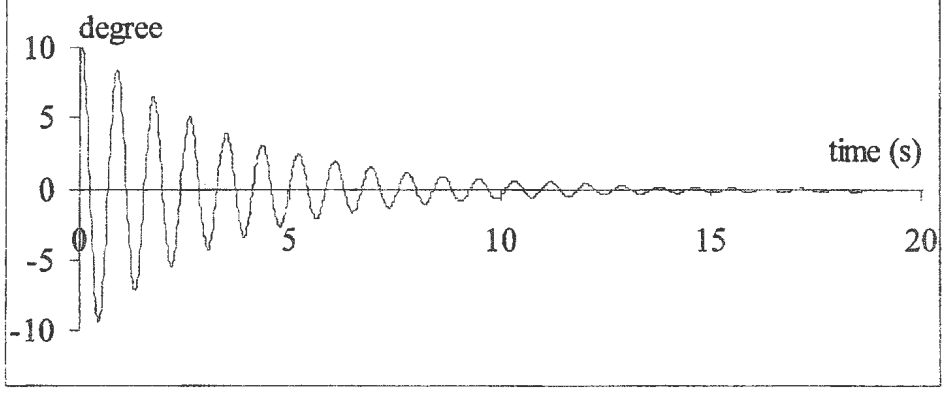

Figure 5.11: 10 degree free decay of "Series 60" case 2

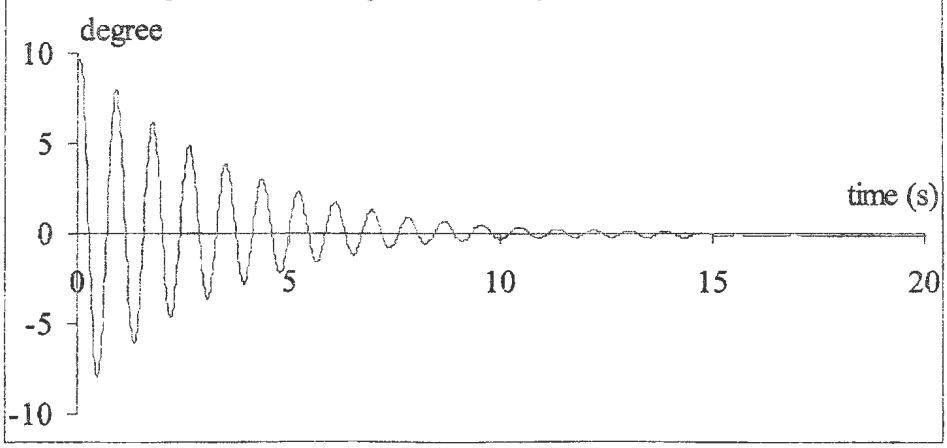

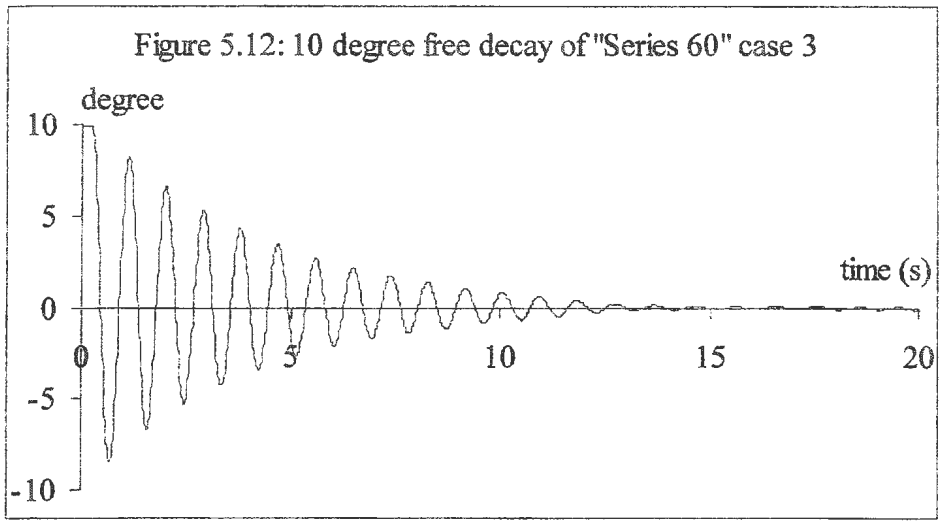

Figure 5.12: 10 degree free decay of "Series 60" case 3

5.4.3 Forced Roll Tests in Random Beam Waves

Following the inclining tests and the free roll tests, the roll tests in random beam waves were performed with the model at the same loading condition. The wave modal frequency f_m was chosen as: 0.5 Hz, 0.6 Hz and 0.7 Hz, which are lower than the natural frequencies in Table 5.5. The shape parameter σ was decided to be equal to 0.09 for $f > f_m$. In setting the JONSWAP wave spectrum, we chose three different significant wave heights. These are 7cm, 10cm and 13 cm. Thus, each model in each loading condition was subjected to 9 different wave excitations. A total of 54 cases were tested, which were tabulated in the Table 5.6 ("Series 60" model) and Table 5.7 ("R-class Icebreaker" model) with the corresponding experimental conditions.

The data sample rate in the random roll tests was kept the same as in free roll tests at 50 points per second, while the sample duration of each record was 600 seconds in order to ensure the stationary requirements and provide enough data for analysis.

Table 5.6: "Series 60" Data Files and Experimental Conditions

Case	File Name	f_m (Hz)	H_s (cm)	GM (cm)
1	S150h70	0.5	7	3.61
	S160h70	0.6	7	3.61
	S170h70	0.7	7	3.61
	S150h10	0.5	10	3.61
	S160h10	0.6	10	3.61
	S170h10	0.7	10	3.61
	S150h13	0.5	13	3.61
	S160h13	0.6	13	3.61
	S170h13	0.7	13	3.61
2	S250h70	0.5	7	3.43
	S260h70	0.6	7	3.43
	S270h70	0.7	7	3.43
	S250h10	0.5	10	3.43
	S260h10	0.6	10	3.43
	S270h10	0.7	10	3.43
	S250h13	0.5	13	3.43
	S260h13	0.6	13	3.43
	S270h13	0.7	13	3.43
3	S350h70	0.5	7	3.23
	S360h70	0.6	7	3.23
	S370h70	0.7	7	3.23
	S350h10	0.5	10	3.23
	S360h10	0.6	10	3.23
	S370h10	0.7	10	3.23
	S350h13	0.5	13	3.23
	S360h13	0.6	13	3.23
	S370h13	0.7	13	3.23

Table 5.7: "R-class Icebreaker" Data Files and Experimental Conditions

Case	File Name	f_m (Hz)	H_s (cm)	GM (cm)
1	R550h70	0.5	7	9.79
	R560h70	0.6	7	9.79
	R570h70	0.7	7	9.79
	R550h10	0.5	10	9.79
	R560h10	0.6	10	9.79
	R570h10	0.7	10	9.79
	R550h13	0.5	13	9.79
	R560h13	0.6	13	9.79
	R570h13	0.7	13	9.79
2	R650h70	0.5	7	10.93
	R660h70	0.6	7	10.93
	R670h70	0.7	7	10.93
	R650h10	0.5	10	10.93
	R660h10	0.6	10	10.93
	R670h10	0.7	10	10.93
	R650h13	0.5	13	10.93
	R660h13	0.6	13	10.93
	R670h13	0.7	13	10.93
3	R750h70	0.5	7	8.66
	R760h70	0.6	7	8.66
	R770h70	0.7	7	8.66
	R750h10	0.5	10	8.66
	R760h10	0.6	10	8.66
	R770h10	0.7	10	8.66
	R750h13	0.5	13	8.66
	R760h13	0.6	13	8.66
	R770h13	0.7	13	8.66

5.5 Experimental Data Analysis Method

All data are analysed using a program "*experimet1.m*" (see Appendix B) to extract the random decrement curves and find out the damped natural frequencies, ω_d, from the curves. Then, the function G is obtained from each random decrement curve using a neural network algorithm. The equivalent natural frequency and the equivalent damping coefficient can then be identified using equations 4.13. Finally, the variance, ψ, of the wave excitation is calculated using equation 4.15.

A Multiple Regression method is used to check the significant levels of the three variables: wave frequency, wave significant height, and GM value. The analysis process of Multiple Regression is outlined here: 1) Checking the results to see if it has any outlier in all estimated results when the variance ψ of the wave exciting moment is modeled as a function of the three variables using ordinary least squares regression. 2) Checking the p-values of all linear terms and interaction terms to test whether each variable had a significant effect on the variance ψ, and whether there was an interaction between these four variables. 3) Checking the R^2 values of each significant term to find their contributions on the variability in estimating the variance ψ of the wave exciting moment.

Chapter 6

Results and Discussion

This chapter will focus on: 1) the validation of the proposed estimation method from the simulated roll motion data; 2) the effect of wave modal frequency, wave significant height, and GM value on the estimated values of the variance ψ of the wave exciting moment in JONSWAP beam waves.

6.1 Simulation Results and Discussion

6.1.1 Validation of Predicted Equivalent Linear Roll Parameters

As explained in section 4.4, the regular responses simulated from equation (4.13) and equation (4.14) are used to validate the method of predicting the equivalent linear roll parameters. The comparison of the regular responses for one case is shown in Figure 6.1. Other comparisons are given in Appendix A. The original parameters values and the predicted equivalent values are shown in Table 6.1. The error in the prediction of the peak amplitude for each case is also given in Table 6.1. We can see that the error in predicting the amplitude in all cases is less than 7%, which means that the predicted values of the roll parameters are accurate enough for the method to be employed in the analysis of actual roll data.

Table 6.1: Comparison of the Regular Responses

Case	ω_n	ζ	ε_1	ε_2	ω_e	ζ_e	ang%error
511	5	0.06	0.01	0.01	4.8640	0.0728	5.7262
513	5	0.06	0.01	0.03	4.8592	0.0711	6.2018
515	5	0.06	0.01	0.05	4.8599	0.0724	6.6230
531	5	0.06	0.03	0.01	4.8744	0.0797	5.0928
533	5	0.06	0.03	0.03	4.8717	0.0765	5.3849
535	5	0.06	0.03	0.05	4.8766	0.0770	5.5959
551	5	0.06	0.05	0.01	4.8703	0.0801	4.5909
553	5	0.06	0.05	0.03	4.8650	0.0751	4.8716
555	5	0.06	0.05	0.05	4.8504	0.0759	5.7396
51010	5	0.06	0.1	0.1	4.8570	0.0774	4.4617
611	3	0.06	0.01	0.01	2.9396	0.0640	0.0894
613	3	0.06	0.01	0.03	3.0138	0.0610	-0.0380
615	3	0.06	0.01	0.05	2.9290	0.0659	-0.1098
631	3	0.06	0.03	0.01	2.9289	0.0655	0.2253
633	3	0.06	0.03	0.03	3.0080	0.0633	-0.0056
635	3	0.06	0.03	0.05	2.9322	0.0661	0.0727
651	3	0.06	0.05	0.01	3.0077	0.0626	-0.0571
653	3	0.06	0.05	0.03	3.0026	0.0634	-0.0654
655	3	0.06	0.05	0.05	2.9979	0.0627	-0.0914
61010	3	0.06	0.1	0.1	2.9296	0.0659	-0.0920
61050	3	0.06	0.1	0.5	2.9987	0.0669	-0.3552
63050	3	0.06	0.3	0.5	2.9995	0.0704	-0.1774
411	3	0.04	0.1	0.1	2.9953	0.0469	-0.3109
413	3	0.04	0.1	0.3	2.9986	0.0424	-2.5166
415	3	0.04	0.1	0.5	2.9950	0.0430	-4.8043
431	3	0.04	0.3	0.1	3.0005	0.0488	-1.0155
433	3	0.04	0.3	0.3	2.9962	0.0473	-1.0875
435	3	0.04	0.3	0.5	2.9996	0.0480	-0.8873
451	3	0.04	0.5	0.1	3.0698	0.0543	0.5013
453	3	0.04	0.5	0.3	3.0043	0.0494	-1.0801
455	3	0.04	0.5	0.5	2.9969	0.0557	0.5153

Figure 6.1: Compare the regular response of case 511

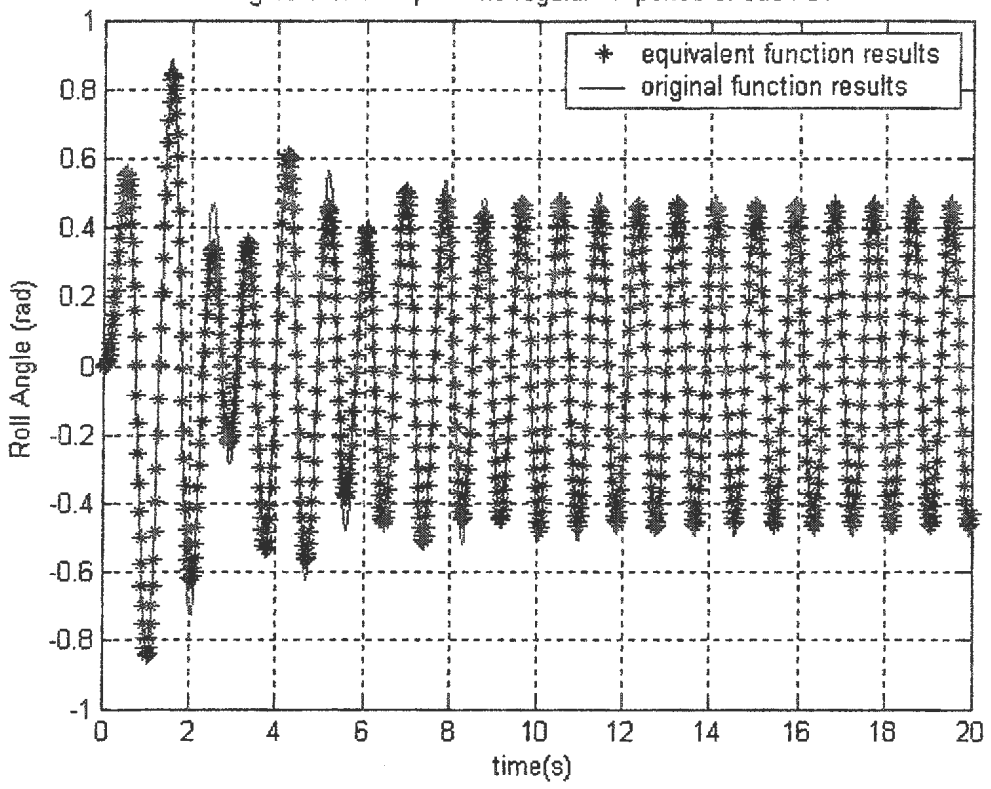

6.1.2 Validation of the Variance ψ Prediction

From equation (4.15), we estimated the variance ψ, and from equation (4.16), the true variance ψ_a could also be determined for each case. The comparison between the estimated variance ψ and the true variance ψ_a of the wave exciting moment for all 31 simulated cases are shown in Table 4.4. We can clearly see that all errors are less than 7%. This indicates that the proposed method is good enough to estimate the variance ψ of wave exciting moment acting on a ship in random waves.

Table 6.2: Comparison of the estimated variance ψ and the true variance ψ_a of wave excitation

Case	ω_e	ζ_e	V_{11}	V_{22}	ψ	n	A_k	ψ_a	% Error
511	4.8640	0.0728	0.0241	0.5707	0.8078	41	0.2	0.82	1.49
513	4.8592	0.0711	0.0242	0.5723	0.7911	41	0.2	0.82	3.52
515	4.8599	0.0724	0.0243	0.5731	0.8069	41	0.2	0.82	1.59
531	4.8744	0.0797	0.0233	0.5545	0.8616	41	0.2	0.82	-5.07
533	4.8717	0.0765	0.0235	0.5579	0.8318	41	0.2	0.82	-1.44
535	4.8766	0.0770	0.0235	0.5583	0.8391	41	0.2	0.82	-2.33
551	4.8703	0.0801	0.0228	0.5409	0.8436	41	0.2	0.82	-2.88
553	4.8650	0.0751	0.0225	0.5317	0.7775	41	0.2	0.82	5.19
555	4.8504	0.0759	0.0231	0.5445	0.8014	41	0.2	0.82	2.27
51010	4.8570	0.0774	0.0216	0.5098	0.7665	41	0.2	0.82	6.52
611	2.9396	0.0640	0.0193	0.1663	0.1253	41	0.08	0.1312	4.53
613	3.0138	0.0610	0.0193	0.1757	0.1291	41	0.08	0.1312	1.61
615	2.9290	0.0659	0.0192	0.1649	0.1273	41	0.08	0.1312	2.96
631	2.9289	0.0655	0.0192	0.1646	0.1264	41	0.08	0.1312	3.63
633	3.0080	0.0633	0.0191	0.1726	0.1314	41	0.08	0.1312	-0.18
635	2.9322	0.0661	0.0189	0.1627	0.1261	41	0.08	0.1312	3.89
651	3.0077	0.0626	0.0190	0.1715	0.1291	41	0.08	0.1312	1.61
653	3.0026	0.0634	0.0190	0.1715	0.1306	41	0.08	0.1312	0.47
655	2.9979	0.0627	0.0188	0.1687	0.1269	41	0.08	0.1312	3.32
61010	2.9296	0.0659	0.0186	0.1597	0.1234	41	0.08	0.1312	5.95
61050	2.9987	0.0669	0.0173	0.1554	0.1246	41	0.08	0.1312	5.00
63050	2.9995	0.0704	0.0166	0.1490	0.1259	41	0.08	0.1312	4.05
411	2.9953	0.0469	0.0271	0.2431	0.1365	41	0.08	0.1312	-4.07
413	2.9986	0.0424	0.0283	0.2542	0.1294	41	0.08	0.1312	1.35
415	2.9950	0.0430	0.0267	0.2394	0.1234	41	0.08	0.1312	5.98
431	3.0005	0.0488	0.0239	0.2153	0.1262	41	0.08	0.1312	3.84
433	2.9962	0.0473	0.0244	0.2188	0.1241	41	0.08	0.1312	5.40
435	2.9996	0.0480	0.0244	0.2192	0.1263	41	0.08	0.1312	3.71
451	3.0698	0.0543	0.0214	0.2017	0.1345	41	0.08	0.1312	-2.54
453	3.0043	0.0494	0.0237	0.2142	0.1272	41	0.08	0.1312	3.03
455	2.9969	0.0557	0.0210	0.1887	0.1260	41	0.08	0.1312	3.95

6.2 Experimental Results and Discussion

The variance ψ of the wave exciting moment has been obtained from the experimental roll time history for the different cases of two ship models and the results are shown in Table 6.3 for the "Series 60" ship model and in Table 6.4 for the "R-class Icebreaker" ship model. Figures 6.2 to 6.19 show a plot of the predicted results as a function of the different variables. In these figures, the points indicate the experimental results while lines show the regression fits.

Figures 6.2 to 6.4 show the variance ψ of the wave exciting moment to "series 60" model as a function of the wave model frequency (f_m) and the wave significant height (Hs). It can be seen that, in general, the variance ψ of the wave exciting moment increases as the wave frequencies and the wave heights increase, except for the case of GM value at 3.43cm, H_s 10cm, f_m 0.5Hz. A similar trend is shown for "R-class Icebreaker" model in Figures 6.5 to 6.7, the variance ψ increase as Hs and Fm increase, except for the case of GM value at 8.66cm, H_s 10 cm, f_m 0.5Hz. As the wave modal frequency increases, it approaches the natural frequency of ship model rolling motion. This will result in an increase of the variance ψ of the wave exciting moment. Also, as the significant wave height increases, we expect the variance ψ to increase. It is difficult to explain the anomalous behaviour of the cases of GM value at 8.66cm, H_s 10cm and f_m 0.5Hz. Maybe, the reason is the value of the point (GM 8.66cm, H_s 10 cm, f_m 0.5Hz) is abnormally big.

Figure 6.8 to Figure 6.10 show the variance ψ of the wave exciting moment for the "series 60" ship model as a function of the GM value and the wave model frequency

(Fm). Figure 6.11 to Figure 6.13 show the variance ψ for the "R-class Icebreaker" ship model as a function of the GM and f_m. Figures 6.8, 6.12, 6.13 show that the wave modal frequency (f_m) has a minor effect on the variance ψ of wave exciting moment when H_s is the same and the GM is at lowest level in our experiments.

Figure 6.14 to Figure 6.16 show that the variance ψ of wave exciting moment to "series 60" ship model as a function of wave significant height (H_s) and the GM value. Figure 6.17 to Figure 6.19 show the variance ψ for the "R-class Icebreaker" as a function of the H_s and GM value. In general, it can seen from Figure 6.14 to Figure 6.19 that the variance ψ of the wave exciting moment increases as H_s increases when f_m and GM are same, except the point in Figure 6.17 corresponding the condition: GM 8.66cm, f_m 0.5Hz, H_s 10cm. The variance ψ of the wave exciting moment for the two models showed nonlinear dependence on the GM values. Figures 6.14 and 6.19 show that the maximum variance ψ occurred at the middle GM value.

Table 6.3: "Series 60" Ship Model Experimental Results

File Name	ω_e	ζ_e	V_{11}	V_{22}	V_H	ψ
S150h70	7.316	0.050	0.006	0.262	3.5234	0.384
S160h70	7.262	0.057	0.010	0.499	3.6251	0.827
S170h70	7.393	0.085	0.012	0.592	3.3937	1.493
S150h10	7.432	0.053	0.018	0.824	9.5701	1.297
S160h10	7.209	0.070	0.016	0.744	7.0206	1.492
S170h10	7.407	0.105	0.021	0.971	7.0019	3.031
S150h13	7.384	0.073	0.015	0.698	11.54	1.504
S160h13	7.401	0.098	0.022	0.958	11.2011	2.788
S170h13	7.288	0.145	0.023	0.952	11.802	4.020
S250h70	7.271	0.072	0.006	0.276	3.6504	0.581
S260h70	7.336	0.152	0.009	0.386	3.6391	3.437
S270h70	7.262	0.056	0.014	0.662	3.3555	1.068
S250h10	7.461	0.101	0.016	0.753	9.5961	2.281
S260h10	7.251	0.115	0.014	0.611	6.9374	2.029
S270h10	7.276	0.081	0.024	1.080	6.8179	2.561
S250h13	7.386	0.079	0.014	0.603	11.3132	1.403
S260h13	7.330	0.077	0.024	1.040	11.5049	2.350
S270h13	7.197	0.114	0.029	1.217	11.8215	4.004
S350h70	7.034	0.012	0.007	0.313	3.5383	0.103
S360h70	7.034	0.013	0.012	0.548	3.6922	0.208
S370h70	7.087	0.011	0.017	0.777	3.4959	0.240
S350h10	7.143	0.030	0.019	0.853	9.8563	0.722
S360h10	7.038	0.037	0.020	0.897	7.1773	0.930
S370h10	7.102	0.064	0.029	1.298	7.3019	2.341
S350h13	7.145	0.035	0.017	0.771	11.523	0.765
S360h13	7.119	0.089	0.027	1.163	11.9242	2.937
S370h13	7.020	0.097	0.037	1.497	12.351	4.061

*V_H is the variance of wave height in the experiment.

Table 6.4: "R-class Icebreaker" Ship Model Experimental Results

File Name	ω_e	ζ_e	V_{11}	V_{22}	V_H	ψ
R550h70	6.121	0.014	0.006	0.215	3.8801	0.075
R560h70	6.162	0.009	0.011	0.403	4.327	0.087
R570h70	6.251	0.040	0.017	0.606	4.3233	0.602
R550h10	6.124	0.022	0.018	0.615	10.54	0.328
R560h10	6.130	0.044	0.020	0.748	8.0787	0.799
R570h10	6.307	0.073	0.032	1.139	8.432	2.092
R550h13	6.127	0.035	0.020	0.690	12.4544	0.594
R560h13	6.220	0.034	0.031	1.128	12.9774	0.947
R570h13	6.182	0.065	0.041	1.432	13.3817	2.308
R650h70	6.655	0.071	0.004	0.164	3.7423	0.308
R660h70	6.598	0.045	0.007	0.278	3.7387	0.327
R670h70	6.643	0.040	0.010	0.407	3.4781	0.430
R650h10	6.690	0.039	0.013	0.518	9.7805	0.539
R660h10	6.548	0.027	0.013	0.521	7.1869	0.365
R670h10	6.735	0.027	0.020	0.796	7.0194	0.578
R650h13	6.695	0.057	0.012	0.457	11.7763	0.697
R660h13	6.642	0.036	0.021	0.827	11.8874	0.786
R670h13	6.645	0.047	0.034	1.270	12.543	1.574
R750h70	5.513	0.004	0.009	0.255	4.0346	0.020
R760h70	5.578	0.002	0.014	0.424	4.3952	0.019
R770h70	5.579	0.019	0.019	0.568	4.3489	0.239
R750h10	5.582	0.030	0.028	0.828	10.9993	0.554
R760h10	5.646	0.016	0.027	0.806	8.3907	0.293
R770h10	5.614	0.022	0.036	1.074	8.0558	0.535
R750h13	5.544	0.011	0.025	0.748	12.7223	0.177
R760h13	5.611	0.013	0.036	1.070	11.8633	0.323
R770h13	5.644	0.018	0.052	1.547	14.3029	0.623

*V_H is the variance of wave height in the experiment.

Figure 6.2: Variance ψ vs. fm for "Series60" GM=3.61cm

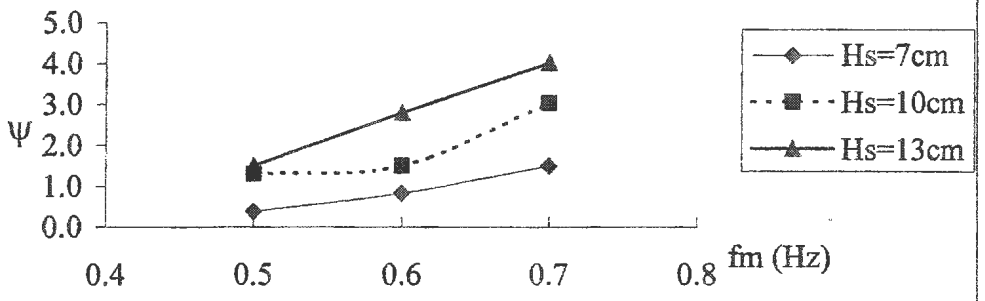

Figure 6.3: Variance ψ vs. fm for "Series60" GM=3.23cm

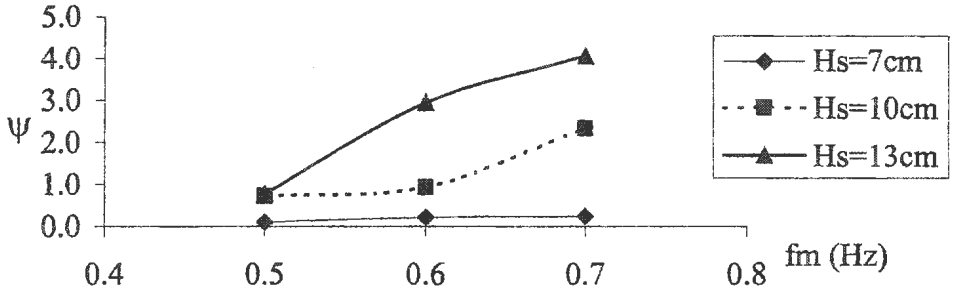

Figure 6.4: Variance ψ vs.fm for "Series60" GM= 3.43cm

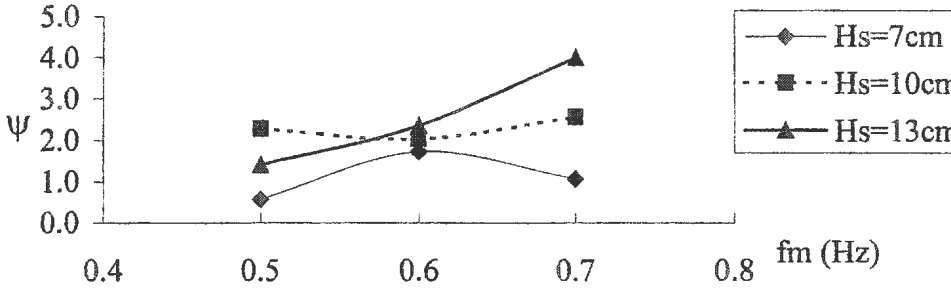

Figure 6.5: Variance ψ vs fm for "R-class" GM= 8.66cm

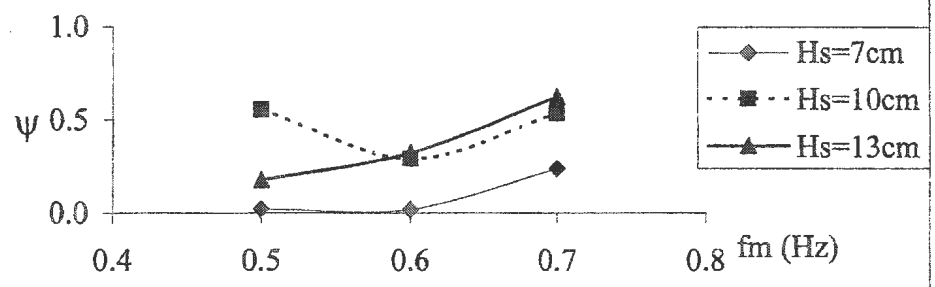

Figure 6.6: Variance ψ vs. fm for "R-class" GM= 9.79cm

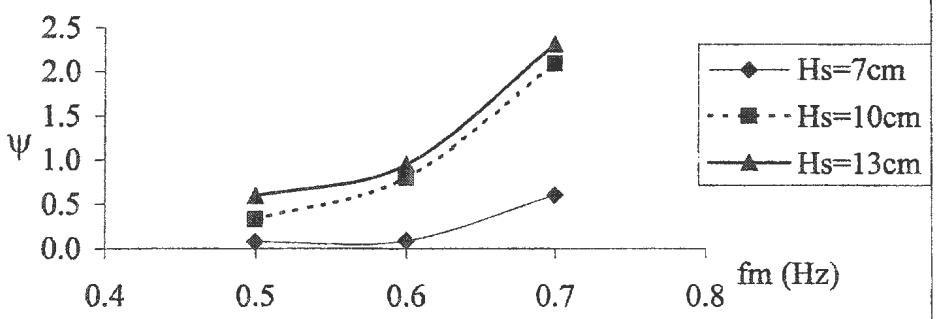

Figure 6.7: Variance ψ vs. fm for "R-class" GM= 10.93cm

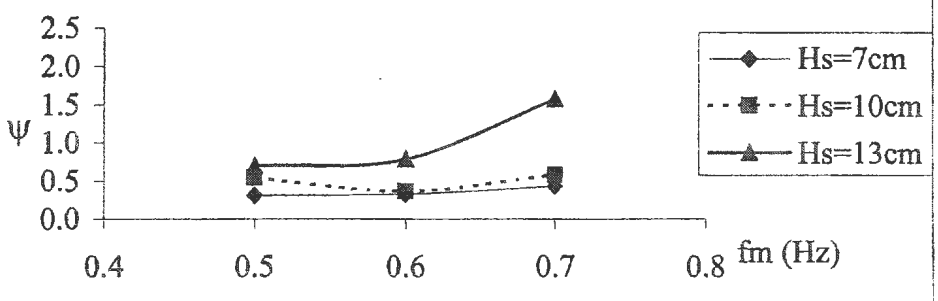

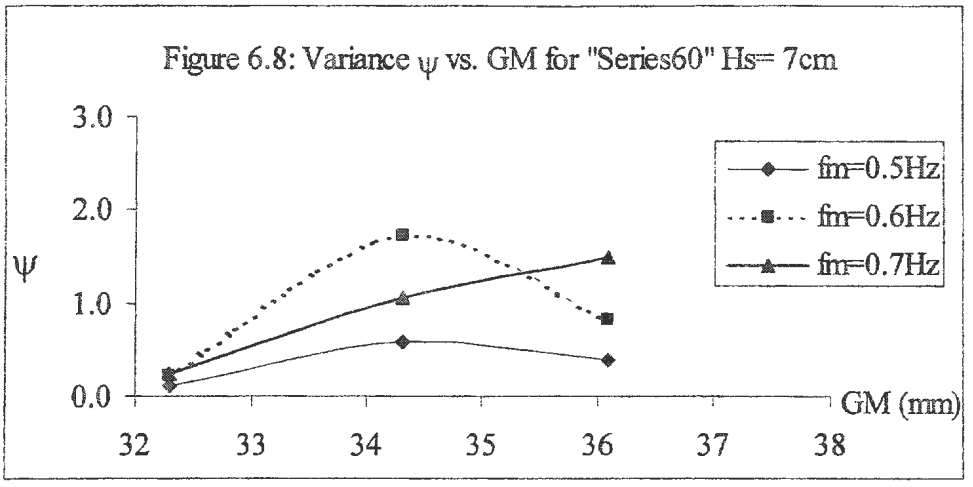
Figure 6.8: Variance ψ vs. GM for "Series60" Hs= 7cm
3.0
2.0
1.0
0.0
ψ
fm=0.5Hz
fm=0.6Hz
fm=0.7Hz
GM (mm)
32
33
34
35
36
37
38

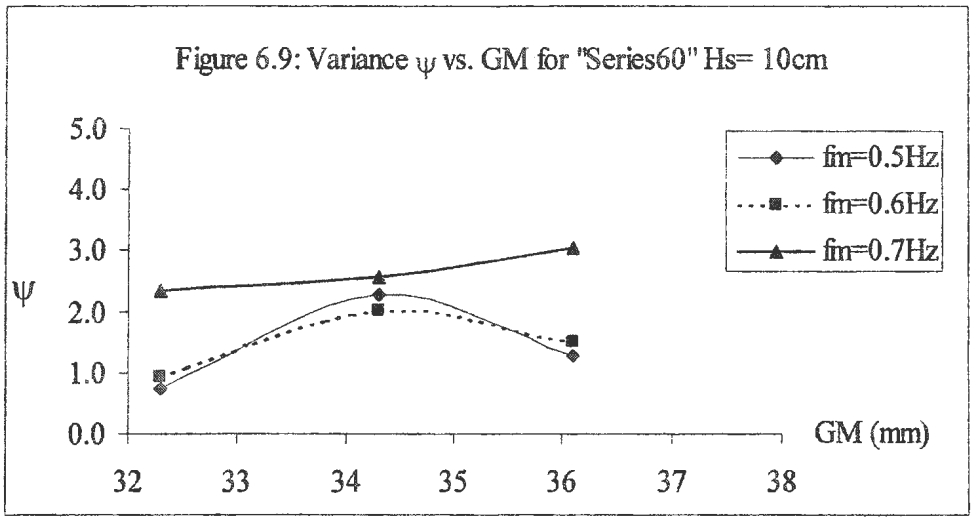
Figure 6.9: Variance ψ vs. GM for "Series60" Hs= 10cm
5.0
4.0
3.0
2.0
1.0
0.0
ψ
fm=0.5Hz
fm=0.6Hz
fm=0.7Hz
GM (mm)
32
33
34
35
36
37
38

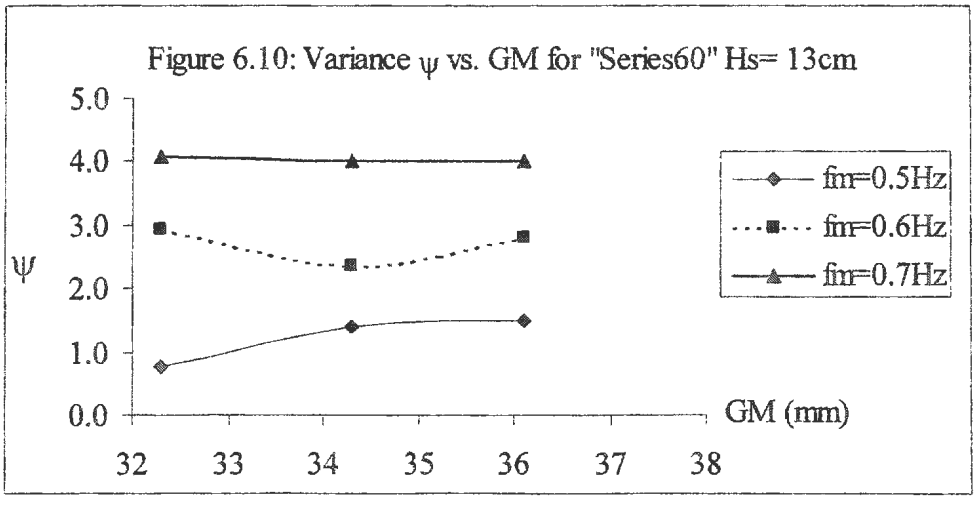
Figure 6.10: Variance ψ vs. GM for "Series60" Hs= 13cm
5.0
4.0
3.0
2.0
1.0
0.0
ψ
fm=0.5Hz
fm=0.6Hz
fm=0.7Hz
GM (mm)
32
33
34
35
36
37
38

Figure 6.11: Variance ψ vs. GM for "R-class" Hs= 7cm

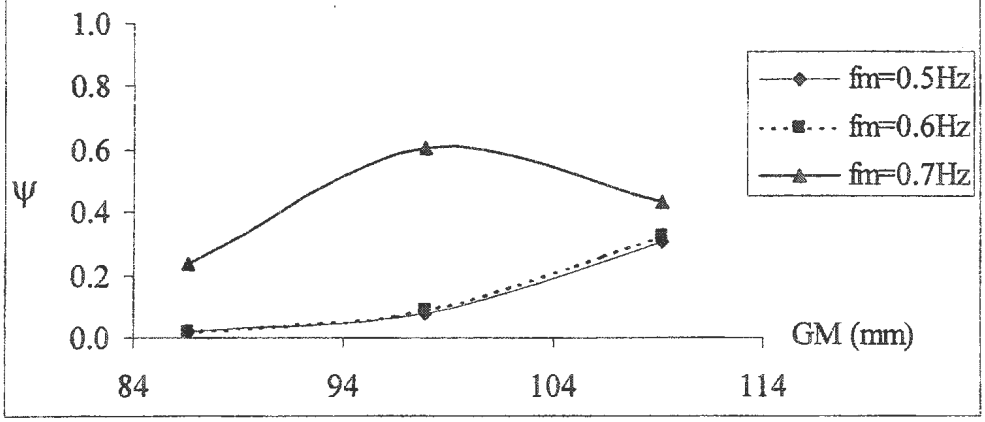

Figure 6.12: Variance ψ vs. GM for "R-class" Hs= 10cm

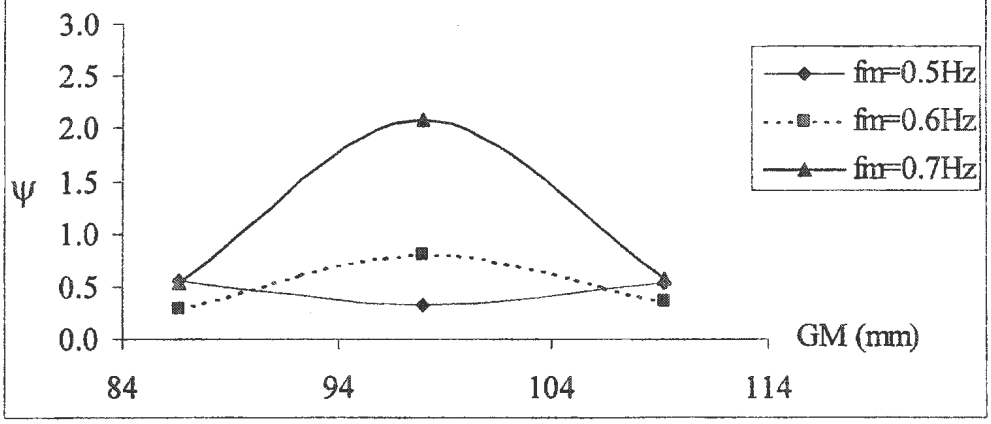

Figure 6.13: Variance ψ vs. GM for "R-class" Hs= 13cm

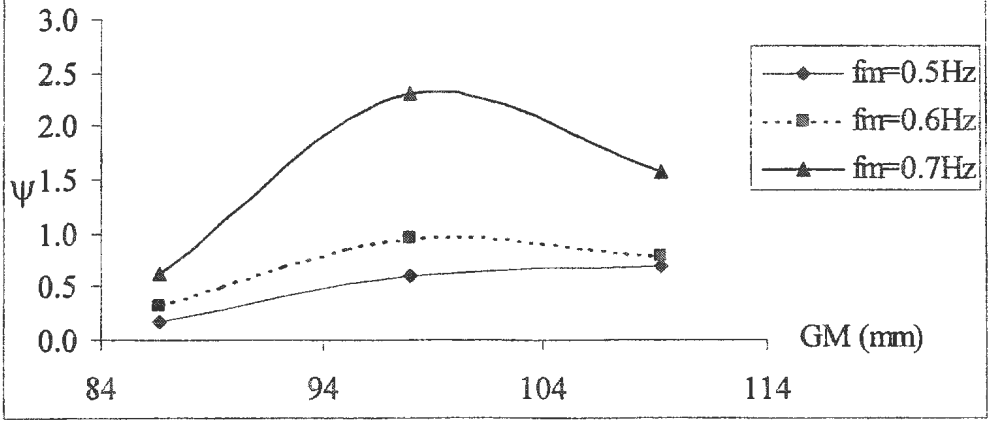

Figure 6.14: Variance ψ vs. Hs for "Series60" fm= 0.5 Hz

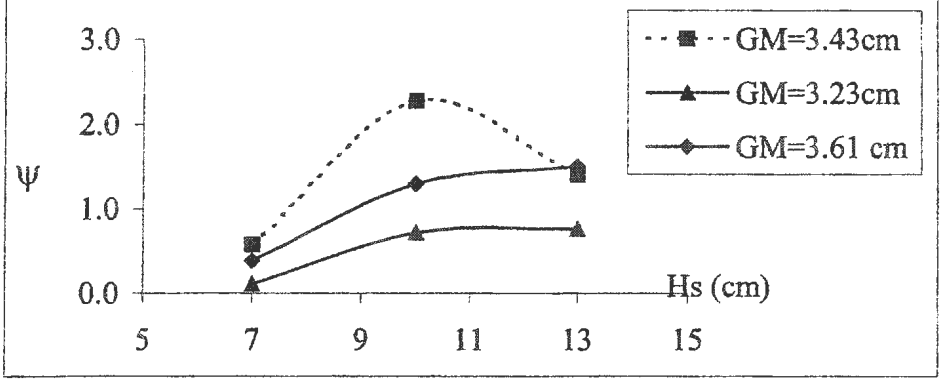

Figure 6.15: Variance ψ vs. Hs for "Series60" fm= 0.6 Hz

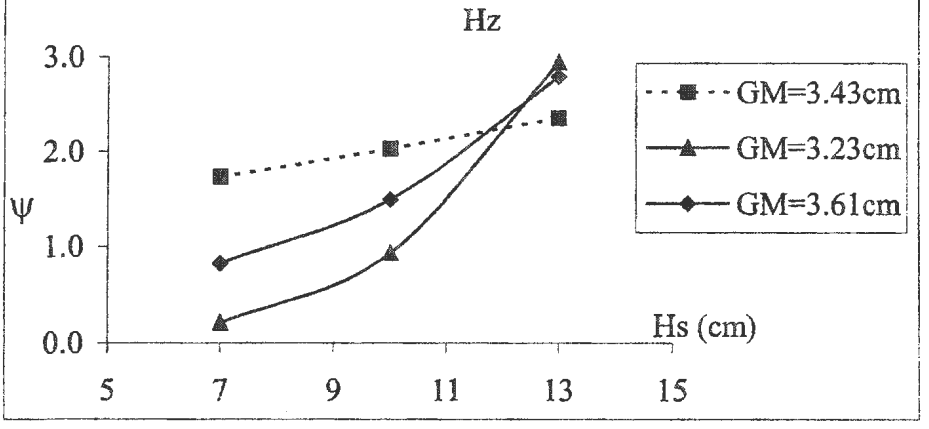

Figure 6.16: Variance ψ vs. Hs for "Series60" fm= 0.7 Hz

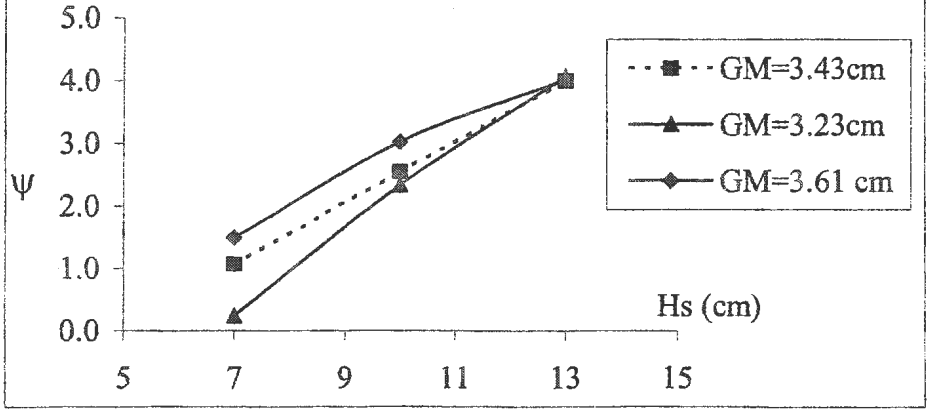

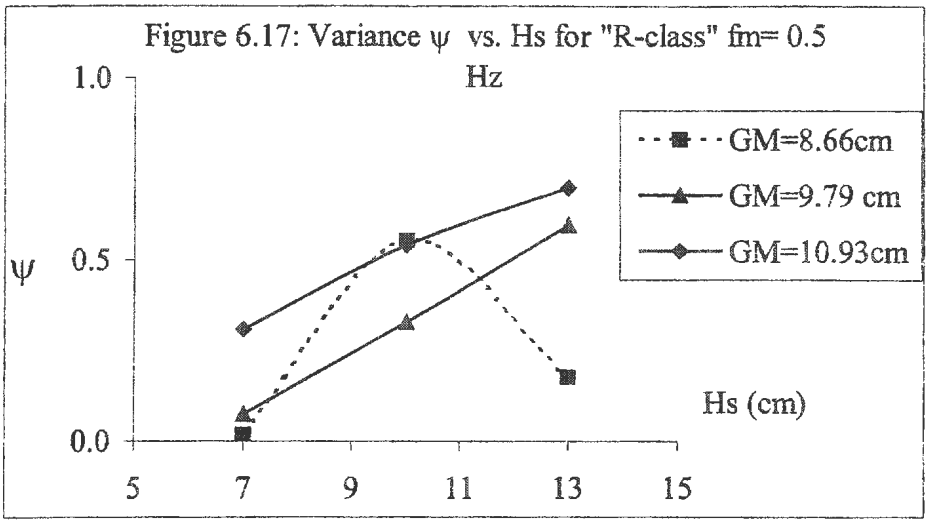
Figure 6.17: Variance ψ vs. Hs for "R-class" fm= 0.5 Hz
1.0
0.5
0.0
ψ
5
7
9
11
13
15
Hs (cm)
GM=8.66cm
GM=9.79 cm
GM=10.93cm

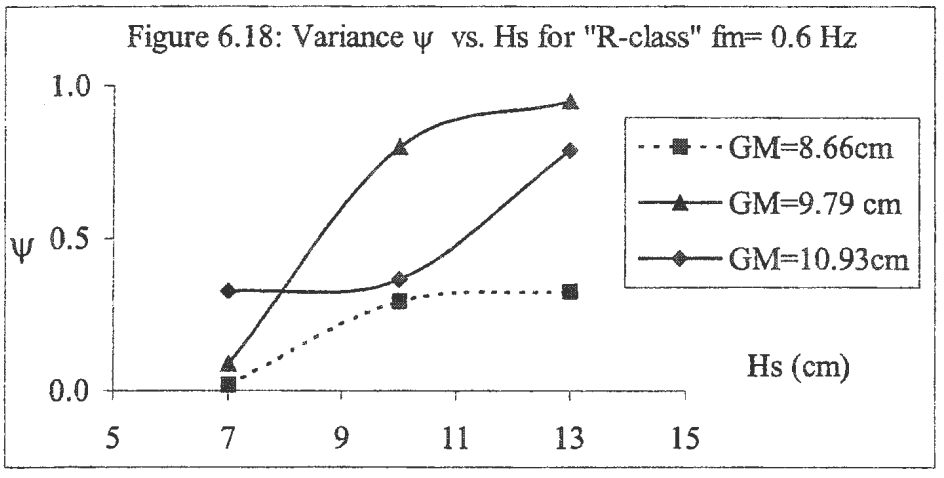
Figure 6.18: Variance ψ vs. Hs for "R-class" fm= 0.6 Hz
1.0
0.5
0.0
ψ
5
7
9
11
13
15
Hs (cm)
GM=8.66cm
GM=9.79 cm
GM=10.93cm

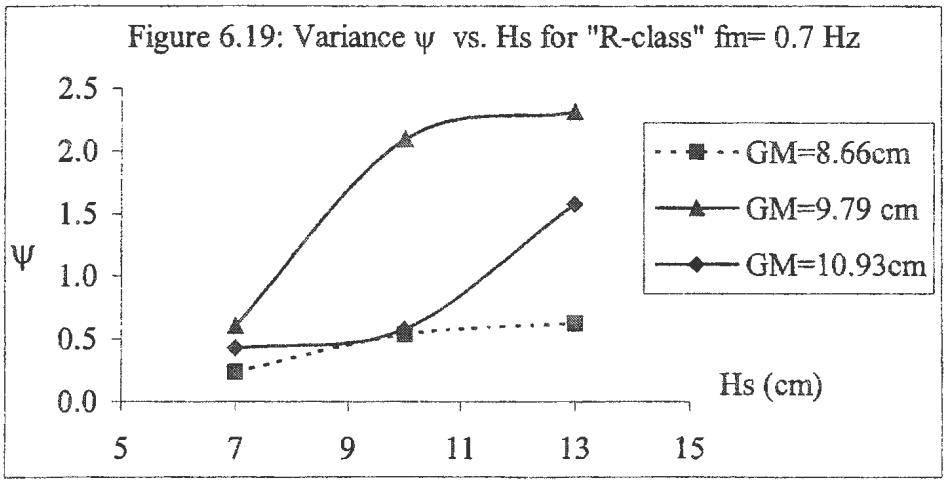
Figure 6.19: Variance ψ vs. Hs for "R-class" fm= 0.7 Hz
2.5
2.0
1.5
1.0
0.5
0.0
ψ
5
7
9
11
13
15
Hs (cm)
GM=8.66cm
GM=9.79 cm
GM=10.93cm

Figure 6.8 to Figure 6.19 show the variance ψ of the wave exciting moment as a function of GM value, wave modal frequency (f_m) and wave significant height (H_s). From these figures, we could not find any quantitative relationship that describe the variance ψ as a function of GM, wave height and wave frequency. So, Multiple Regression method is applied.

The purpose of multiple regressions is to establish a quantitative relationship between a group of parameters and a response. This relationship is useful for: 1. Understanding which parameters has the greatest effect. 2.Knowing the direction of the effect (i.e., increasing x increases/decreases y). 3.Using the model to predict future values of the response when only the parameters are currently known. Here, the multiple regression method is used to find the significant level of each variable on the predicted value of the variance ψ of the wave exciting moment.

Figure 6.20 shows the residuals plotted in case order for "Series60" model (upper part) and "R-class Icebreaker" model (lower part). The case number in Fig 6.20 is the order number from the upmost case to the lowest case in Table 6.3 and in Table 6.4 respectively. The 95% confidence intervals about these residuals are plotted as error bars. The 12th and the 22nd estimated the variance ψ values for "Series 60" model, and the 15th and 18th ones for "R-class Icebreaker" model are outliers since their error bars do not cross the zero reference line.

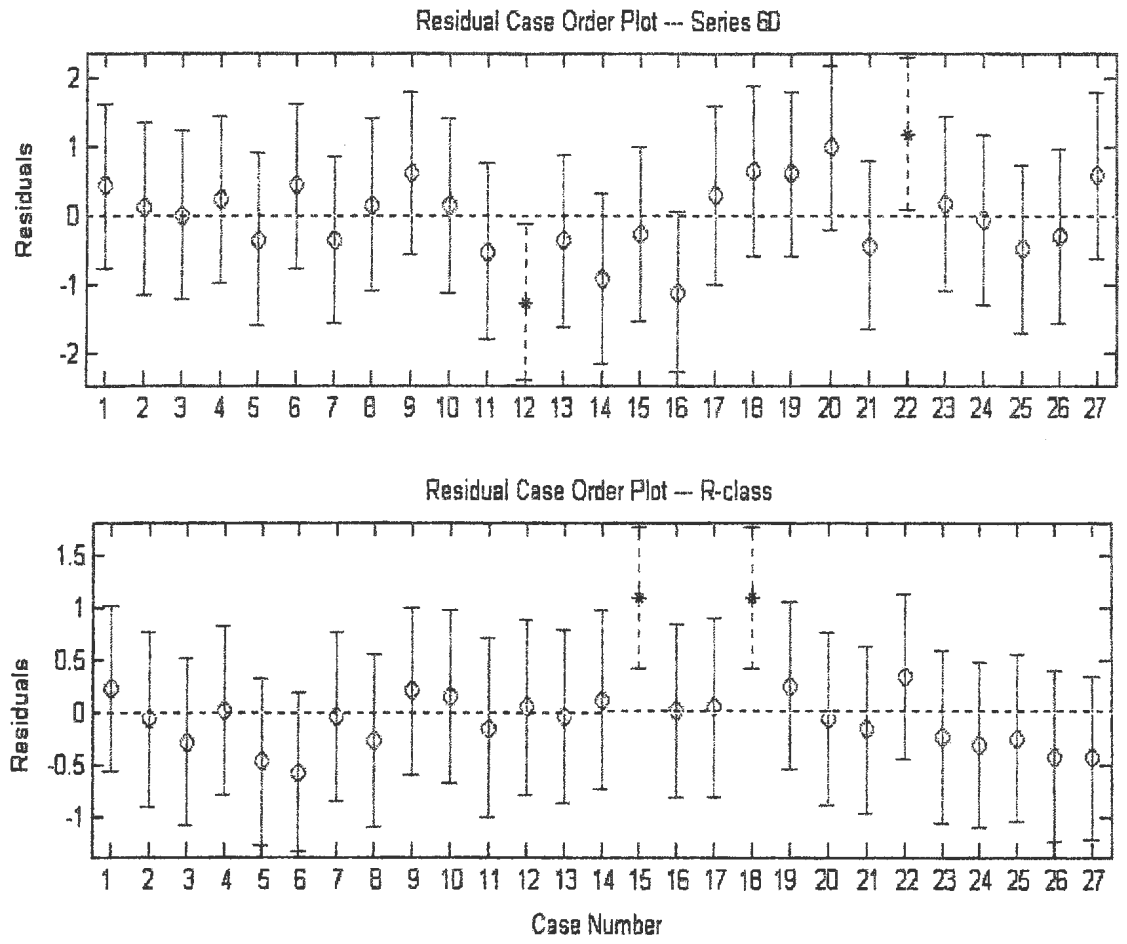

Figure 6.20: Residual vs. Case Number Plot

The corresponding experimental conditions are GM 3.23cm, Hs 7cm, fm 0.7Hz for "series 60" 12th case; GM 3.43cm, Hs 10cm, fm 0.5Hz for "series 60" 22nd case, which point has been found unreasonable in former analysis; GM value 9.79cm, Hs 10cm and 13cm, fm 0.7Hz for "R-class Icebreaker" 15th case and 18th case, separately. I cannot explain these four outliers after checking and comparing the original experiment data and the each partial result in estimation process for these four cases with those for other cases. So, these four cases were not thrown away from the further Multiple Regression analysis (MR).

Table 6.5: MR including all Interaction Terms

Terms	Parameter	p-value
Constant	4.7195	0.3044
Ship form	1.1169	0.0008
GM	-0.2357	0.7048
H_s	-1.0551	0.0199
f_m	-14.7269	0.0536
$GM*H_s$	0.0805	0.1818
$GM*f_m$	1.1871	0.2456
H_s*f_m	2.4520	0.0014
$GM*H_s*f_m$	-0.1851	0.0654

The 'parameter' in Fig. 6.5 to Fig.6.9 is a coefficient that means a given constant value for a specified variable (e.g. GM, H_s or H_s*f_m) in a regression model. The 'p-value' is the probability of observing a value of the test statistic that is at least as contradictory to the null hypothesis, and supportive of the alternative hypothesis, as the actual one computed from the sample data. (McClave et al. 1997)

Table 6.5 shows that the Multiple Regression (MR) result returned from all 54 cases data when the variance ψ of the wave exciting moment as a function depends on ship form, GM, Hs, fm, and their interaction terms. For the data of ship form, we use "1" to represent "Series 60" model and "-1" to represent "R-class" model in the multiple regression analysis. The p-value of ship form term is 0.34%, which is far less than 5% reference level. It shows that ship form is a significant factor in determining the variance ψ of the wave exciting moment.

Thus, Table 6.6 showed the MR analyses results for the two ship models separately. The p-values of all terms in Table 6.6 show that all linear and interaction terms are not significant because their p-values are far bigger than 5% reference level.

Table 6.6: MR including Interaction Terms for Two Models

	"Series 60" model		"R-class" model	
Terms	Parameter	p-value	Parameter	p-value
Constant	73.37	0.2443	-7.08	0.8007
GM	-19.94	0.2771	0.85	0.7663
Hs	-7.87	0.2004	0.61	0.8231
fm	-146.39	0.1629	13.29	0.7742
GM*Hs	2.07	0.2472	-0.088	0.7511
GM*fm	39.58	0.1945	-1.65	0.7263
Hs*fm	15.04	0.1411	-1.29	0.7747
GM*Hs*fm	-3.85	0.1937	0.1931	0.6720

Table 6.7: MR Results for Two Models

	"Series 60" model		"R-class" model	
Terms	Parameter	p-value	Parameter	p-value
Constant	-10.68	0.0007	-3.74	0.0025
GM	1.36	0.0827	0.28	0.1318
Hs	0.32	0.0000	0.11	0.0032
fm	7.66	0.0000	3.16	0.0043

Then, deleting all interaction terms, MR results are shown in Table 6.7 for two models separately. Table 6.7 shows that only GM term is not significant. From both Table 6.5 and Table 6.6, it also can be found that GM term, GM*H_s term and GM*f_m term are not

significant in determining the variance ψ. So, GM term is deleted, and the variance ψ as a function depends only on wave parameters.

Table 6.8: MR excluding GM Term for Two Models

	"Series 60" model		"R-class" model	
Terms	Parameter	p-value	Parameter	p-value
Constant	-6.03	0.000	-2.3923	0.0026
Hs	0.32	0.000	0.11	0.0039
fm	7.66	0.000	3.16	0.0052

The p-value in Table 6.8 shows that the variance ψ of the wave exciting moment basically depends on wave significant height and wave modal frequency in JONSWAP beam waves.

Now, returning to study Figure 6.2 to Figure 6.19, it seemed that the dependence of the variance ψ on GM and H_s is nonlinear. Then, GM^2 and Hs^2 terms are introduced, and H_s^2 term replaced with the variance V_H of the wave height in the experiment because the H_s^2 value is proportional to the V_H value. The multiple regression result is shown in Table 6.9.

Table 6.9: MR Results including GM^2 and V_H Terms

	"Series 60" model		"R-class" model	
Terms	Parameter	p-value	Parameter	p-value
Constant	-199.43	0.0431	-31.5142	0.0089
V_H	0.2190	0.0000	0.0790	0.0005
GM^2	-16.2310	0.0537	-0.2923	0.0187
fm	8.4785	0.0000	3.3380	0.0008
GM	112.48	0.508	5.8943	0.0159

Table6.9 shows that the variance ψ of the wave exciting moment depends on V_H and GM^2 value. However, the p-values of GM and GM^2 term for the "Series 60" model are a little bigger than the reference level 5%. The reason probably is too small changes between the GM values of the "Series 60" model in our experiments.

Finally, the multiple regression model for "Series 60" ship model is shown as:

$$\psi = -199.43 + 0.219V_H + 8.4785f_m + 112.48GM - 16.231GM^2$$

The multiple regression model for "R-class Icebreaker" ship model is shown as:

$$\psi = -31.5142 + 0.079V_H + 3.338f_m + 5.8943GM - 0.2923GM^2$$

Table 6.10: R^2 value for Different Function

Variables	R^2 value	
	Series60	R-class
V_H, GM^2, fm, GM	0.7244	0.6518
GM^2, fm, GM	0.3471	0.3872
V_H, fm, GM	0.6724	0.5497
V_H, GM^2, GM	0.3980	0.4113
V_H, GM^2, fm	0.6710	0.5437

The 'R^2 value' is called the coefficient of multiple determination, which is defined as:

$$R^2 = \frac{SSR}{SSTO} = 1 - \frac{SSE}{SSTO}$$

Here SSTO is the total error sum of square; SSR is the regression error sum of square; SSE is the error sum of square.

The general nonlinear model of the variance ψ as a function of V_H, Gm^2, GM and fm explained 72.44% of the variation of the variance ψ for the "Series 60" ship model in random waves, and explained 62.14% of the variation of the variance ψ for the "R-class Icebreaker" ship model (Table 6.10). The GM and GM^2 terms contribute about 10% to the variation of the variance ψ for the "Series 60" model, and above 20% to "R-class Icebreaker" model. The main contribution comes from wave modal frequency and the variance of wave height.

Chapter 7

Conclusions and Recommendations

7.1 Conclusions

In this study, a new method has been developed for estimating the variance ψ of the wave exciting moment per unit virtual mass moment inertia from the time history of the roll displacement in random waves. The variation of the variance ψ depends on wave frequency, wave height, ship form, and GM and GM square value in JONSWAP beam waves.

The validation of the proposed method covered various waves and different nonlinear restoring moments and damping moments to generate simulated roll data. The random decrement technique and the neural networks technique were successfully combined in the process of identifying equivalent linear restoring coefficient and equivalent linear damping coefficient. The comparison between the estimated variance ψ value and the true variance ψ value showed very small errors, which indicate that it is reasonable to use the method for the variance ψ of the wave exciting moment identification in random waves.

The method was used to predict the variance ψ of the wave exciting moment from experimental data of "Series 60" and "R-class Icebreaker" ship models under different JONSWAP beam waves. The method could not be verified using experimental results because the wave excitation to the models could not be measured in the experiments. However, through a series of Multiple Regression analyses combining with studying the regression fit figures of the variance ψ, several conclusions can be achieved.

- Wave frequency and the variance of wave height are the main factors in determining the variance ψ of the wave exciting moment in random waves.
- GM value shows quadratic nonlinear effect in determining the variance ψ of wave exciting moment in random waves.
- No interaction terms between GM value, wave frequency and wave height are significant in determining the variance ψ of the wave exciting moment.

7.2 Recommendations

Based on this study, the following recommendations have been made and should be studied in further research.

- Using sensitive instrument to measure the wave excitation in ship model experiment, calculating the true variance ψ of wave exciting moment, further verifying the proposed method.
- The effect of ship form on the variance ψ of the wave exciting moment should be investigated through testing more ship models.
- The effect of GM value on the variance ψ of the wave exciting moment should be investigated through testing more ship models and GM values.
- A more accurate method is needed to predict the parameters of ship roll motion in random waves.
- Using other time history records of ship motions (for example, pitch record) to estimate the variance ψ of wave exciting moment.

References

Bass, D.W. and Haddara, M. R. (1988) "Nonlinear Models of Ship Roll Damping Moment", International Shipbuilding Progress, Vol. 35, No. 401, pp. 5-24.

Caughey, T.K. and Stumpt, H.J. (1961) "Transient Response of a Dynamic System Under Random Excitation", Journal of Applied Mechanics, pp. 563-566.

Cole, H.A. (1973) "On-line Failure Detection and Damping Measurement of Aerospace Structures by Random Decrement Signatures", NASA CR-2205.

Dalzell, J.F. (1978) "A Note on the Form of Ship Roll Damping", Journal of Ship Research, Vol. 35, No. 22, pp. 178-185.

Froude, W. (1955) "The Papers of William Froude", The Inst. Of Naval Arch., London.

Haddara, M. R. (1971) "On the Stability of Ship Motion in regular Oblique Waves", International Shipbuilding Progress, Vol. 18, No. 207, pp. 416-434.

Haddara, M. R. (1974) "A Modified Approach for the Application of Fokker-Planck Equation to the Nonlinear Ship Motions in Random Waves", International Shipbuilding Progress, Vol. 21, No. 242, pp. 283-288.

Haddara, M. R. (1980) "On the Parametric Excitation of Nonlinear Rolling Motion in Random Seas", International Shipbuilding Progress, Vol. 27, No. 315, pp. 291-293.

Haddara, M. R. (1983) "A Note on the Power Spectrum of Nonlinear Rolling Motion", International Shipbuilding Progress, Vol. 30, No. 342, pp. 41-43.

Haddara, M. R. (1984) "A Note on the Effect of Damping Moment Form on Rolling", International Shipbuilding Progress, Vol. 31, No. 363, pp. 285-290.

Haddara, M. R. and Bennett, P. (1989) "A Study of the Angle Dependence of Roll Damping Moment", Ocean Engineering, Vol. 16, No. 4, pp. 411-427.

Haddara, M. R. (1992) "On the Random Decrement for Nonlinear Rolling Motion", Proceedings of the 11th International Conference on Offshore Mechanics and Arctic Engineering, Vol. II, Safety and Reliability, pp. 321-324.

Haddara, M. R. and Wu, X. (1993) "Parameter Identification of Nonlinear Rolling Motion in Random Seas", International Shipbuilding Progress, Vol. 40, No. 423, pp. 247-260.

Haddara, M. R. Wishahy, M. and Wu, X. (1994) "A Study of the Angle Dependence of Roll Damping Moment", Ocean Engineering, Vol. 21, No. 8, pp. 781-800.

Haddara, M. R. and Zhang, S. (1994) "Effect of Forward Speed on the Roll Damping of three Small Fishing Vessels", Journal of Offshore Mechanics and Arctic Engineering, Vol. 116, No. 2, pp. 102-108.

Haddara, M. R. (1995) "On the Use of Neural Network Techniques for the Identification of Ship Stability Parameters at Sea", Proceedings of the 14th International Conference on Offshore Mechanics and Arctic Engineering, Vol. II, Safety and Reliability, pp. 321-324.

Haddara, M. R. and Hinchey, M. (1995) "On the Use of Neural Network Techniques in the Analysis of Free Decay Curves", International Shipbuilding Progress, Vol. 42, No. 430, pp. 166-178.

Haddara, M. R. (2000) "On the Roll Damping Characteristics of a Series 60 Block 60 Model", Ocean Engineering International, Vol. 5, No. 1, pp. 54-60.

Ibrahim, S.R. and Mikulcik, E.C. (1976) "The Experimental Determination of Vibration Parameters from Time Responses", Shock and Vibration Bulletin,Bull. No. 46, part 5.

Ibrahim, S.R. (1977) "Random Decrement Technique for Modal Identification of Structures", The AIAA Journal of Spacecraft, Vol. 14, No. 11, pp. 696-700.

Ljung,L. (1999) "System Identification Theory for the User", Second Edition, Prentice Hall PTR.

Lloyd, A.R.J.M. (1998). "Seakeeping: Ship Behaviour in Rough Weather", Second Edition, Ellis Horwood Series in Marine Technology.

Mathiesen, J.B. and Price, W.G. (1984) "Estimation of Ship Roll Damping Coefficients" Transaction of the Royal Institution of Naval Architects, pp. 295-307.

McClave,J.T., Dietrich, F.H. and Sincich T. (1997) "Statistics", Seventh Edition, Prentice Hall, New Jersey.

Roberts, J.B. (1985) "Estimation of Nonlinear Ship Roll Damping from Free-decay Data", Journal of Ship Research. Vol. 29, No. 2, pp. 127-138.

Roberts, J.B., Dunne, J.F. and Debonos, A., (1991) "Estimation of Ship Roll Parameters in Random Waves", Proceedings of the 10th International Conference on Offshore Mechanics and Arctic Engineering, Vol. II, Safety and Reliability. Pp. 97-106.

Vandiver, J.K., Dunwoody, A.B., Campbell, R.B. and Cook, M.F. (1982) "A Mathematical Basis for the Random Decrement Vibration Signature Analysis Technique", Journal of Mechanical Design, Vol. 104, pp. 307-313.

Xing, Zhiliang. (1999) "Estimation for the Maximum Amplitude of Ship Roll Motion in Random Waves", Thesis, Ocean University of Qingdao.

Appendix A

Comparison of Regular Response Curves

Figure A.1: Compare the regular response of case 513

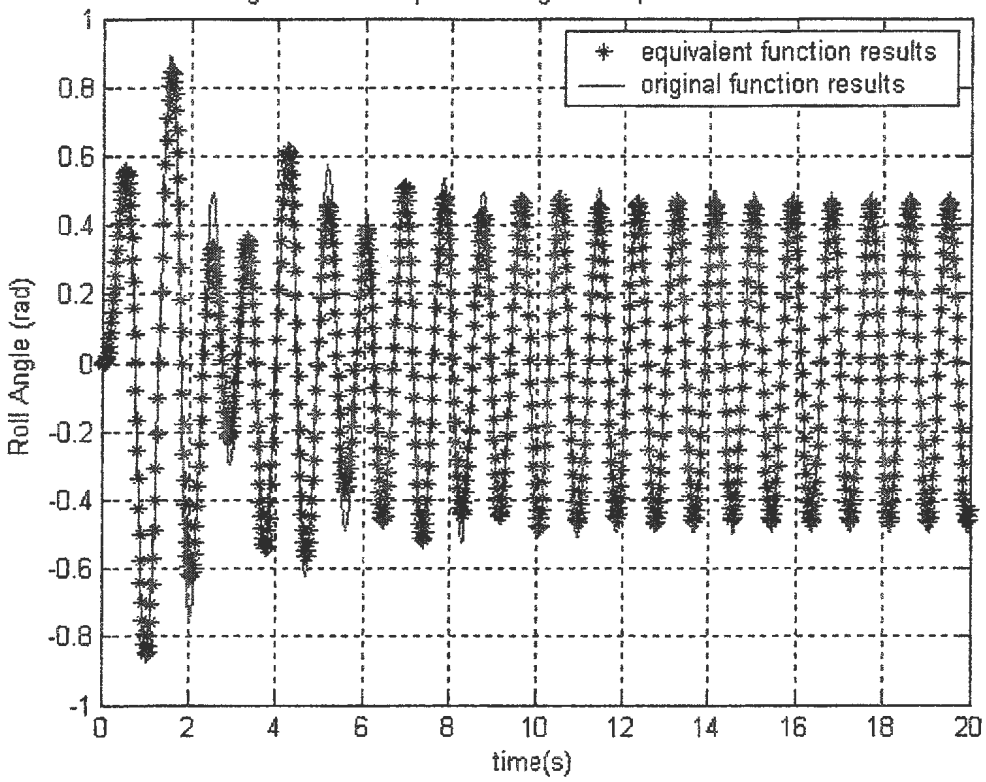

Figure A.2: Compare the regular response of case 515

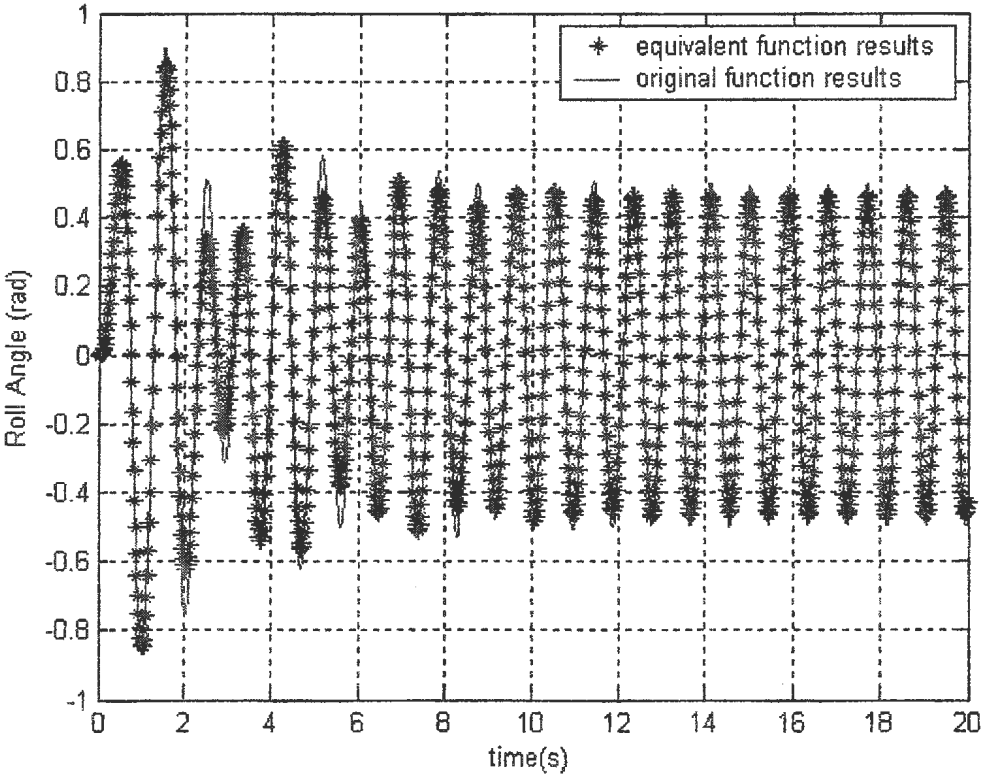

Figure A.3: Compare the regular response of case 531

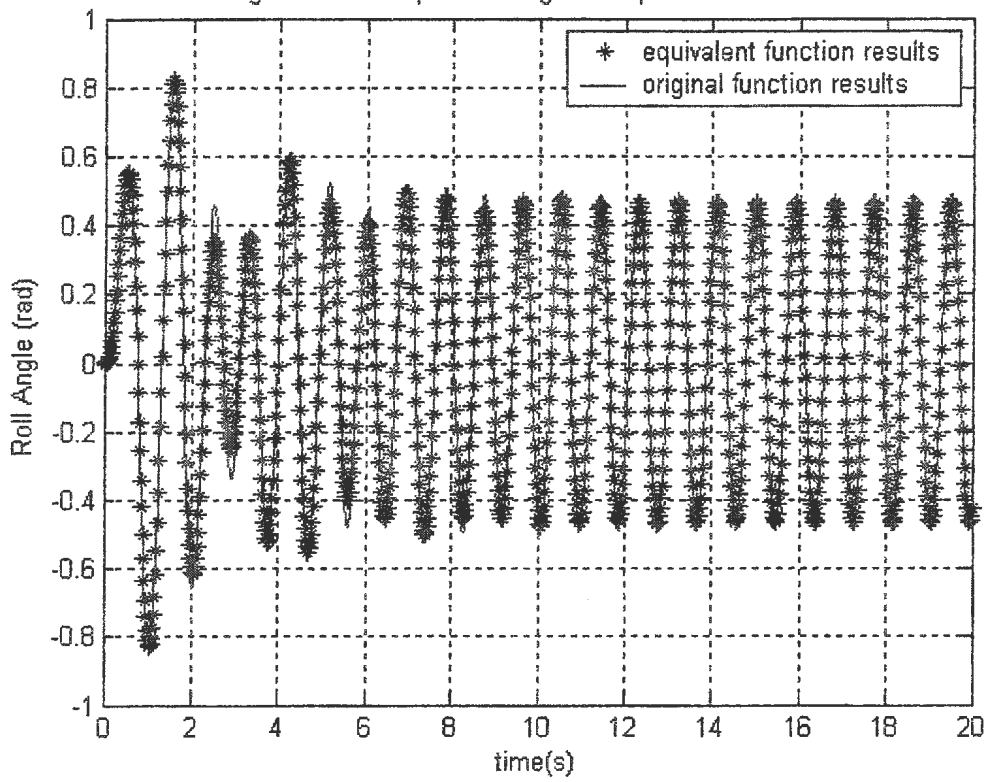

Figure A.4: Compare the regular response of case 533

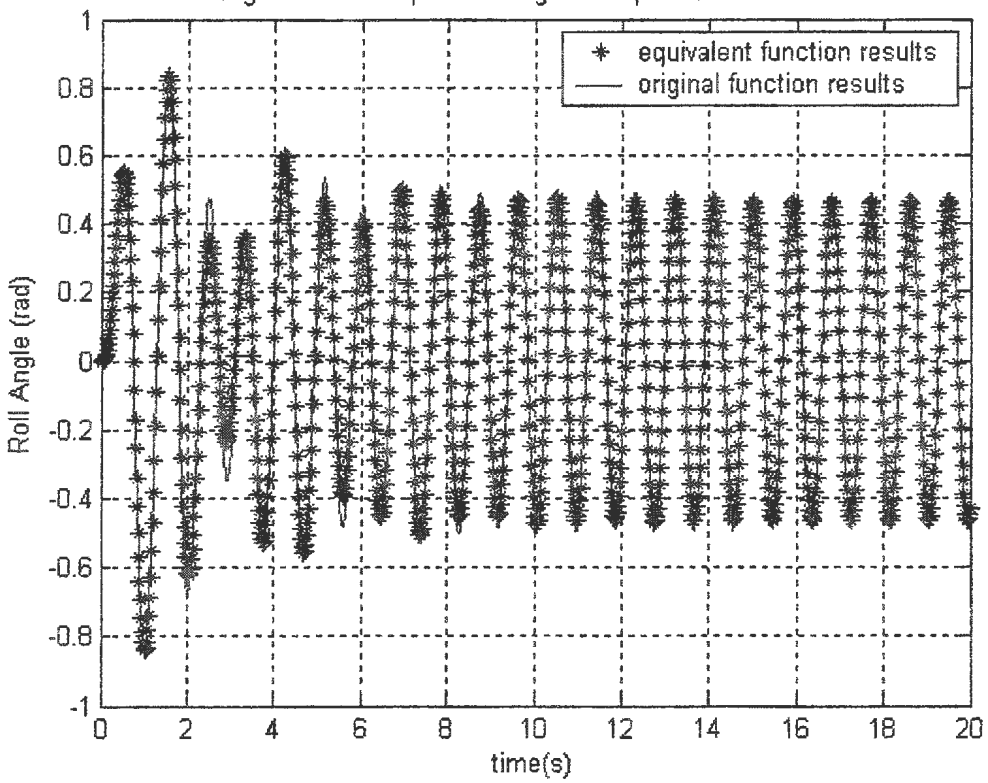

Figure A.5: Compare the regular response of case 535

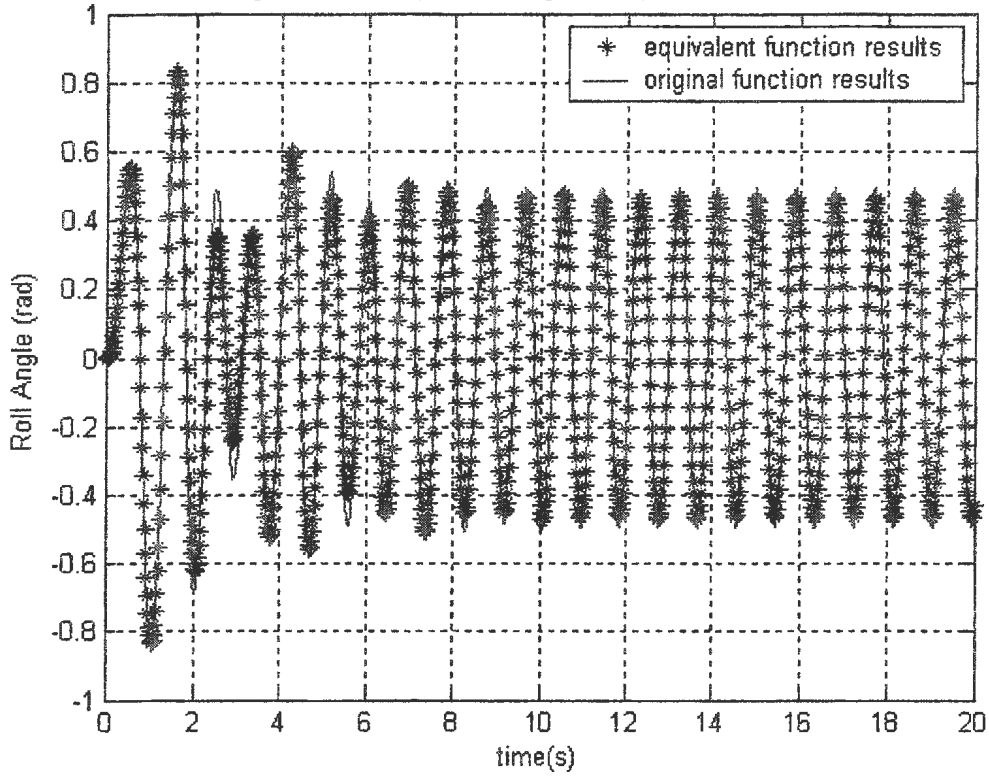

Figure A.6: Compare the regular response of case 551

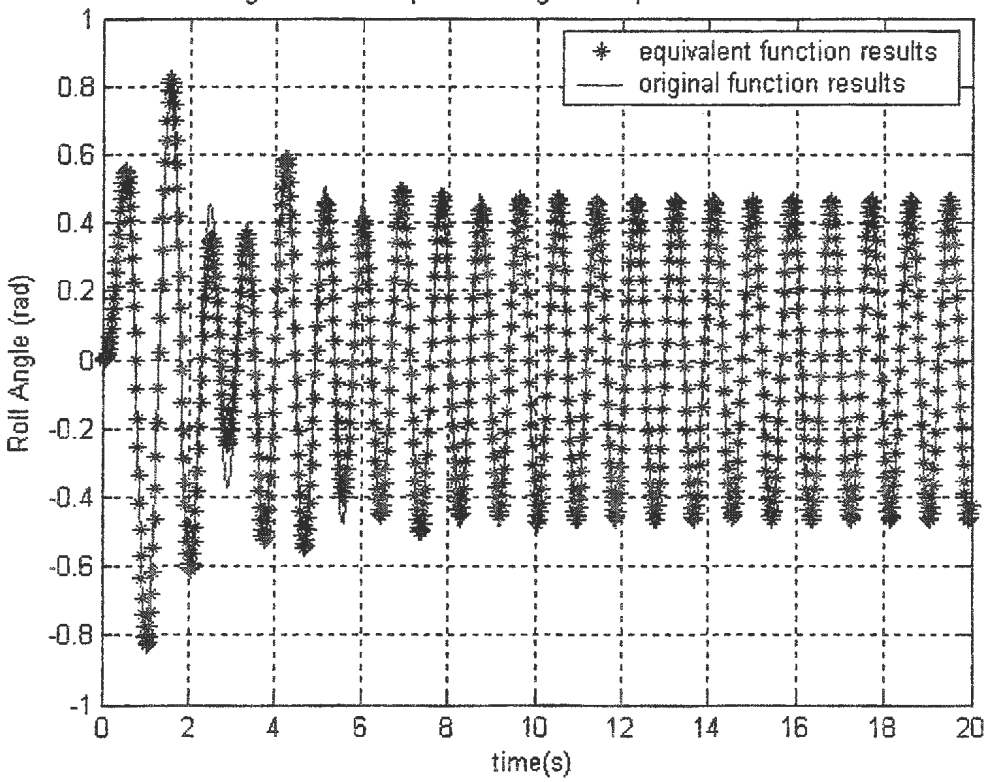

Figure A.7: Compare the regular response of case 553

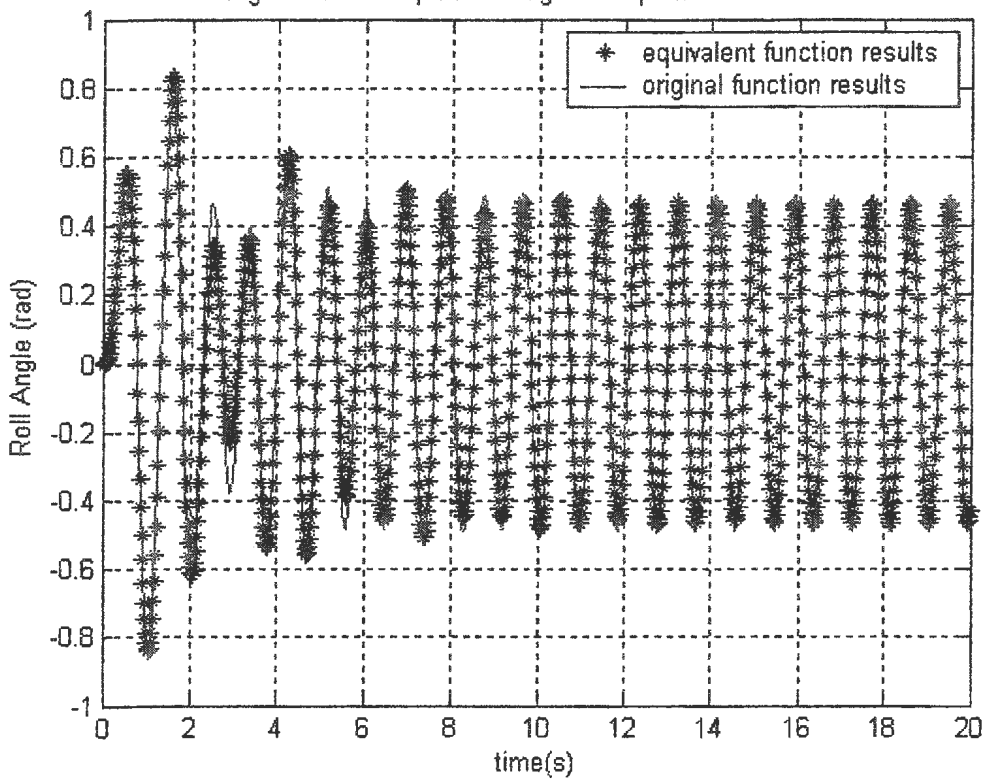

Figure A.8: Compare the regular response of case 555

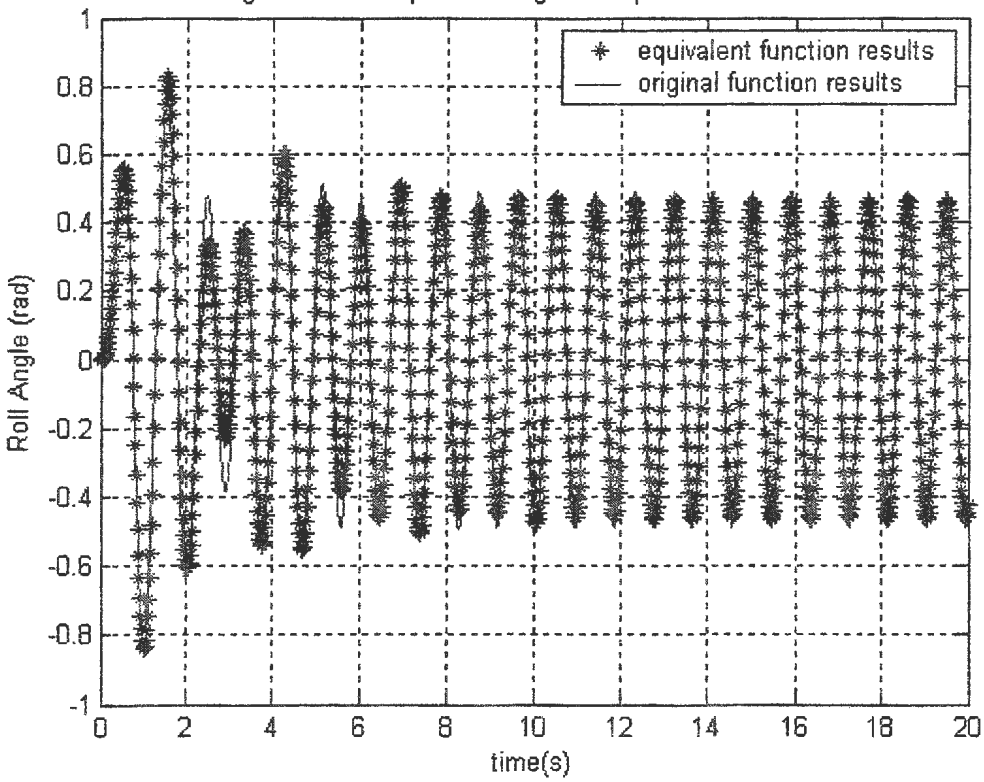

Figure A.9: Compare the regular response of case 51010

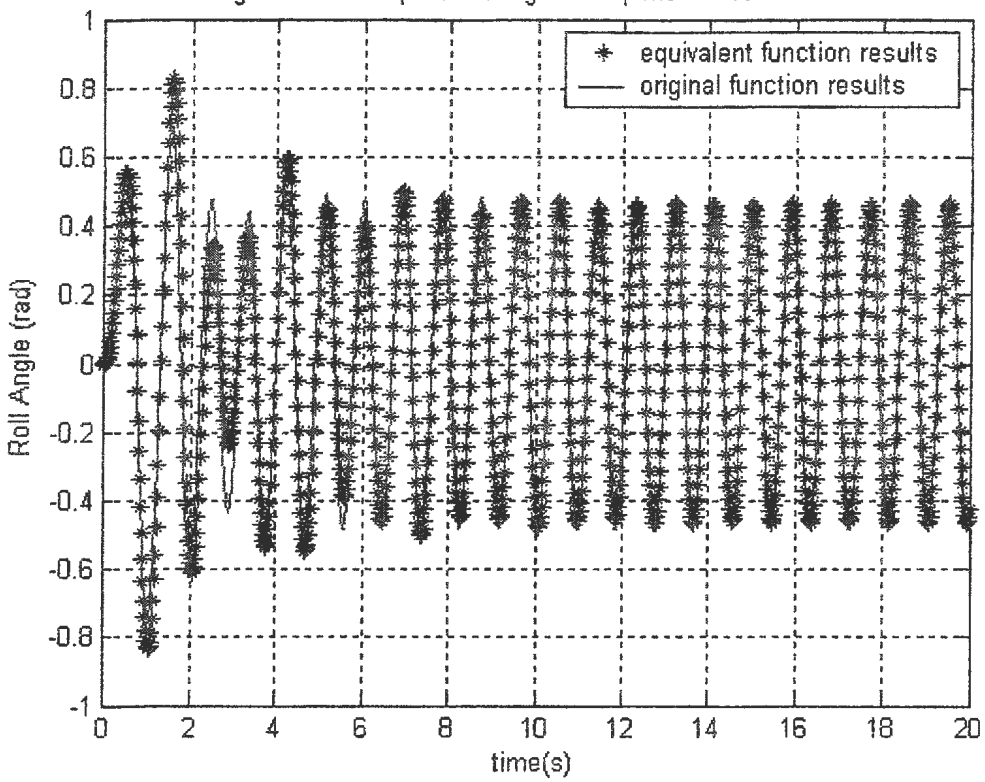

Figure A.10: Compare the regular response of case 611

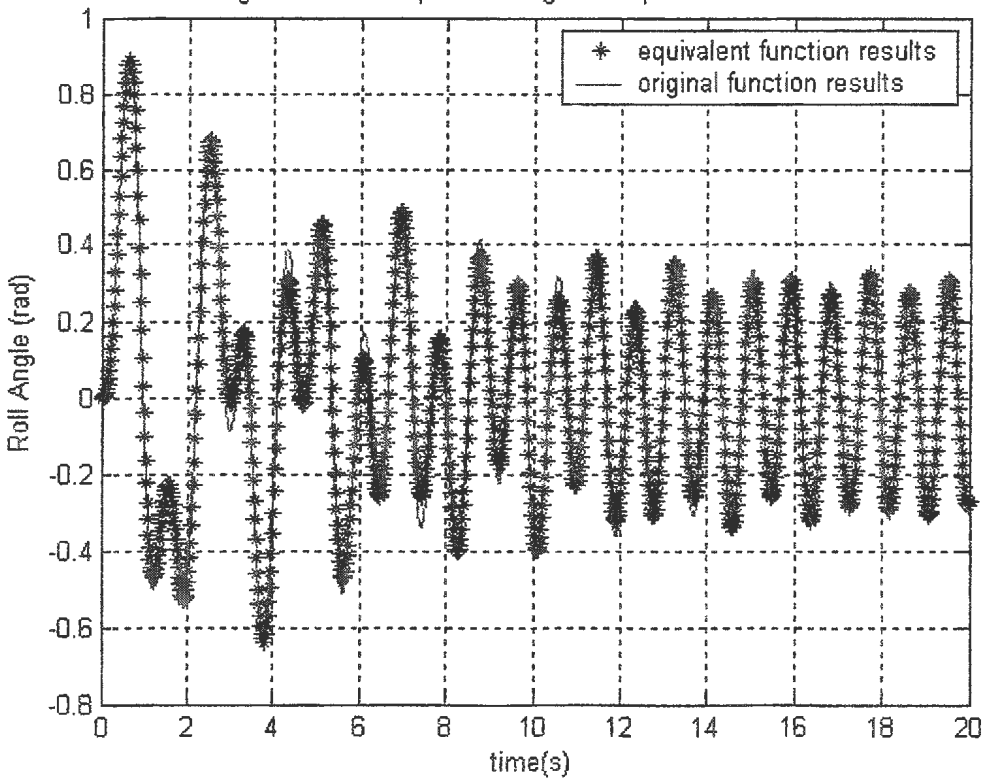

Figure A.11: Compare the regular response of case 613

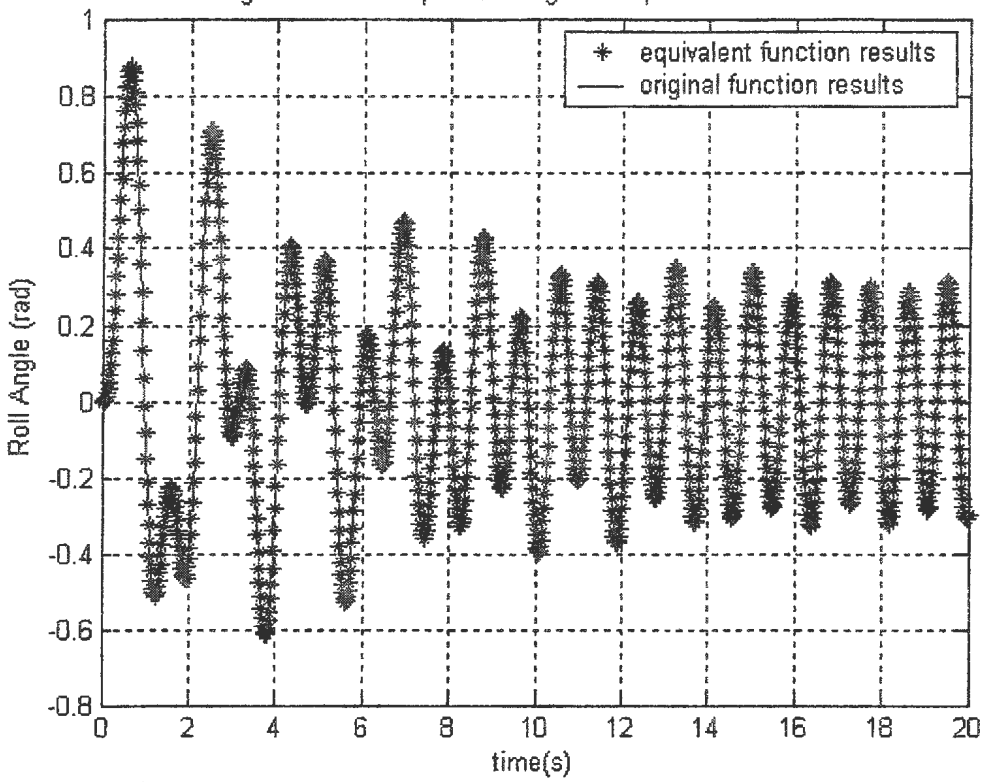

Figure A.12: Compare the regular response of case 615

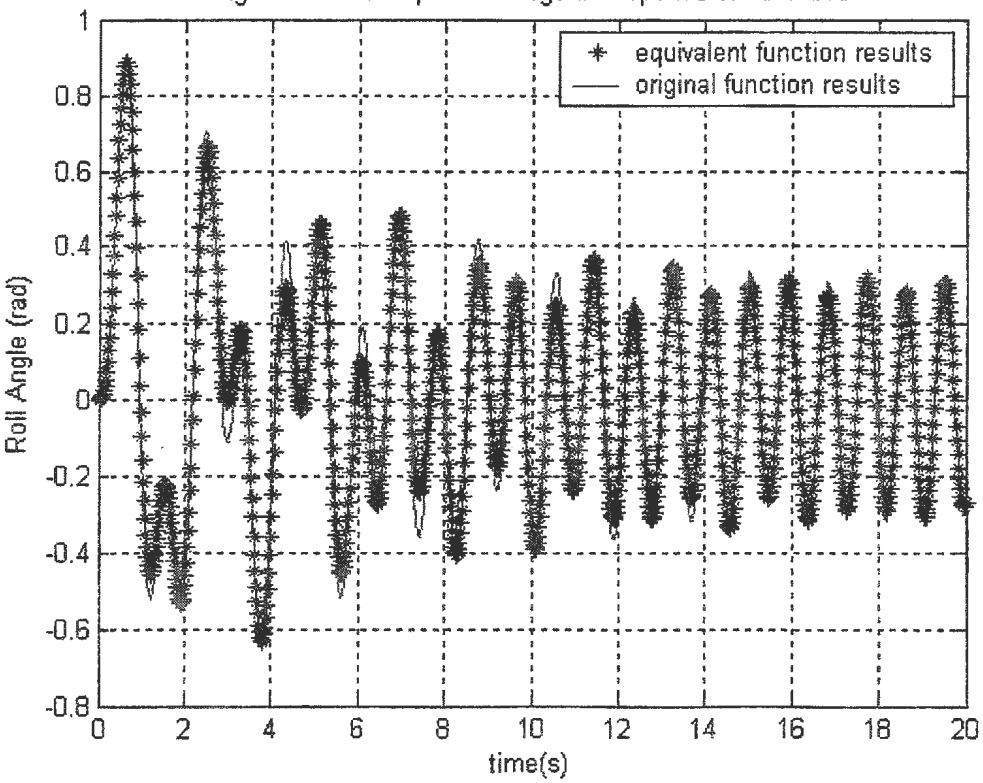

Figure A.13: Compare the regular response of case 631

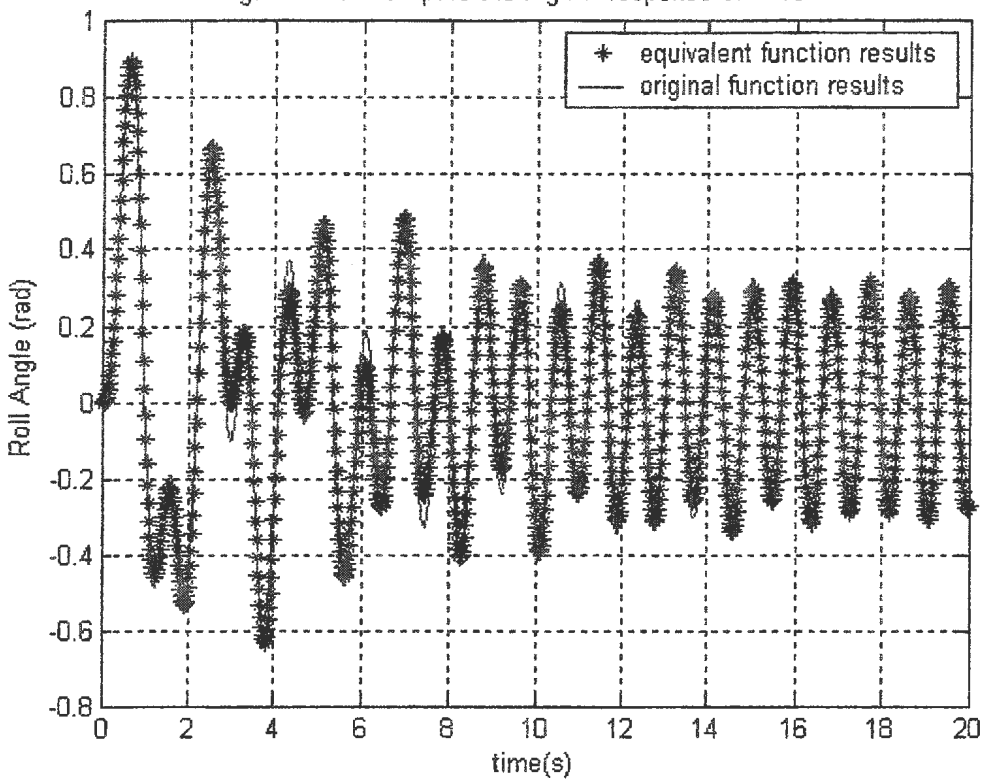

Figure A.14: Compare the regular response of case 633

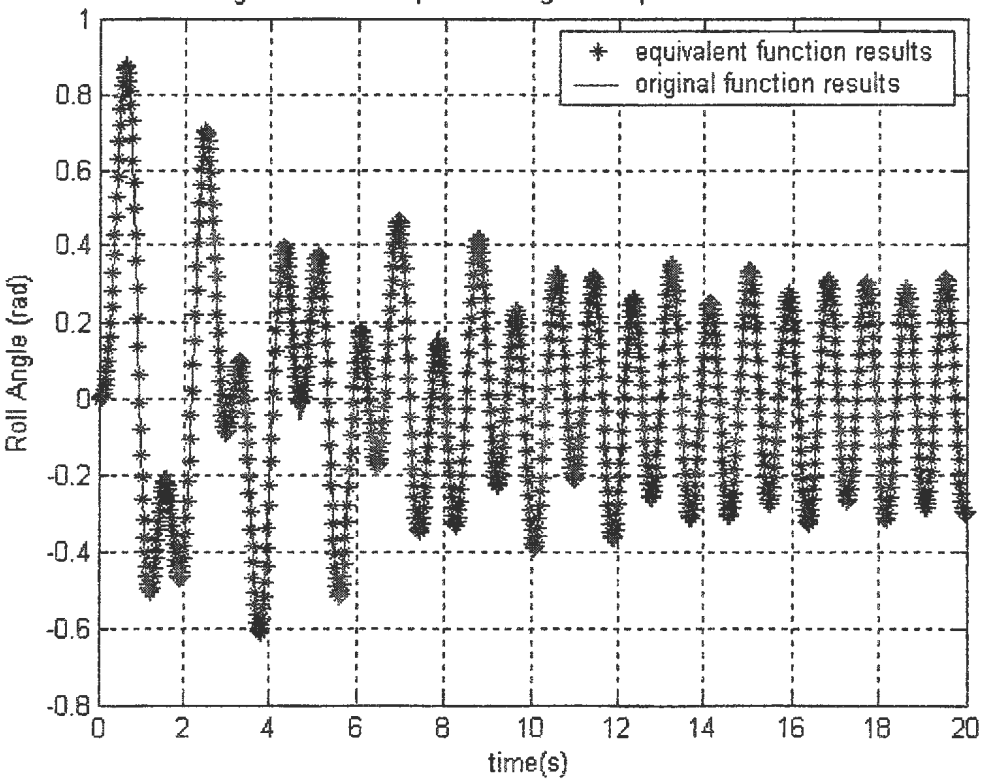

Figure A.15: Compare the regular response of case 635

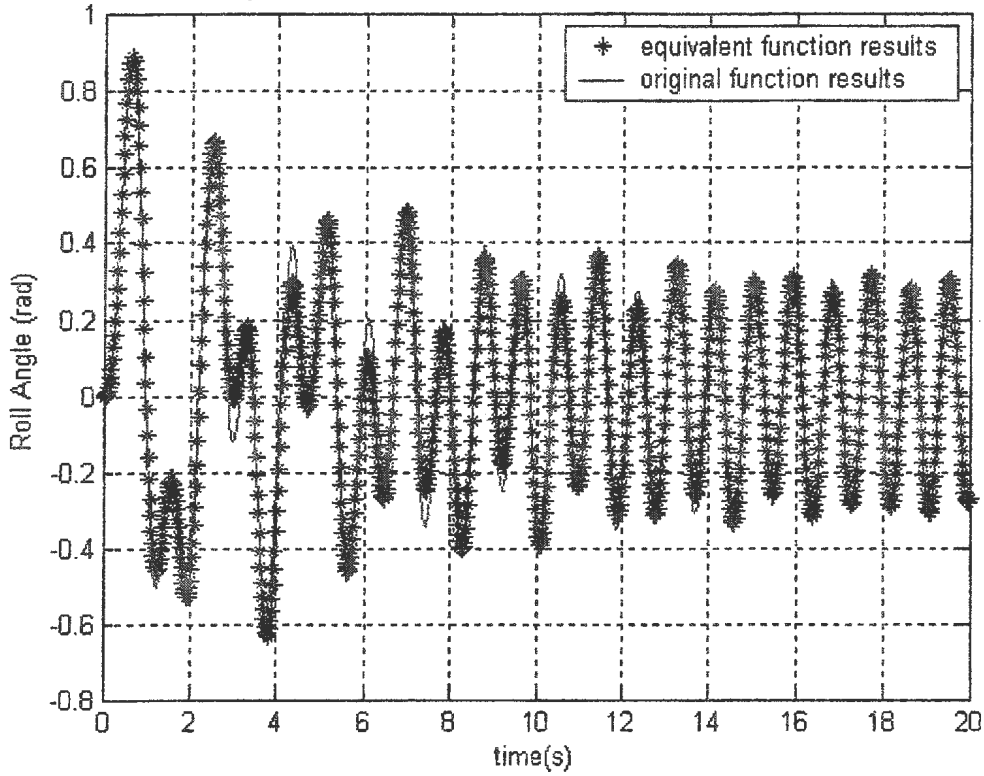

Figure A.16: Compare the regular response of case 651

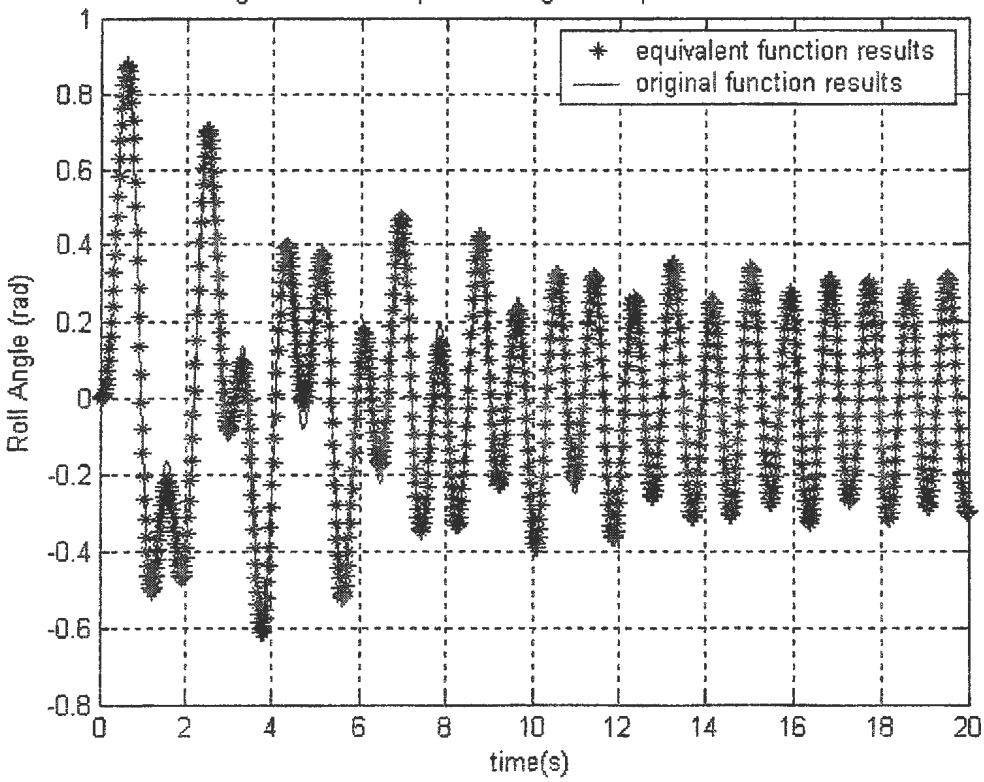

Figure A.17: Compare the regular response of case 653

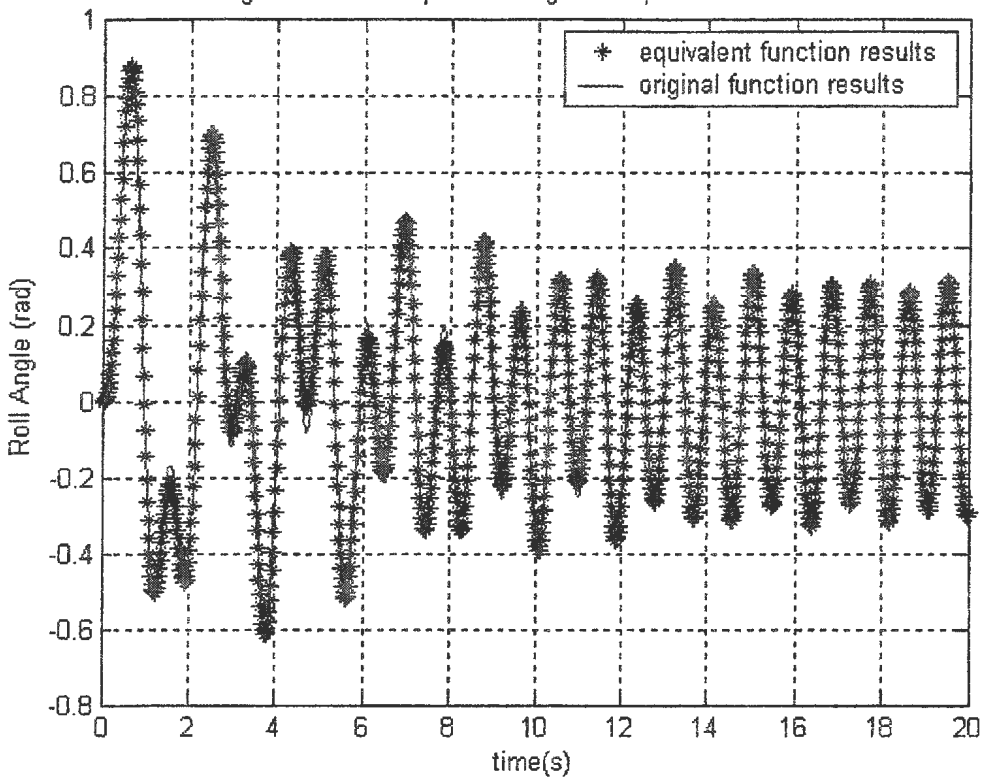

Figure A.18: Compare the regular response of case 655

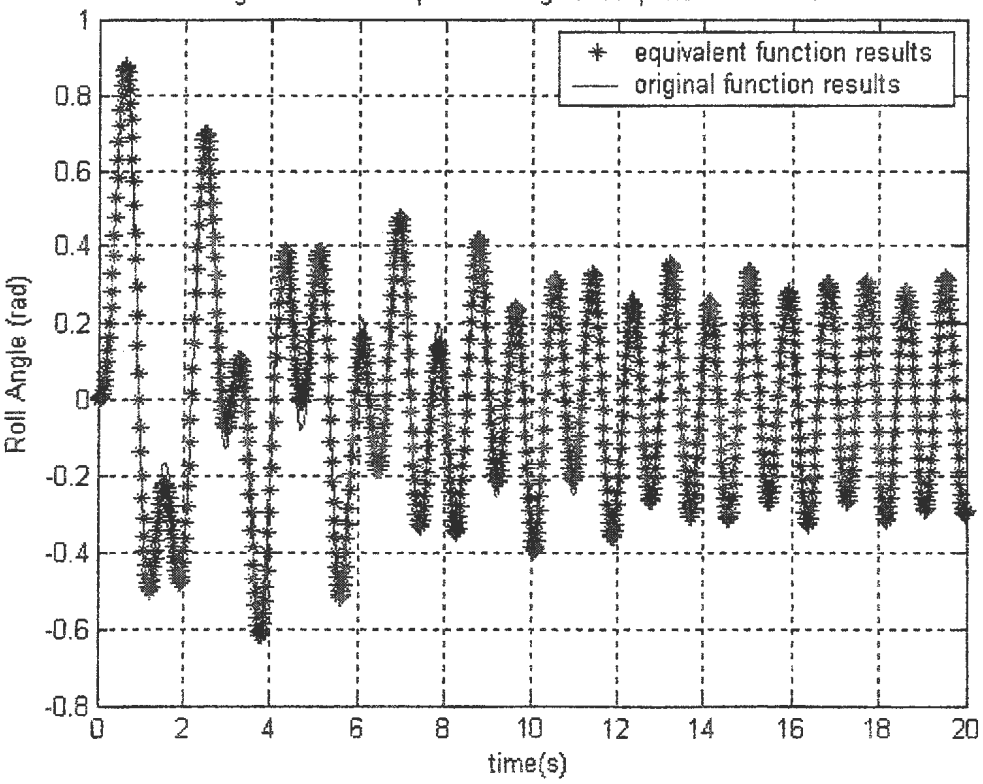

Figure A.19: Compare the regular response of case 61010

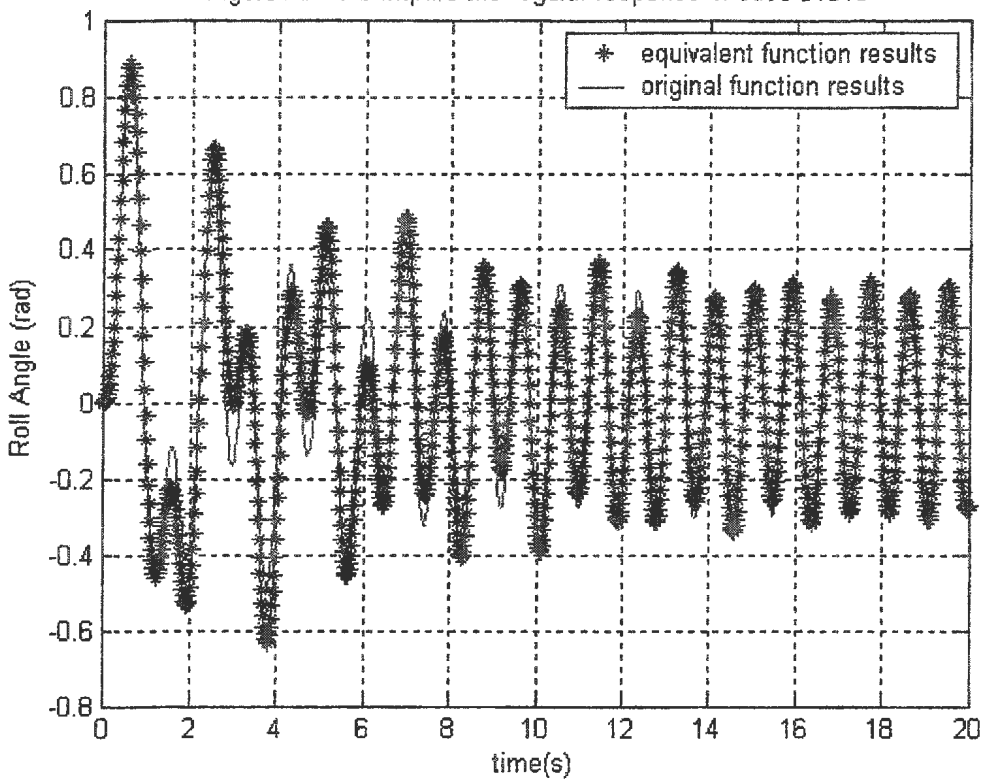

Figure A.20: Compare the regular response of case 61050

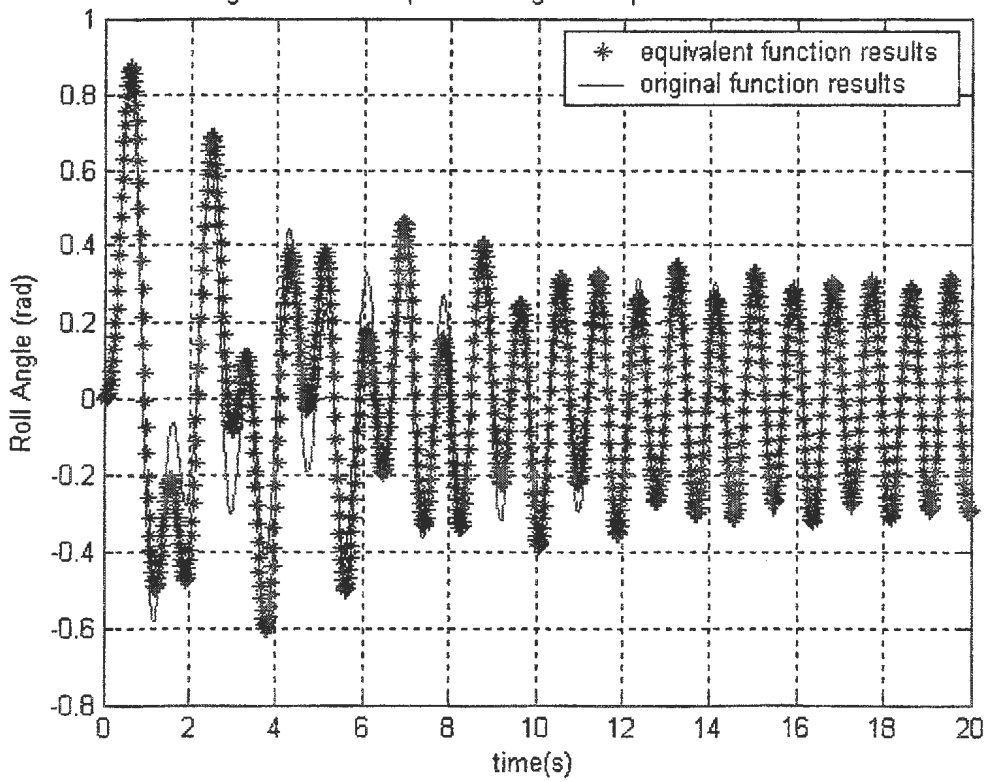

Figure A.21: Compare the regular response of case 63050

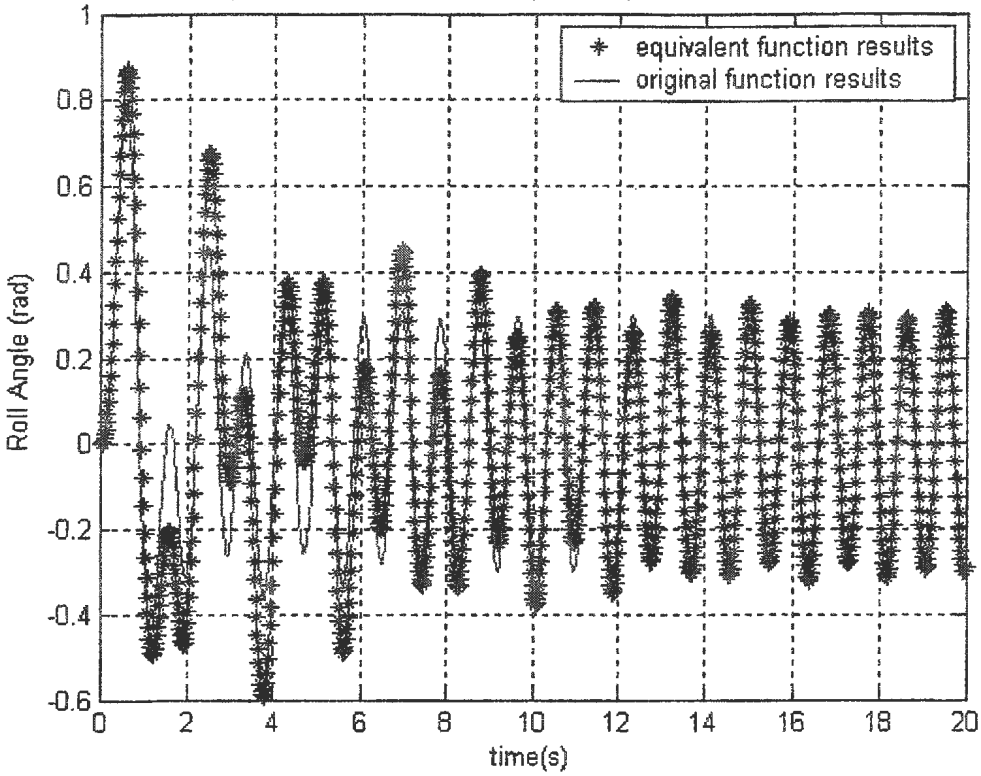

Figure A.22: Compare the regular response of case 411

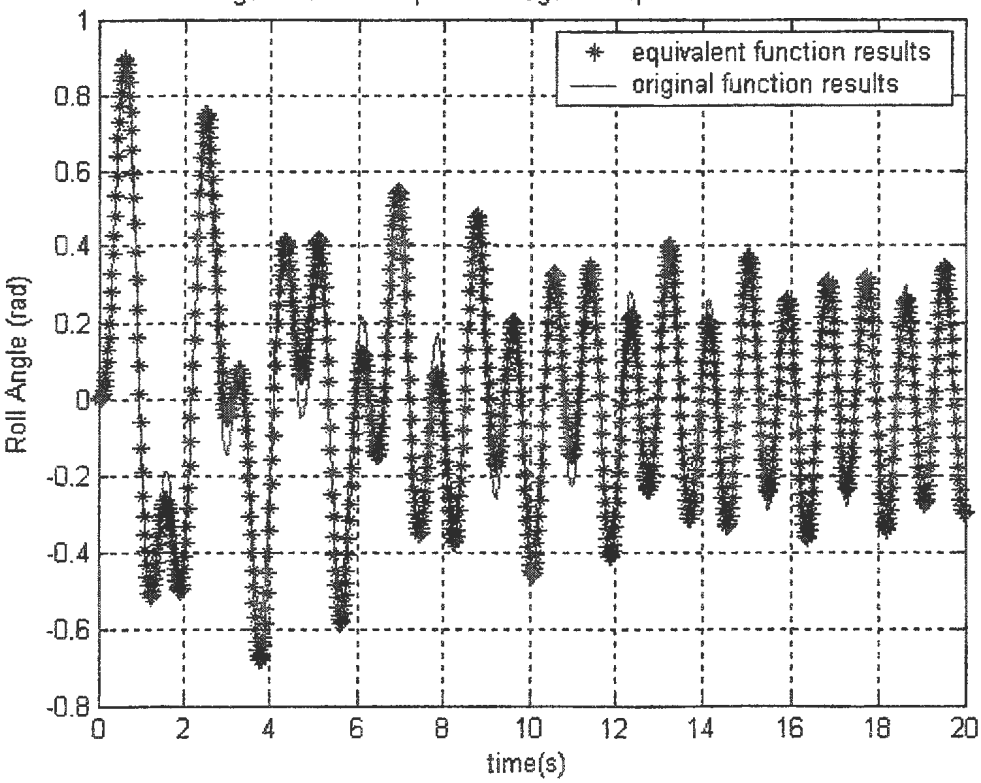

Figure A.23: Compare the regular response of case 413

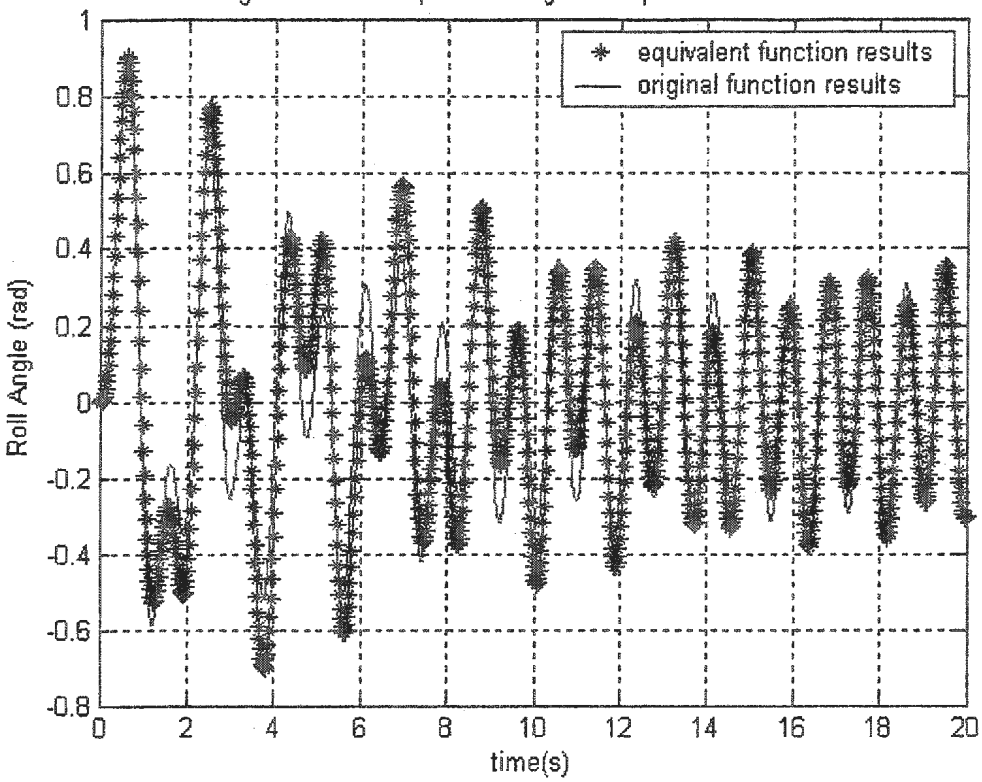

Figure A.24: Compare the regular response of case 415

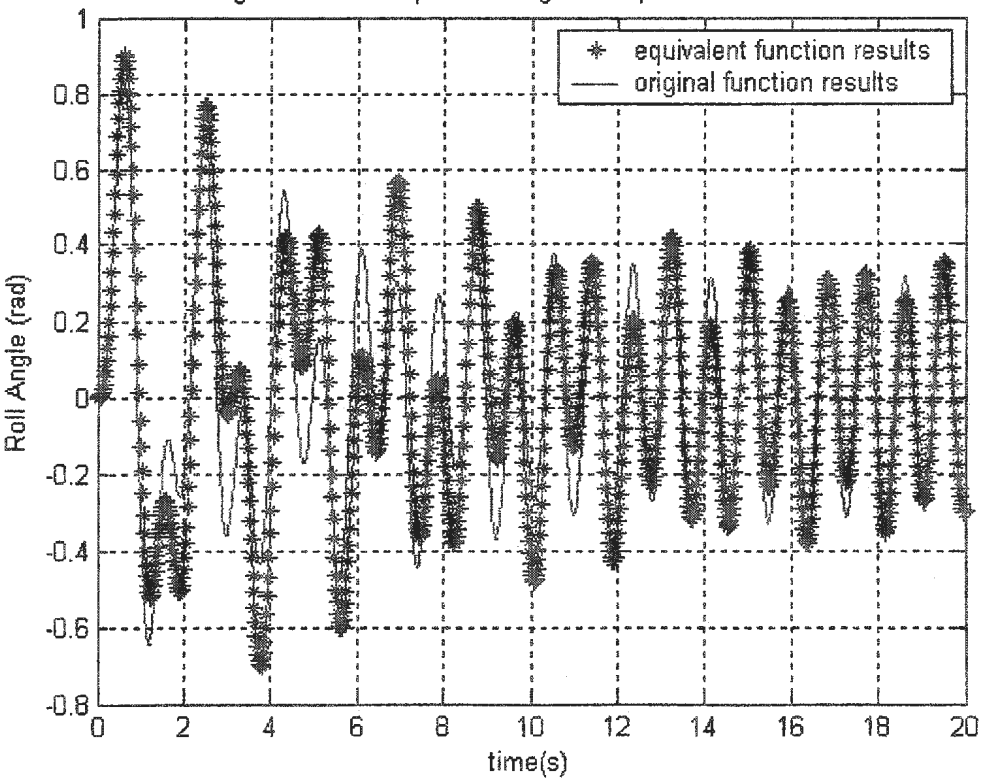

Figure A.25: Compare the regular response of case 431

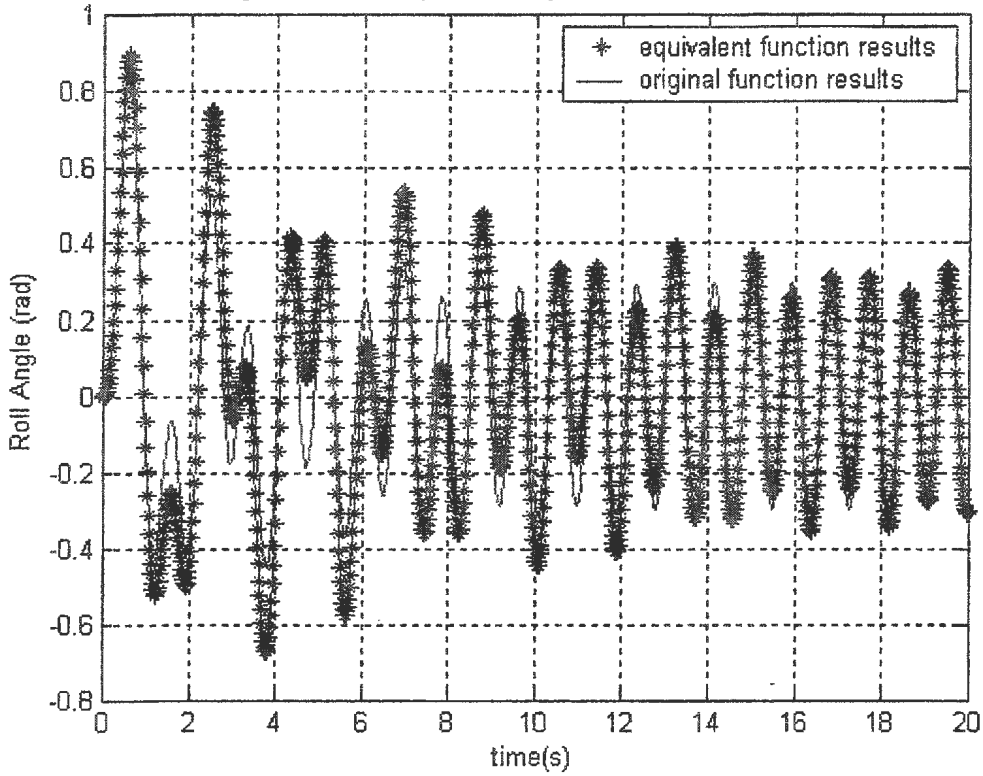

Figure A.26: Compare the regular response of case 433

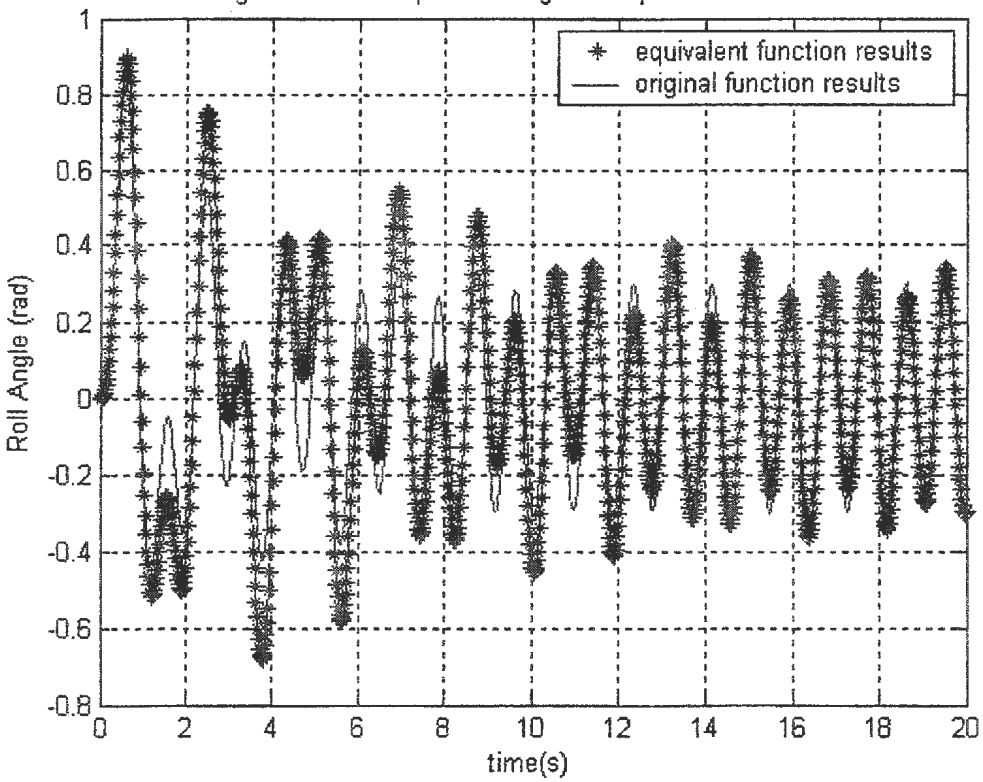

Figure A.27: Compare the regular response of case 435

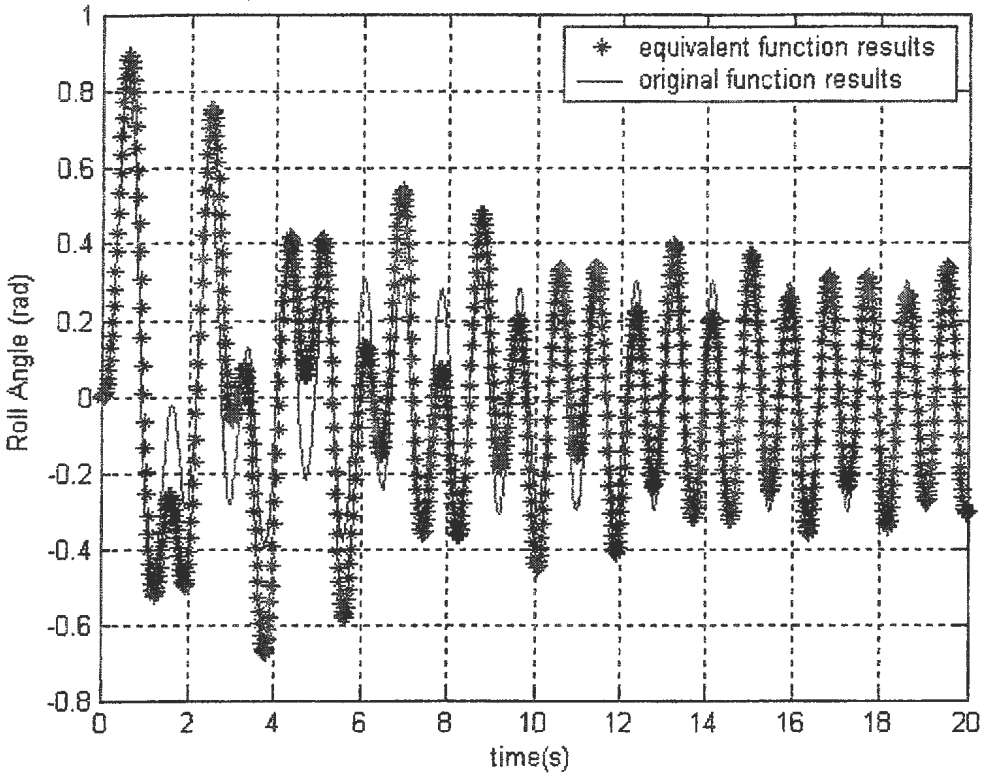

Figure A.28: Compare the regular response of case 451

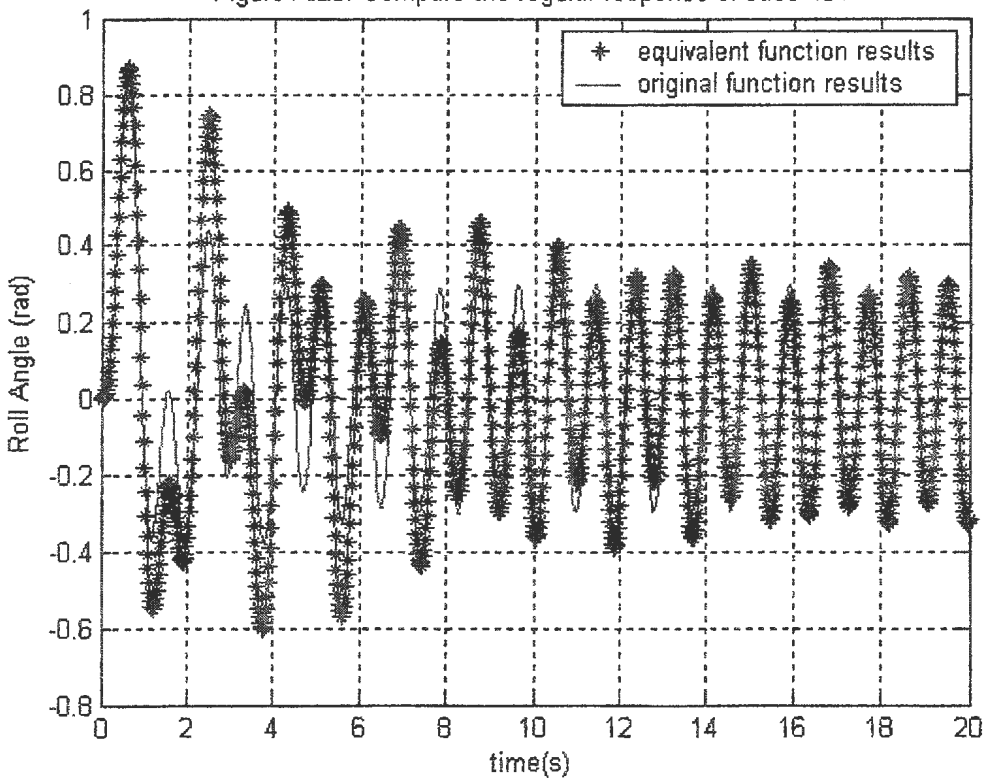

Figure A.29: Compare the regular response of case 453

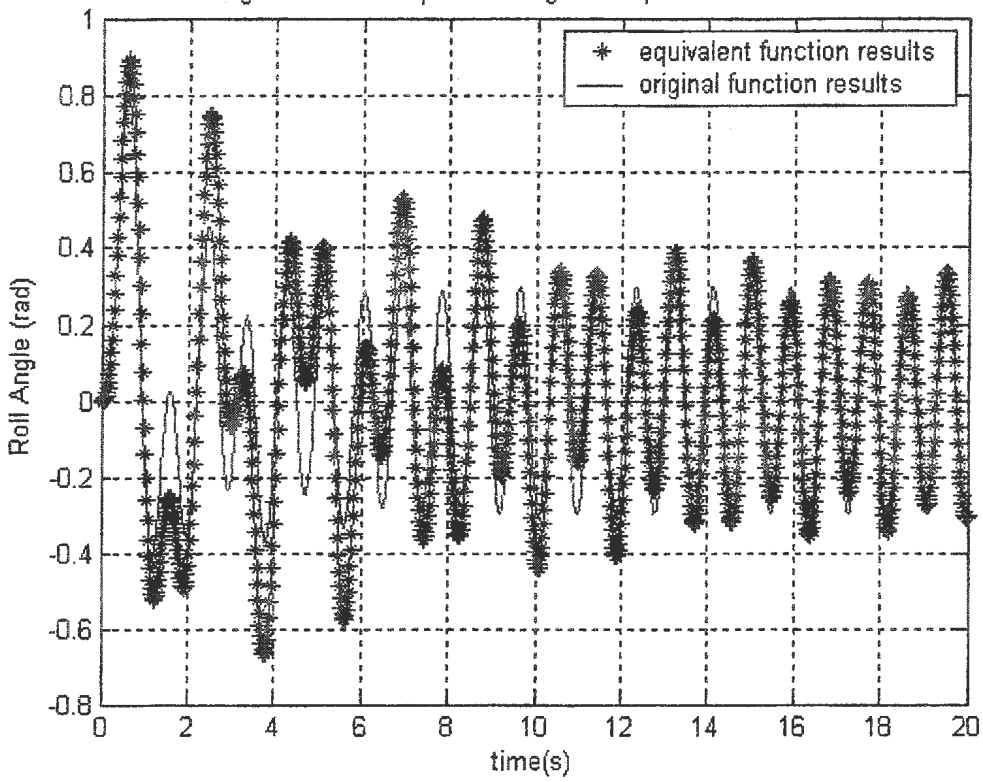

Figure A.30: Compare the regular response of case 455

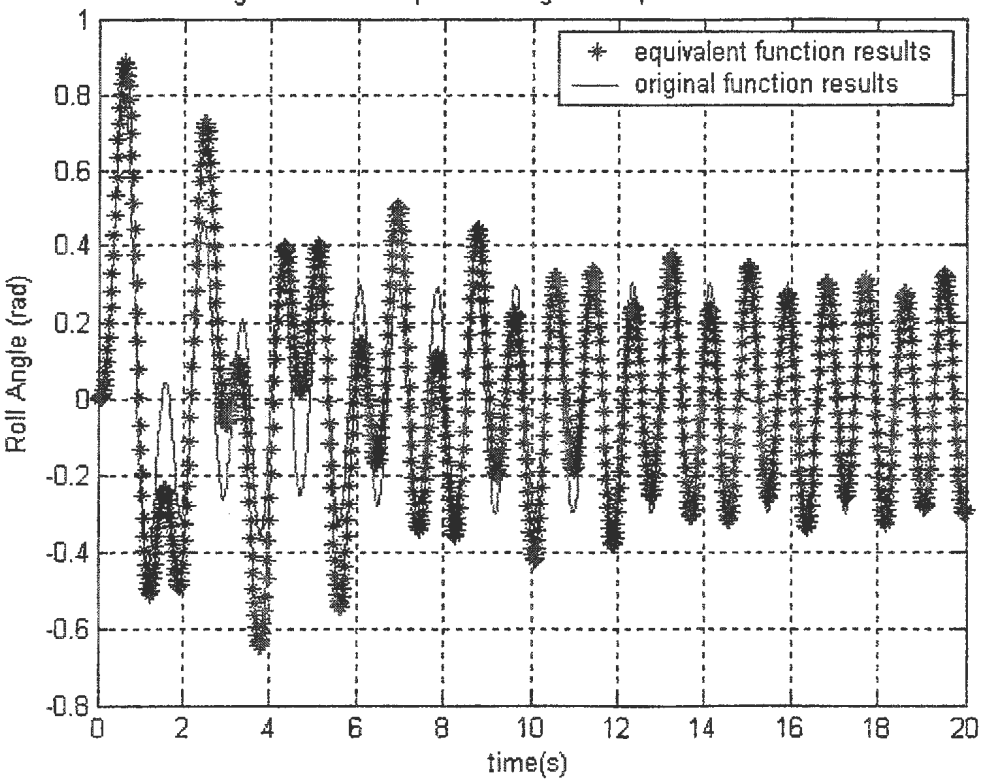

Appendix B

Computer programs

The Following MATLAB program "*simulation1.m*" was used to generate the roll motion history from the random wave excitation, and also calculate the random decrement curves. The program "*xzl_oct3.m*" was used to create ship roll motion equation, which would be solved by "ode45" command in the program "*simulation1.m*". The FORTRAN 90 program "*roll.f*" was used for neural network training to identify the damping function G. The MATLAB program "*Compare.m*" was used to compare the regular response results of estimated parameters and original parameters. The programs "*xzl_Oct5.m*" and "*xzl_5.m*" were used to create ship regular roll motion equation, which would be solved by "ode45" command in the program "*Compare.m*". Finally, the MATLAB program "*experiment1.m*" was used to deal with the experimental data of each case to calculate the random decrement curve.

Simulation1.m

```
%Oct3,2002
%simulation of ship roll motion
%Random decrement to extract the free roll decay curve
global zeta Wn Ak w q a1 a2
zeta=0.06;
Wn=5.00;
Ak=0.2;
w=3:0.075:6;
q=2*pi*rand(1,41);
a1=0.01;
a2=0.01;
time=4000;
tspan=[0:0.05:time];
Y0=[0.1,0.1];
[t,y]=ode45('xzl_Oct3',tspan,Y0);
z=y(:,2);       % simulated Roll Angle
dz=y(:,1);      % simulated Roll Velocity
nn=length(t);
dT=time/(nn-1);
v11=sum(z.^2)/(nn-1);
v22=sum(dz.^2)/(nn-1);
v12=sum(z.*dz)/(nn-1);
%x0=input('X0=?????');
x0=0.2;
TT=4;
```

```
num=round(TT/dT);
T=0;
for n=1:num;
    tn=n*dT;
    T=[T,tn];
end
k=zeros(1,num+1);
kk=zeros(1,num+1);
count=0;
dk=zeros(1,num+1);
dkk=zeros(1,num+1);
for m=1:(nn-num);
 if z(m)>0;
    if (z(m)-x0)*(z(m+1)-x0)<0;
        mm=m+num;
        kk=z(m:mm);
        k=k+kk';
        dkk=dz(m:mm);
        dk=dk+dkk';
        count=count+1;
     end
 end
end
U=k/count;
dU=dk/count;
x11=U';
x22=dU';
Tm=T';

Pk=[x0];
Tt=[0];
for h=7:(num-1)
    if U(h)>0
       if (U(h)-U(h+1))>0
          if (U(h-1)-U(h))*(U(h)-U(h+1))<0
           Pk=[Pk;U(h)];
           tT=h*dT-dT;
           Tt=[Tt;tT];
          end
       end
     end
end
NX=3;
PT=[Pk,Tt];
Td=(Tt(NX)-Tt(1))/(NX-1);
Wd=2*pi/Td;

data=[Tm,x11,x22];
save Nov511.dat data /ascii;

data_2=[Wd,v11,v22,v12];
save Nov511_rr.dat data_2 /ascii;

clf
figure(1)
subplot(211)
plot(t,z);
```

```
title('Roll Angle 511');
xlabel('Time (sec)');
ylabel('Roll Angle (rad)');
grid

subplot(212)
plot(T,U);
title('the Shape of the Random Decrement 511');
xlabel('Time (sec)');
ylabel('Mean value U (rad)');
grid
```

xzl_oct3.m

```
%ship roll motion equation

function dy=xzl_Oct3(t,Y)
global zeta Wn Ak w q a1 a2

dy=zeros(2,1);

FF=Ak*sum(sin(w*t+q));
dy(1)=FF-Wn^2*(Y(2)+a2*Y(2).^3)-2*zeta*Wn*(Y(1)+a1*Y(1).^3);
%accelaration

dy(2)=Y(1);    %velocity

% Y(1)is velocity;
% Y(2) is roll angle.
```

roll.f

```
* Input layer weight--->wi
* Output layer weight-->wo
* Suspension inputs---->ri
* Suspension outputs--->ro
* Middle layer outputs->rm
* Roll natural frequency>rr
* Time end & time step-->tend & delt
* Middle layer neurons-->Net
* Number of inputs------>kin
* Number of outputs----->kon
```

```
* variation of data points--> rate
* # of iterations:kit, and Counter for iterations: it
* Logical IF operator mig
* Natural roll Frequency rr
* If statment condition for RM(i) - power
* Weight manipulator del
* Number of input velocities,and angles data npoint
* Use old or new wieghts CHOICE (choice < 0 old, choice > 0 new)
* Declare variables
      implicit real*8 (a-z)
      integer i,j,count1,kin,kon,net,met,jf
      integer npoint,mf,mig,kit,it,nfiles

      character*20 ff,ff1
      dimension timer2(2500),result3(2500),sense(25000)
      dimension res1(2500),res2(2500)
      common/block1/ met,net,kin,kon,big,choice,power,del,rr,tend,
     *  delt,time,count1,mig,wig,wrong,yi(2),wo(15,15),wi(15,15),rm(15)
     *  ,ri(15),ro(15),k1(2),k2(2),k3(2),k4(2),rsim(2500,4),
     *  result1(2500),result2(2500),oo(15,15,15),oi(15,15,15)

* input constants and initial variable values
      open(1,file='initial.d',status = 'old')
      read(1,*) rate,big,wig,mig,power,del
      read(1,*) net,kin,kon
      read(1,*) delt,tend,kit
      read(1,*) choice,ddel
      close(1)
      print *,' rate:?????:',rate
      print *,'# of Middle layer neurons: net = ',net
      print *,'Number of inputs:kin = ',kin
      print *,'Number of outputs:kon = ',kon
      print *,'Total time ',tend,'and time step',delt
      print *,'big',big,'wig',wig
      print *,'# of iterations:',kit,'Counter for iterations: it'
      print *,'Logical IF operator mig: ',mig

      print *,'If statment condition for RM(i): power = ',power
      print *,'Weight manipulator: del = ',del

      print *,'Use old or new wieghts(choice > 0 old, choice < 0 new)'
      print *, 'choice = ',choice
      open(1,file='data1.d',status = 'old')
      write(1,*)' rate:?????:',rate
      write(1,*)'# of Middle layer neurons: net = ',net
      write(1,*)'Number of inputs:kin = ',kin
      write(1,*)'Number of outputs:kon = ',kon
      write(1,*)'Total time ',tend,'and time step',delt
      write(1,*)'big',big,'wig',wig
      write(1,*)'# of iterations:',kit,'Counter for iterations: it'
      write(1,*)'Logical IF operator mig: ',mig

      write(1,*)'If statment condition for RM(i): power = ',power
      write(1,*)'Weight manipulator: del = ',del


      write(1,*) 'choice = ',choice
```

```
      close(1)
* input weight inputs and outputs
      met = net + 1
      open(1,file='tt.txt', status = 'old')

      read(1,*) nfiles

      do jf = 1, nfiles

            read(1,*) ff

            ff1 = trim(ff) // ".d"


* input ship roll and roll rate


      open(2, file= ff1 ,status ='old')

      read(2,*) rr, npoint
       do  count1 = 1,npoint
         read(2,*) dummy,rsim(count1,1),rsim(count1,2)

       end do
      close(2)



      do count1 = 1, npoint

            rsim(count1,2) = rsim(count1,2)

      end do

      npoint = 100

      print *,'Natural roll Frequency rr',rr

      print *,'Number of input velocities,and angles data = ',npoint
      call intweight(ff)

      it = 1

      crit = 1
       sense(it) = 1
*     do while (it.lt.kit)
* loops to end of program
      do while (crit.gt.ddel )
      time = 0.d0
      count1 = 1
      deep = 0.d0
      result1(1) = rsim(1,1)
      result2(1) = rsim(1,2)

      mf = 2
      do while(time .lt. tend)
* call Middle layer and net output subroutine
```

```
            ri(1) = result1(mf-1)
            ri(2) = result2(mf-1)

            ri(kin) = 1.d0
            call mid_net_out
            call runge
            result3(mf - 1) = ro(1)
            mf = mf + 1
            result1(mf-1)= ri(1)
            result2(mf-1)= ri(2)
            count1 = count1 + 1
            wrong = ri(1) - rsim(count1,1)

      if (mig.eq.0) then
             deep = deep + wrong**2
      else if (mig.eq.1)then
             deep = deep + DABS(wrong)
      end if
* do while time < tend loop ends
      end do

      it = it + 1
      Sense(it) = sqrt(deep)/npoint

      crit = sense(it)/rsim(1,1)

      write(*,*) it,sense(it), crit
      call wi_oi(result3)
      call wo_oo(timer2,result3)
      call corcalc(cor,rate)
      if (it > kit) then

      go to 3

      else if (it < kit) then

      go to 5

      end if



* do while it < kit loop ends
5     end do
3     call results(npoint,timer2,result3,sense,kit,ff,ff1)
      end do

      close (1)

      end

      subroutine intweight(ff)
      implicit real*8 (a-z)
      integer met,net,kin,kon,i,j,count1
      integer mig
      integer*4 iseed
```

```
      character*30 string,string1

      character*20 ff,ff3


      common/block1/ met,net,kin,kon,big,choice,power,del,rr,tend,
     *  delt,time,count1,mig,wig,wrong,yi(2),wo(15,15),wi(15,15),rm(15)
     *  ,ri(15),ro(15),k1(2),k2(2),k3(2),k4(2),rsim(2500,4),
     *  result1(2500),result2(2500),oo(15,15,15),oi(15,15,15)

      ff3 = trim(ff) //".w"


      If (choice.GE.0) Then

      open(3,file=ff3,status = 'old')

            read(3,5) string
5               format(a)
            do 20 j = 1,met
            do 20 i = 1,kon
                  read (3,*) wo(j,i)
20              continue
            read(3,15) string1
15              format(a)
            do 30 j = 1,net
            do 30 i = 1,kin
                  read (3,*) wi(j,i)
30              continue
            close(3)
      else
*  initialize random layer weight input and output
            iseed = 123457
            do 40 j = 1,met
            do 40 i = 1,kon
                  gwo = RAN(iseed)*big
                  wo(j,i)=gwo
40              continue
*
            do 50 j = 1,net
            do 50 i = 1,kin
                  gwo = ran(iseed)*big
                  wi(j,i) = gwo
50              continue
      end if
      return
      end


      subroutine mid_net_out
      implicit real*8 (a-z)
      integer i,j,net,met,kin,kon,count1
      integer mig
      common/block1/ met,net,kin,kon,big,choice,power,del,rr,tend,
     *  delt,time,count1,mig,wig,wrong,yi(2),wo(15,15),wi(15,15),rm(15)
     *  ,ri(15),ro(15),k1(2),k2(2),k3(2),k4(2),rsim(2500,4),
     *  result1(2500),result2(2500),oo(15,15,15),oi(15,15,15)
```

```
* middle layer output

            do 60 i = 1,net
            rm(i) = 0.d0
            do 70 j = 1,kin
               rm(i)= rm(i) + wi(i,j)*ri(j)
70              continue
            if(rm(i).ge.power) then
                  rm(i)=1.0d0/(1.0d0+dexp(-rm(i)))
            else if(rm(i).lt.power) then
              rm(i)=0.d0
            end if
            rm(i) = 2.d0*(rm(i)- 0.5d0)
60              continue
            rm(met)=1.0d0
* net ouput calculation
            do 80 i=1,kon
              ro(i)= 0.d0
            do 80 j=1,met
              ro(i)= ro(i) + wo(j,i)*rm(j)
80              continue
            return
            end


      Subroutine runge
      implicit real*8 (a-z)
      integer n,i,net,met,kin,kon,count1
      integer mig
      common/block1/ met,net,kin,kon,big,choice,power,del,rr,tend,
     *  delt,time,count1,mig,wig,wrong,yi(2),wo(15,15),wi(15,15),rm(15)
     *  ,ri(15),ro(15),k1(2),k2(2),k3(2),k4(2),rsim(2500,4),
     *  result1(2500),result2(2500),oo(15,15,15),oi(15,15,15)

      n = 2
      ti = time
      do 90 i = 1,n
             yi(i) = ri(i)
90      continue

             rslt = - rr**2* ri(1) - ro(1)
             k1(1) = delt*ri(2)
             k1(2) = delt* rslt
            do 100 i = 1,n
                  ri(i) = yi(i) + k1(i)/2.d0
100             continue
             call mid_net_out
             time = ti + delt/2
             rslt = - rr**2*ri(1) - ro(1)
             k2(1) = delt*ri(2)
             k2(2) = delt*rslt
             do 150 i = 1,n
            ri(i) = yi(i) + k2(i)/2.d0
150           continue
             call mid_net_out
             rslt = -rr**2* ri(1) - ro(1)
             k3(1) = delt*ri(2)
```

```
            k3(2) = delt*rslt
            do 120 i = 1,n
           ri(i) = yi(i) + k3(i)
120           continue
            call mid_net_out
            time = ti + delt
            rslt = -rr**2* ri(1) - ro(1)
            k4(1) = delt*ri(2)
            k4(2) = delt * rslt
            do 130 i = 1, n
            ri(i)= yi(i) + (k1(i) +2.d0*(k2(i) + k3(i))
     *           + k4(i))/6.d0
130           continue
            call mid_net_out
            return
            end

      subroutine corcalc(cor,rate)

      implicit real*8 (a-z)
      integer n,i,net,met,kin,kon,count1
      integer mig
      common/block1/ met,net,kin,kon,big,choice,power,del,rr,tend,
     *  delt,time,count1,mig,wig,wrong,yi(2),wo(15,15),wi(15,15),rm(15)
     *  ,ri(15),ro(15),k1(2),k2(2),k3(2),k4(2),rsim(2500,4),
     *  result1(2500),result2(2500),oo(15,15,15),oi(15,15,15)

      do i = 1,kon
      do j = 1,met
      cor = (oo(j,i,1)-oo(j,i,2))/2.d0/del
      wo(j,i) = wo(j,i) - cor*rate
      end do
      end do
      do i = 1,kin
      do j = 1,net
      cor = (oi(j,i,1)-oi(j,i,2))/2.d0/del
      wi(j,i) = wi(j,i) - cor*rate
      end do
      end do
      return
      end

      subroutine wi_oi(result3)
      implicit real*8 (a-z)
      integer n,i,net,met,kin,kon,count1,ii,jj,kk
      integer mig
      dimension result3(2500),result4(2500),result5(2500)
     *  ,result6(2500),res1(2500),res2(2500)
      common/block1/ met,net,kin,kon,big,choice,power,del,rr,tend,
     *  delt,time,count1,mig,wig,wrong,yi(2),wo(15,15),wi(15,15),rm(15)
     *  ,ri(15),ro(15),k1(2),k2(2),k3(2),k4(2),rsim(2500,4),
     *  result1(2500),result2(2500),oo(15,15,15),oi(15,15,15)

            do 999 jj = 1,net
            do 999 ii = 1,kin
              wi(jj,ii) = wi(jj,ii)+del
              do 888 kk=1,2
```

```
              oi(jj,ii,kk)=0.d0
              time = 0.d0
              count1 = 1
              result5(1) = rsim(1,2)
              result4(1) = rsim(1,1)

              mf = 2
              do while(time .lt. tend)
              ri(1) = result4(mf-1)
              ri(2) = result5(mf-1)

              ri(kin) = 1.d0
              call mid_net_out
              call runge
              result6(mf - 1) = ro(1)
              mf = mf + 1
              result4(mf-1)= ri(1)
              result5(mf-1)= ri(2)
                  count1 = count1 + 1
                  wrong = ri(1) - rsim(count1,1)
                  wrong = wrong/wig
               if (mig.eq.0) then
                  oi(jj,ii,kk)=oi(jj,ii,kk)+wrong**2
               else if (mig.eq.1)then
                  oi(jj,ii,kk)=oi(jj,ii,kk)+DABS(wrong)
               end if
* end of do while TIME loop
            end do
            wi(jj,ii)=wi(jj,ii)-2.d0*del
888             continue
            wi(jj,ii)=wi(jj,ii)+del
999             continue
            return
            end

      subroutine wo_oo(timer2,result3)
      implicit real*8 (a-z)
      integer n,i,net,met,kin,kon,count1,ii,jj,kk
      integer mig
      dimension timer2(2500), result3(2500),result7(2500)
     *  ,result8(2500),res1(2500),res2(2500)
      common/block1/ met,net,kin,kon,big,choice,power,del,rr,tend,
     *  delt,time,count1,mig,wig,wrong,yi(2),wo(15,15),wi(15,15),rm(15)
     *  ,ri(15),ro(15),k1(2),k2(2),k3(2),k4(2),rsim(2500,4),
     *  result1(2500),result2(2500),oo(15,15,15),oi(15,15,15)
            do 777 jj = 1,met
            do 777 ii = 1,kon
              wo(jj,ii) = wo(jj,ii)+del
              do 666 kk=1,2
              oo(jj,ii,kk)=0.d0
              time = 0.d0
              count1 = 1

              result8(1) = rsim(1,2)
              result7(1) = rsim(1,1)

              timer2(1) = time
```

```
              mf = 2
              do while(time .lt. tend)
              ri(1) = result7(mf-1)
              ri(2) = result8(mf-1)

              ri(kin) = 1.d0
              call mid_net_out
              call runge
              mf = mf + 1
              timer2(mf -1) = time
              result7(mf-1)= ri(1)
              result8(mf-1)= ri(2)
                  count1 = count1 + 1
                  wrong = ri(1) - rsim(count1,1)
                  wrong = wrong/wig
                if(mig.eq.0)then
                  oo(jj,ii,kk)=oo(jj,ii,kk)+wrong**2
                else if (mig.eq.1)then
                  oo(jj,ii,kk)=oo(jj,ii,kk)+DABS(wrong)
                end if

* end of do while TIME loop
            end do
              wo(jj,ii)=wo(jj,ii)-2.d0*del
666               continue
              wo(jj,ii)=wo(jj,ii)+del
777             continue
            return
            end

      subroutine results(npoint,timer2,result3,sense,kit,ff,ff1)
      implicit real*8(a-z)
      integer i,j,net,met,kin,kon,count1,npoint,count3
      integer mig,kit

      character*20 ff,ff1,ff2,ff3,ff4,ff5,ff6
      dimension timer2(2500),result3(2500),sense(25000)
      common/block1/ met,net,kin,kon,big,choice,power,del,rr,tend,
     *  delt,time,count1,mig,wig,wrong,yi(2),wo(15,15),wi(15,15),rm(15)
     *  ,ri(15),ro(15),k1(2),k2(2),k3(2),k4(2),rsim(2500,4),
     *  result1(2500),result2(2500),oo(15,15,15),oi(15,15,15)

* print net outputs
      ff2 = trim(ff) //".a"
      ff3 = trim(ff) //".w"
      ff4 = trim(ff) //".v"
      ff5 = trim(ff) //".r"
      ff6 = trim(ff) //".e"
      open(2,file=ff2,status = 'replace')
      open(3,file=ff3,status = 'replace')
      open(4,file=ff4,status = 'replace')
      open(5,file=ff5,status = 'replace')
      open(6,file=ff6,status = 'replace')
      do 140 count3 = 1, npoint
      write(2,*) timer2(count3),rsim(count3,1),result1(count3)
140     continue
      do 170 count3 = 1,npoint
```

```
      write(4,*) timer2(count3),rsim(count3,2),result2(count3)
170     continue
      do 180 i = 1, npoint
      write(5,*) result1(i),result3(i)
180     continue
      do 190 i =1, kit
      write(6,*) sense(i)
190     continue
      write(3,*) 'WO - Output layer weights'
      do 150 j = 1,met
      do 150 i = 1,kon
        write(3,*) wo(j,i)
150     continue
      write(3,*) 'WI - Input layer weights'
      do 160 j = 1, net
      do 160 i = 1,kin
        write(3,*) wi(j,i)
160     continue
      close(3)
      close(4)
      close(2)
      close(5)
      close(6)
      return
      end
```

Compare.m

```
%Compare Oct5,2002
global ze we F0 w zeta Wn a1 a2

we=4.864;
ze=0.073;

Err=[];
NN=[];
for F0=12:12;
w=7;
time=20;
tspan=[0:0.02:time];
Y0=[0,0];
[t,ye]=ode45('xzl_Oct5',tspan,Y0);
Re=ye(:,2);       % Equivalent Roll Angle
dRe=ye(:,1);      % Equivalent Velocity

Pe=[];
num=length(Re);
for h=2:(num-1)
    if Re(h)>0
       if (Re(h)-Re(h+1))>0
          if (Re(h-1)-Re(h))*(Re(h)-Re(h+1))<0
           Pe=[Pe;Re(h)];
          end
```

```
        end
      end
end

zeta=0.06;
Wn=5.00;
a1=0.01;
a2=0.01;
[t,y]=ode45('xzl_5',tspan,Y0);
R=y(:,2);       % Roll Angle
dR=y(:,1);      % Velocity

P=[];
N=length(R);
for h=2:(N-1)
    if R(h)>0
       if (R(h)-R(h+1))>0
          if (R(h-1)-R(h))*(R(h)-R(h+1))<0
           P=[P;R(h)];
          end
       end
     end
end
l_p=length(P);
l_pe=length(Pe);
error=sum(1-Pe(l_pe-9:l_pe)./P(l_p-9:l_p))*100/10;
Err=[Err;error];
NN=[NN;F0];
end
Peak=sum(P(l_p-9:l_p))/10;
Error=[NN,Err]

figure(1)
plot(t,Re,'*',t,R,'r')
xlabel('time(s)');ylabel('Roll Angle');
legend('equivalent function results','real function results')
title('Compare the regular response of case 511')
grid
```

xzl_Oct5.m

```
%Oct.05,2002
%Equivalent Linear Function

function dy=xzl_Oct5(t,Y)
global ze we F0 w

dy=zeros(2,1);

dy(1)=F0*sin(w*t)-we^2*Y(2)-2*ze*we*Y(1);  %accelaration
dy(2)=Y(1);    %velocity
```

```
% Y(1)is velocity;
% Y(2) is roll angle.
```

xzl_5.m

```
%original parameters function
function dy=xzl_5(t,Y)
global zeta Wn F0 w a1 a2

dy=zeros(2,1);

dy(1)=F0*sin(w*t)-Wn^2*(Y(2)+a2*Y(2).^3)-2*zeta*Wn*(Y(1)+a1*Y(1).^3);
%accelaration

dy(2)=Y(1);    %velocity

% Y(1)is velocity;
% Y(2) is roll angle.
```

experiment1.m

```
%Feb21, 2003
%"R-class icebreaker" and "Series 60" models roll tests
% in the towing tank at MUN
%analysis the experimental data

load j770h13.dat

RA_1=j770h13(:,3)-mean(j770h13(1:3000,3)); %Roll angle
dt=1/50;  %time step
dRA_1=(RA_1(2:end)-RA_1(1:end-1))/dt; %Roll velocity

RA_1=RA_1(3001:end)*pi/180;  %degree to radian
dRA_1=dRA_1(3000:end)*pi/180;   %degree per second to radian per second
nn=length(RA_1);
time=nn*dt;
v11=sum(RA_1.^2)/(nn-1);
v22=sum(dRA_1.^2)/(nn-1);
v12=sum(RA_1.*dRA_1)/(nn-1);
%x0=input('X0=?????');
```

```
x0=0.1;
TT=10;
num=round(TT/dt);
T=0;
for n=1:num;
    tn=n*dt;
    T=[T,tn];
end
t=[0.02:0.02:time];

k=zeros(1,num+1);
kk=zeros(1,num+1);
K=zeros(1,num+1);
count=0;
dk=zeros(1,num+1);
dkk=zeros(1,num+1);
DK=zeros(1,num+1);
DDk=zeros(1,num+1);
for m=1:(nn-num);
 if RA_1(m)>0;
    if (RA_1(m)-x0)*(RA_1(m+1)-x0)<0;
        mm=m+num;
        kk=RA_1(m:mm);
        k=k+kk';
        dkk=dRA_1(m:mm);
        dk=dk+dkk';

        count=count+1;
     end
 end
end
U=k/count;
dU=dk/count;
Tm=T';

Pk=[x0];
Tt=[0];
for h=7:(num-1)
    if U(h)>0
       if (U(h)-U(h+1))>0
          if (U(h-1)-U(h))*(U(h)-U(h+1))<0
           Pk=[Pk;U(h)];
           tT=h*dt-dt;
           Tt=[Tt;tT];
          end
       end
     end
end
NX=4;
PT=[Pk,Tt];
X1=Pk(1);
X2=Pk(NX);
Td=(Tt(NX)-Tt(1))/(NX-1);
Wd=2*pi/Td;
Tm=[0:0.02:2]';
U11=U(1:101)';
U22=dU(1:101)';
```

```
data=[Tm,U11,U22];
save e770h13.dat data /ascii;
data_2=[Wd,v11,v22,v12];
save e770h13_rr.dat data_2 /ascii;

clf
figure(1)
plot(T,U);
title('the Shape of the Random Decrement(j770h13)');
xlabel('Time (sec)');
ylabel('Mean value U (rad)');
grid

figure(2)
plot(t(10000:10300),RA_1(10000:10300),'R',t(10000:10300),dRA_1(10000:103
00));
title('Comparison of Roll Angle & Velocity');
xlabel('Time (sec)');
ylabel('Roll Angle (rad) & Velocity(rad/s)');
legend('roll angle','roll velocity');
grid
```